

Eindhoven University of Technology
Department of Biomedical Engineering

Development of a numerical analysis pipeline to study the influence of the Infinity Total Ankle System on hindfoot range of motion

Jeroen Norg
1456741

Examination committee:
dr. ir. Bert van Rietbergen
prof. dr. ir. Gabriëlle Tuijthof
drs. Joris Hermus
dr. Vito Conte

Final version

Eindhoven, April 17, 2025

Abstract

Ankle arthritis is a chronic disease that affects approximately 1% of the world's population. Ankle arthritis patients can experience significant pain, dysfunction and disability in their ankle. Ankle arthritis is most commonly caused by previous trauma, and it therefore affects younger people than primary osteoarthritis. Ankle arthritis is most commonly treated through conservative means, but if they prove unsuccessful, ankle arthrodesis or total ankle arthroplasty are the most used solutions. Total ankle arthroplasty replaces the distal end of the tibia and proximal surface of the talus with metal implants which articulate through a polyethylene component and simulate ankle movement. The influence of total ankle arthroplasty with the Infinity Total Ankle System on the range of motion is not known. If the range of motion of the hindfoot is limited by the Infinity Total Ankle System, subsequent osteoarthritis in adjacent bones could occur. Therefore, it is necessary to study the hindfoot range of motion before and after total ankle arthroplasty with the Infinity Total Ankle System by acquiring CT scans of the foot in multiple positions and computing the translation and rotation between foot positions.

This study focuses on the development of a pipeline which segments the acquired CT scans into separate 3D bone models used for 3D registration to obtain the range of motion of hindfoot joints. CT scan segmentation was performed by an nnU-Net segmentation model which was trained with 23 healthy ankle CT scans and one ankle CT scan with the Infinity Total Ankle System implanted left and right. The trained nnU-Net model segmented the left and right tibia, talus, calcaneus, and navicular of six ankle CT scans with a Dice similarity index of over 90%. Segmentation of three total ankle arthroplasty post-op CT scans achieved an average Dice similarity index of over 80%.

A bayesian coherent point drift algorithm was adapted to perform 3D registration. It was adapted by minimising the mean absolute error for 3D registration of 20 3D hindfoot models, for 48 combinations of parameters. This was done by prescribing an arbitrary transformation to the 3D hindfoot models and computing the 3D registration from the original to the transformed orientation. The combination of parameters with the smallest error in both translation and rotation was used. The mean absolute translation error was 0.0846 mm, and the mean absolute rotation error was 0.0155°, which is smaller than other verified 3D registration methods.

Whilst a limited number of human ankle CT scans were used during the model development and algorithm validation, this research primarily centres on establishing the segmentation and 3D registration pipeline. To fully evaluate hindfoot range of motion after total ankle arthroplasty with the Infinity Total Ankle System, future studies with newly acquired CT scans of the foot in multiple positions will be necessary.

A research application was developed to enable this analysis, and will be used for future human subject studies at the Maastricht University Medical Center+.

Contents

1 General Introduction	4
1.1 Anatomy of the hindfoot	4
1.2 Ankle arthritis	4
1.3 Treatments	4
1.3.1 Conservative treatment	4
1.3.2 Ankle arthrodesis	5
1.3.3 Total ankle arthroplasty	5
1.4 INFINITY Total Ankle System	6
1.5 Hindfoot range of motion	7
1.6 3D CT stress test	7
1.7 Goals of this study	7
2 Segmentation of total ankle arthroplasty CT scans	8
2.1 Introduction	8
2.1.1 Segmentation of ankle CT scans	8
2.1.2 Metal artefact reduction	9
2.2 Methods	10
2.2.1 Training nnU-Net on ankle CT scans	10
2.2.2 Segmentation of ankle CT scans with Infinity TAS implant	12
2.2.3 Accuracy testing	14
2.3 Results	15
2.3.1 Accuracy of the nnU-Net Ankle segmentation model	15
2.3.2 Accuracy of the nnU-Net TAA segmentation model for a CT scan with Infinity TAS	16
2.4 Discussion	16
2.4.1 Major findings testing the accuracy of the nnU-Net Ankle segmentation model	16
2.4.2 Major findings testing the influence of MAR on the nnU-Net TAA segmentation model	17
2.4.3 Visual comparison of Infinity TAS CT scan segmentation with and without MAR	17
2.4.4 Limitations	18
2.5 Conclusion	18
3 Analysis of hindfoot range of motion with 3D registration	19
3.1 Introduction	19
3.1.1 Volume merge	19
3.1.2 Bayesian Coherent Point Drift	19
3.2 Methods	20
3.2.1 Adapting BCPD	20
3.2.2 3D registration of separate bones for joint range of motion	21
3.2.3 Robustness test	22
3.3 Results	22
3.3.1 Parameter search	22
3.3.2 Accuracy of joint 3D registration	24
3.3.3 Robustness test	25
3.4 Discussion	25
3.4.1 Major findings for the parameters search	25
3.4.2 Major findings testing the accuracy of 3D registration of separate joints	26
3.4.3 Major findings of the robustness test	26

3.4.4 Limitations	26
3.4.5 Future work	26
3.5 Conclusion	27
4 Development of an METC application for medical hindfoot ROM analysis	28
4.1 Introduction	28
4.2 Research protocol	28
4.2.1 Objectives	28
4.2.2 Study design	28
4.3 METC application process	29
4.4 Limitations throughout the application process	30
4.5 Next steps	30
Appendix A Results of the nnU-Net segmentation tests	35
A.1 nnU-Net Ankle segmentation model, accuracy	35
A.2 nnU-Net TAA segmentation model, influence of MAR	36
A.3 Visual comparison of Infinity TAS CT scan segmentation with and without MAR	38
Appendix B 3D registration	39
B.1 Equations for postprocessing of 3D registration results	39
B.1.1 Denormalisation of the translation vector	39
B.1.2 Derivation of the rotation vector	39
B.2 Joint 3D registration, accuracy	40
B.3 3D registration robustness	41
Appendix C METC application	41
Appendix D nnU-Net manual	94

1 General Introduction

1.1 Anatomy of the hindfoot

The hindfoot contains several joints that are all involved in the range of motion of the ankle and hindfoot: the tibiotalar, talocalcaneal, and talonavicular joint (Figure 1) [1]. The tibiotalar joint is located between the distal tibia and the proximal and medial talus. The joint allows for dorsal flexion and plantar flexion, the primary movement of the ankle [2]. The talocalcaneal joint, or subtalar joint, is the joint between the inferior talus and superior calcaneus, and allows for inversion and eversion of the hindfoot [2]. The talonavicular joint connects the talus and the navicular, and supports hindfoot range of motion in all six degrees of freedom, mainly plantar flexion and dorsal flexion [1, 2]. A healthy hindfoot is essential for normal movement, but unfortunately the ankle is prone to injuries, leading to ankle arthritis.

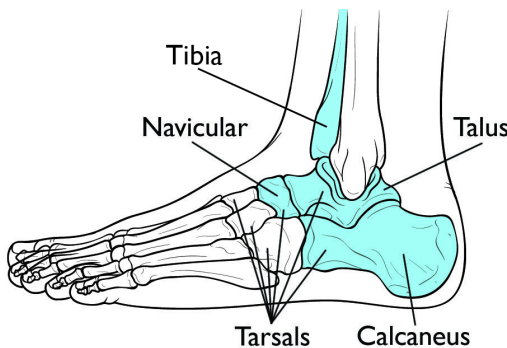


Figure 1: Anatomy of the hindfoot [3]

1.2 Ankle arthritis

Osteoarthritis (OA) is a chronic disease that is increasingly more prominent [4]. Ankle arthritis affects approximately 1% of the world's population [4]. Patients with ankle arthritis can experience significant pain, dysfunction, and disability, not unlike end-stage hip arthritis [4]. Research on ankle arthritis is limited and the cause and aetiology are not as widely analysed and understood as hip and knee OA [4].

Whereas primary OA primarily causes hip and knee arthritis, ankle arthritis is most often the result of previous trauma [5] and pa-

tients with post-traumatic ankle osteoarthritis (PTAOA) are generally younger than patients with primary OA [6, 7]. PTAOA is most common with 70% cases, followed by rheumatoid OA (12%) and primary ankle OA (7%) [7].

PTAOA is predominantly caused by ankle fractures, but also by previous ligament injuries as a result of repetitive ankle sprains in sports [6]. PTAOA results from cartilage damage at the time of injury, leading to decreased ankle stability and eventually cartilage overloading [6]. PTAOA can occur as early as one year or as late as 52 years after injury, with most cases after 20.9 years [8]. The time period between injury and PTAOA is influenced by the type of injury, complications during healing, the patient's age, and varus malalignment of the hindfoot [8].

1.3 Treatments

Traumatic ankle fractures are treated by stimulating bone healing through internal or external fixation [7]. If bone healing goes well, the fracture is resolved, but degenerative changes to the ankle can still occur, leading to PTAOA [7]. Ankle arthritis can be treated in multiple ways, starting with conservative treatment and then surgery [7].

1.3.1 Conservative treatment

Conservative treatment of ankle arthritis aims to alleviate symptoms, improve mobility, delay or avoid the need for surgical intervention [7]. This treatment includes lifestyle modifications such as reducing high-impact activities and maintaining a healthy weight which reduce mechanical load and decrease pain in the ankle joint [7]. Physical therapy is used to improve the muscle strength and range of motion of the ankle joint [6]. In case these therapies have not worked, orthotic support is sought to improve stability and reduce pain [9]. This can be an ankle brace which provides external support, or custom insoles which redistribute weight and improves walking efficiency [9]. Finally, pharmacologic pain management and intra-articular injections are used to reduce inflammation and provide pain relief [9].

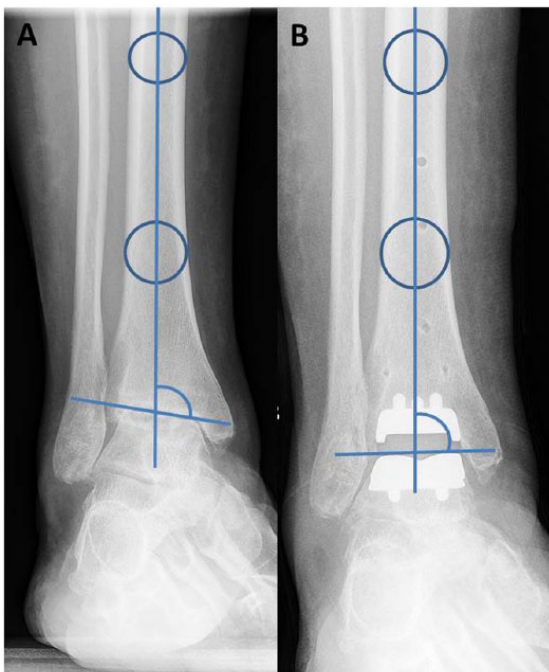


Figure 2: Weightbearing anteroposterior radiographs showing (A) preoperative tibiotalar coronal alignment, and (B) postoperative tibiotalar alignment, defined as the angle between the anatomical axis of the tibia and a line tangential to the superior surface of the talar implant [10].

1.3.2 Ankle arthrodesis

If conservative treatment of ankle arthritis is not successful, surgery is performed to remove the cause of pain and discomfort [11]. Ankle arthrodesis used to be the gold standard treatment for ankle arthritis [11]. Fusion of the tibia and talus bones, and therefore removing the arthritic tibiotalar joint, proved successful in pain relief and improved quality of life, despite the inability to move the ankle afterwards [11]. However, fusion of the ankle joint leads to increased motion of adjacent hindfoot joints as compensation [11]. During walking and double heel-rise, dorsiflexion-plantarflexion of the talocalcaneal joint increases significantly [12]. In the long term, this can lead to degeneration and arthritis in the talocalcaneal and talonavicular joint and additional arthrodesis surgery [11].

1.3.3 Total ankle arthroplasty

Total ankle arthroplasty (TAA) was developed and tested in the 1970s as an alternative for arthrodesis, returning mobility to the ankle

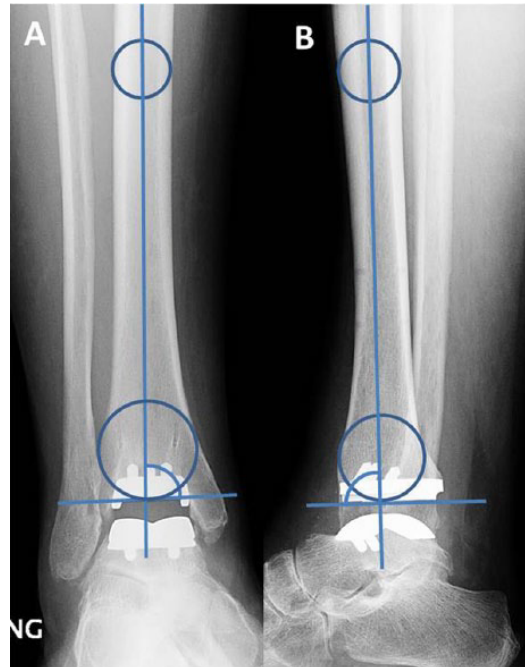


Figure 3: Tibial implant alignment defined as the angle between the anatomical axis of the tibia and a line drawn through the inferior border of the tibial component. Measured in weightbearing radiographs of the ankle (A) in anteroposterior view and (B) lateral view [10].

[13]. The early versions proved unsuccessful and caused more damage, and TAA was abandoned in favour of the more reliable arthrodesis [13]. However, recent advancements in prosthesis design and improvement of ankle anatomy have led to TAA being adopted as the new gold standard operative treatment [13]. Follow-up studies of TAA have shown an improvement in quality of life, movement, and reduced pain [10, 14, 15].

The positioning of the implant during TAA surgery is determined using pre-operative CT scans which allows for an accurate fit. Yet it is often necessary to perform concomitant procedures such as Gastrocnemius recession, Achilles lengthening, and prophylactic fixation of the medial malleolus, among others [10]. The most common cause for subsequent surgery is gutter impingement by the implant, which can cause pain in the ankle after TAA due to the talar implant impinging against either malleolus [16]. Impingement is caused by multiple factors including implant placement and presents itself during ankle movement [16].

Follow-up of the TAA surgery often consists

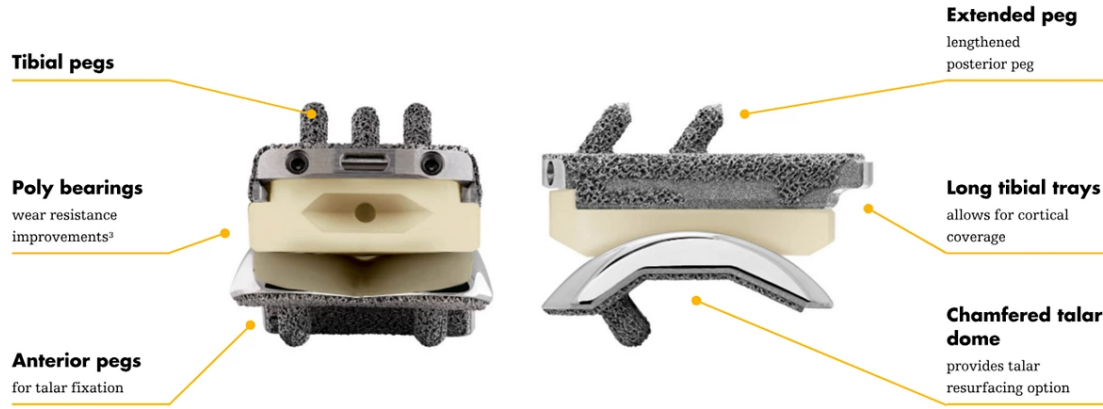


Figure 4: The INFINITY® Total Ankle System component parts [17].

of a clinical assessment, where patients are asked to evaluate pain, activities of daily living, and quality of life using the Foot and Ankle Outcome Score (FAOS) [18]. Saito et al. found significant improvement for all FAOS components after TAA compared to before surgery [10]. The second part of follow-up is radiographic analysis, where weight-bearing radiographs are taken in anteroposterior view and lateral view. These radiographs are analysed for positioning of the implant, checking whether the angle between the anatomical axis of the tibia and a line tangential to the talar dome is close to 90°. The same angle is measured for the tibial component, (Figure 2 and 3). These radiographs are further used to check for complications, such as gutter impingement, postoperative stress fractures, subsidence of components, and more [10].

Although TAA restores mobility in the ankle, the range of motion of older implants is observed to be smaller than of a normal healthy ankle [19]. Due to this difference in range of motion, osteoarthritis can still occur in the adjacent talocalcaneal and talonavicular joint, leading to joint fusion [20]. Although the incidence is low (<5%), it is important that modern total ankle replacements restore the range of motion of the ankle as much as possible such that adjacent joints do not become arthritic [19].

1.4 INFINITY Total Ankle System

At the Maastricht University Medical Center+ (MUMC+), the most used ankle prosthesis is the INFINITY® Total Ankle System (Infinity TAS) (Figure 4). The Infinity TAS is a mod-

ern, fourth-generation, fixed-bearing, total ankle replacement consisting of a tibial tray, an ultra-high molecular weight polyethylene (UHMWPE) component, and a talar dome.

The tibial tray is engineered from titanium alloy (approximately 90% titanium, 6% aluminium, and 4% vanadium). The superior surface is coated with a titanium plasma spray (approximately 100% titanium with traces of iron). Tibial fixation is achieved by the porous titanium coating and three press-fit pegs in an anterior triangular configuration [21].

The UHMWPE component is non-cross-linked compression-molded GUR-1020 polyethylene which locks into the tibial tray after implantation of the tibial tray and talar dome. The UHMWPE is front loaded and can be exchanged without removing the metallic implant components. Depending on implant size, the thickness of the UHMWPE component can range from 6 millimetres to 13 mm [21].

Finally, the talar dome is made from a cobalt chrome alloy (approximately 60% cobalt, 28% chromium, 6% molybdenum, and 1% nickel). The inferior surface is coated with the same titanium plasma spray as the tibial tray. The porous coating and anterior press-fit pegs fixate the dome to the talus. Rotational stability is provided by the anterior talar pegs and chamfer cuts. The talar dome is designed to maintain frontal plane stability when articulating with the corresponding sulcus design of the UHMWPE component [21]. The prosthesis is designed to replicate the shape of the talotibial joint such that it functions like the physiological joint.

Some advantages of the Infinity TAS over

other fixed-bearing total ankle replacements is that its components are smaller and easier to place, which requires removing fewer bone during placement, keeping bone strength intact. However, gutter impingement is still a common complication and reason for additional surgery. Although new placement techniques are being developed to prevent gutter impingement, there is no gold standard placement.

Although the Infinity TAS is widely accepted and proved successful in follow-up, it is currently not known how implanting this prosthesis affects the range of motion of the ankle and hindfoot joints. Reduced tibiotalar, and/or increased talocalcaneal or talonavicular range of motion, similar to in a fused ankle, could lead to more osteoarthritis in the hindfoot.

1.5 Hindfoot range of motion

The range of motion of the ankle and hindfoot can be studied in different ways. The standard technique to measure ankle and hindfoot range of motion is through a manual stress test where a clinician moves the foot as far as possible and measures the movement of the complete foot [22]. This however, depends on the clinician's own interpretation of the movement and does not quantify the individual joint movement involved in the ankle rotation.

A study by Imai et al. investigated the 3D kinematics of the tibiotalar joint, talocalcaneal joint, and the talonavicular joint using a rotational footplate to place the foot in plantar flexion and dorsal flexion and make digital models of the hindfoot bones from CT scans [2].

Nichols et al. studied the range of motion during walking by using near-IR camera gait analysis and dual-fluoroscopy to get the full range of motion [23].

1.6 3D CT stress test

The 3D CT stress test has been developed to overcome the problem of the manual stress test [24]. This test uses a medical device called the 3D Foot Plate (Figure 5) and mimics the manual stress test by positioning the foot relative to the lower leg and holds this position whilst performing 3D imaging to obtain quantitative data of the positions of the bones. The 3D Foot Plate has been

redesigned and made available via open-source by Masih at the University of Twente [25].

This 3D foot plate can hold the foot in multiple different positions whilst making a CT scan of the foot in each position. These scans can then be analysed to study the range of motion of an ankle after TAA with the Infinity TAS and find the influence of impingement on the range of motion.

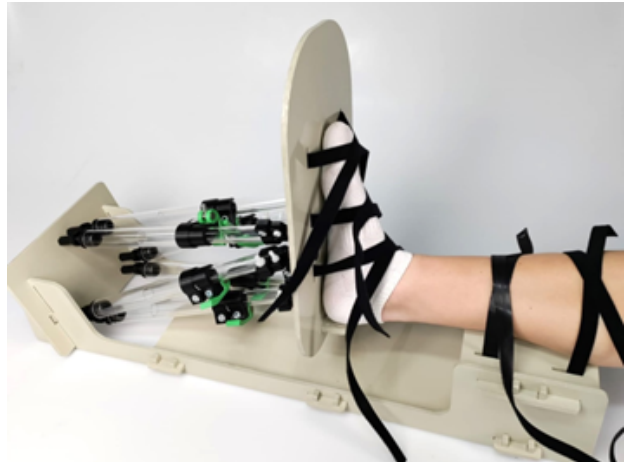


Figure 5: The redesigned 3D Foot Plate [25]

1.7 Goals of this study

As it is currently not known what the influence is of the Infinity TAS on the range of motion of the hindfoot, the risk of developing subsequent osteoarthritis in the hindfoot is not known. The goal of this research is to study the range of motion of the hindfoot after total ankle arthroplasty. This will be done using the 3D Foot Plate, placing the foot in extreme positions and making CT scans in each position. These CT scans allow for accurate quantification of the movement of each hindfoot bone and joint. This quantification requires the CT scans to be segmented to obtain digital bone models and the components of the Infinity TAS. This will be covered in chapter 2. These digital bone models are then used for 3D registration from one position to another, obtaining the movement of the hindfoot joints. This will be covered in chapter 3. Finally, to study the influence of the Infinity TAS on the range of motion of the hindfoot on human subjects, a research application should be submitted to the medical research ethics committee (medisch-ethische toetsingscommissie, or METC, in Dutch). This will be covered in chapter 4.

2 Segmentation of total ankle arthroplasty CT scans

2.1 Introduction

To quantify the range of motion of the hindfoot, digital hindfoot bone models should be created from segmented ankle CT scans. For CT scans of Infinity TAS implanted ankles, the metal artefacts caused by the metal implant could be reduced to improve bone model segmentation. In this chapter, an nnU-Net segmentation model is developed which can accurately segment ankle CT scans. This model is then adapted to segment Infinity TAS implanted ankle CT scans and determine the influence of MAR on ankle segmentation quality.

2.1.1 Segmentation of ankle CT scans

Medical image segmentation is the process of dividing an image into multiple segments to identify areas to be studied [26]. For a CT scan of the ankle, segmentation is used to segment the bones involved in the ROM of the ankle [26]. There are multiple methods to segment ankle CT scans. The first is performing manual segmentation using medical image analysis software such as Materialise Mimics [27] or 3D Slicer [28]. Using this software, ankle CT scans can be segmented accurately by the operator, obtaining individual digital models for the tibia, talus, calcaneus, and navicular [28]. Whilst manual segmentation makes detailed segmentation of bone possible, the reproducibility is operator dependent [29], is labor-intensive and time consuming [30], and scalability issues arise with large datasets [31].

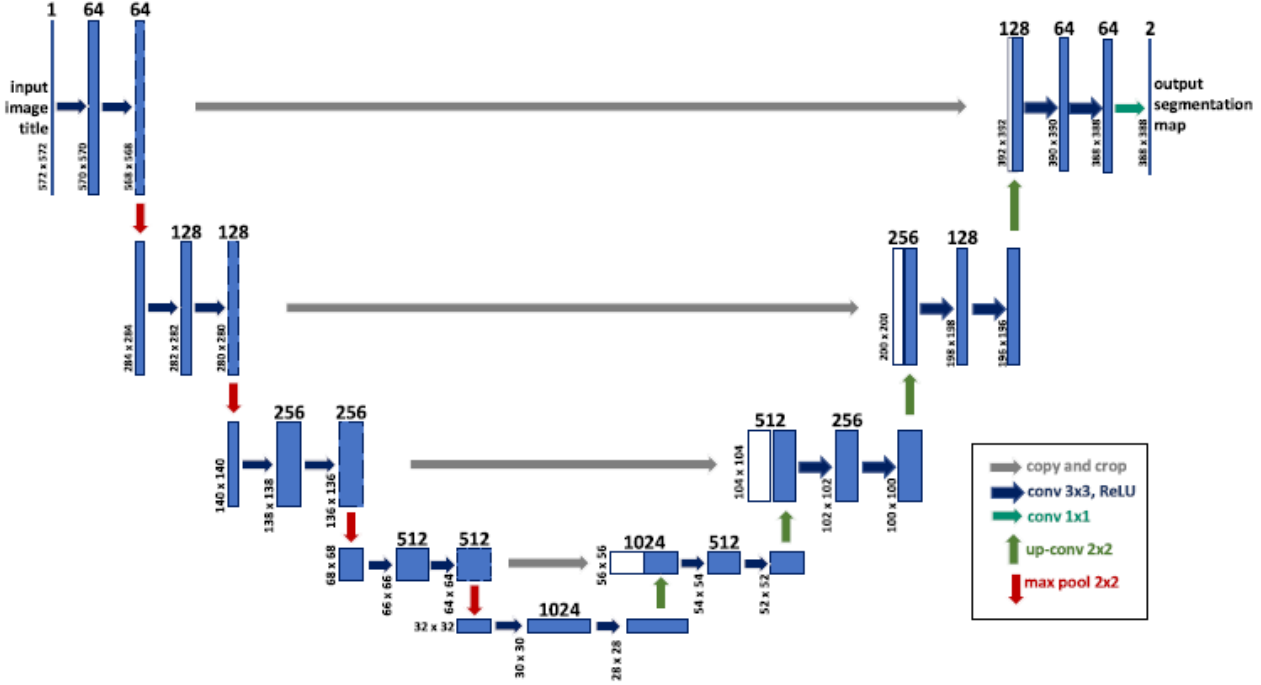
Recent development in artificial intelligence, mainly deep learning (DL), has shown significant improvement in image segmentation [32]. DL-algorithms can train a model to segment CT scans with higher accuracy and speed than traditional machine learning techniques, and much greater speed than manual segmentation [32]. DL models work very well for image segmentation applications because they can extract complex hierarchical features and patterns from raw pixel values [32]. A widely used model is a convolutional neural network (CNN) [33]. CNN's consist of multiple layers of convolution, pooling, and up-

sampling, which take an input image and return an output label [32, 33]. The CNN formed the basis to the U-Net network which is specialised for medical images due to its inherent ability to focus on specific objects in an image [33] (Figure 6). The U-Net, unlike the CNN which is linear, has a U-channel architecture and skip connections which copy the uncompressed images from the encoding blocks to their mirrored counterpart in the decoding blocks [32, 33]. The U-channel down-samples the image and then upsamples the label to provide a labelmap for each pixel. The skip connections allow for label and image linking [33] (Figure 6).

A U-Net model which has shown vast adaptability and high accuracy is nnU-Net [35]. nnU-Net is a DL-based biomedical image segmentation framework that automatically configures itself for any given dataset [35]. The working architecture behind nnU-Net is based on the U-Net (Figure 6). Unlike traditional segmentation models that require manual tuning, nnU-Net systematically optimises the training process by splitting the architecture into three groups: fixed parameters, rule-based parameters, and empirical parameters [35]. Fixed parameters remain unchanged across datasets, such as using a U-Net-like architecture [35]. Rule-based parameters adapt dynamically based on dataset properties, such as voxel spacing and image size [35]. Finally, empirical parameters, such as model selection and post-processing steps, are determined based on cross-validation performance [35]. nnU-Net generates multiple configurations, including 2D and 3D U-Net architectures, and then evaluates them using a five-fold cross-validation process to select the optimal model or ensemble [35].

nnU-Net evaluates model performance using the Sørensen-Dice index (SDI) [35]. The SDI provides information into the agreement between a groundtruth segmentation and model segmentation, or the similarities between two segmentations [36]. If we have segmentation A and B, the SDI is defined as,

$$SDI(A, B) = \frac{2|A \cap B|}{|A| + |B|} \quad (1)$$



ated as a cube 50 pixels around the metal implant. Everything within this region will be affected by the MAR correction. The next step is pre-processing the FPR by segmenting the bones in the original image and setting their HU values to zero. K-means clustering was used to segment the air, soft tissue, and bone within the FPR. Thereafter, the HU values of bone and everything outside of the FPR was set to zero, and the air and soft tissue inside the FPR are kept as the

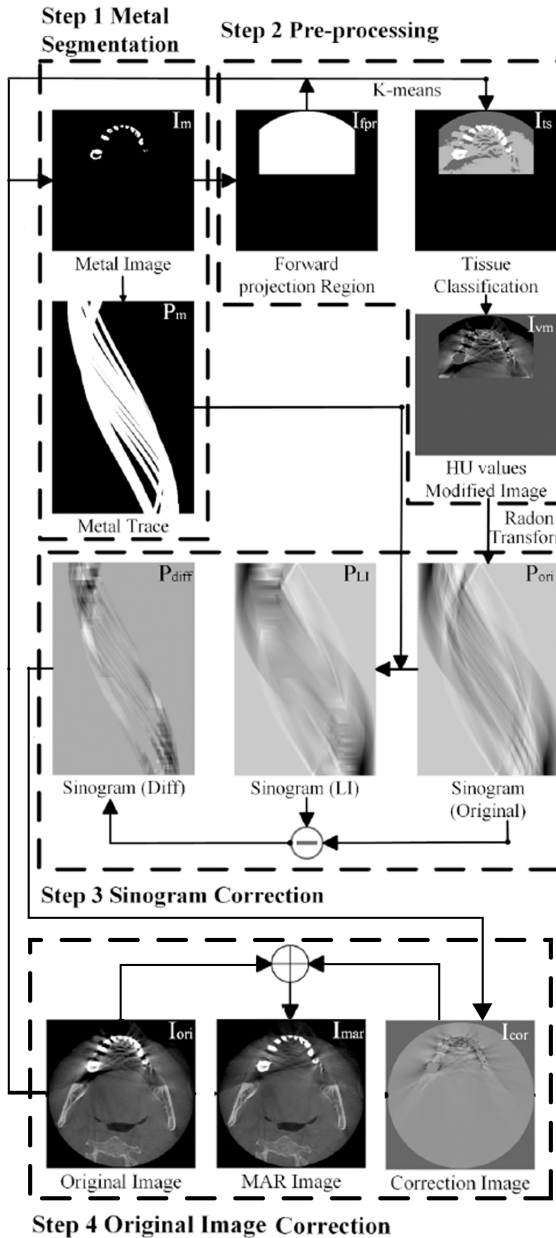


Figure 7: Flow chart of the proposed MAR algorithm consisting of four steps: (1) metal segmentation, (2) pre-processing, (3) sinogram correction, (4) original image correction [40].

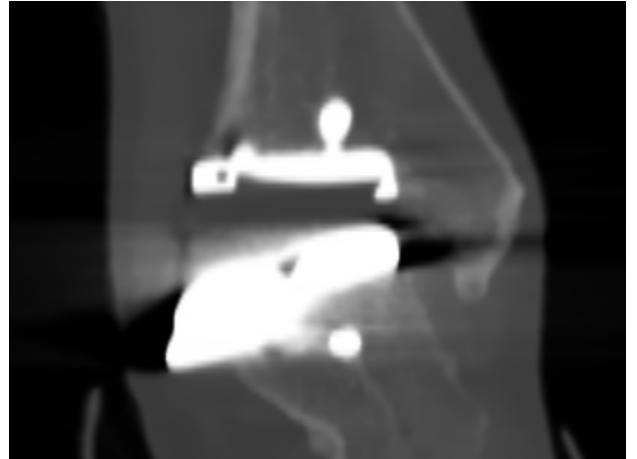


Figure 8: Right ankle CT scan with Infinity TAS, showing metal artefacts around the implant

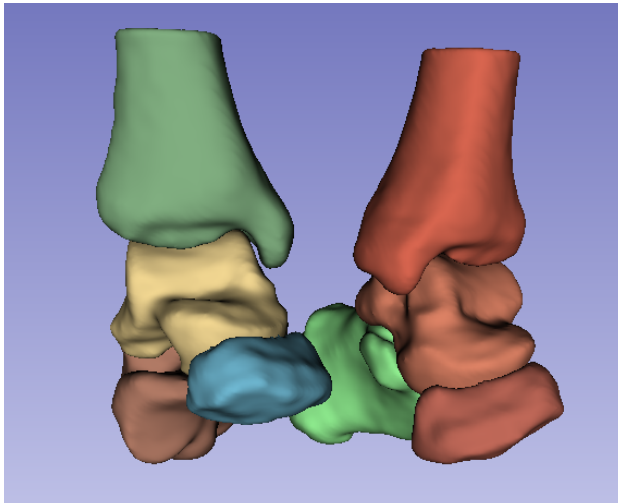
original image. This image was forward projected by the Radon transform. This sinogram is corrected with the metal trace to obtain a corrected sinogram. From the corrected sinogram, the inverse Radon transform creates a correction image which is added to the original image, resulting in the MAR image (Figure 7, Step 4) [40].

2.2 Methods

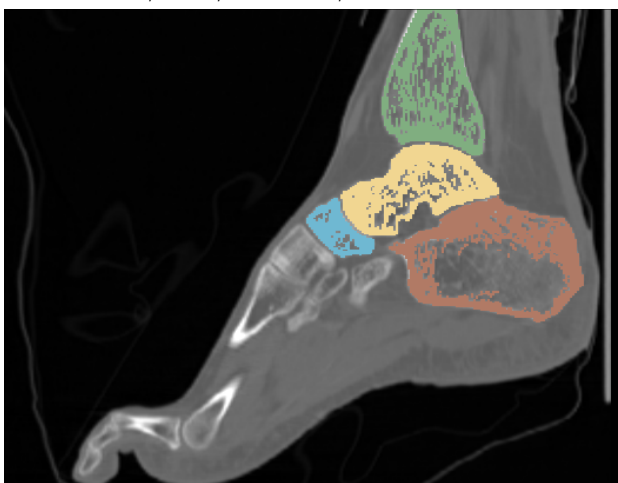
2.2.1 Training nnU-Net on ankle CT scans

2.2.1.1 Ankle CT data

The CT scans used for training nnU-Net are adapted from lower limb CT scans by Fischer [41]. Fischer created a database of 29 lower limb CT scans with segmentations of all the bones. These scans and segmentations were loaded into 3D Slicer 5.6.2 [28], where the volume of interest was reduced to only include the foot and 5 cm of distal tibia. Furthermore, the fibula, phalanges, metatarsals, and tarsals, not including the navicular, were removed from the segmentation, see Figure 9a and b. The segmentations were exported to a binary label map and saved as a NIfTI file. The label map is a matrix with an integer corresponding to a label. The background is 0, and the labels for Tibia_R, Talus_R, Calcaneus_R, Navicular_R, Tibia_L, Talus_L, Calcaneus_L and Navicular_L are 1 to 8, respectively. The cropped CT scan was also saved as a NIfTI file. The training set includes the first 23 CT scans with their segmentation, and the test set consists of the remaining 6 scans.



(a) 3D view of the cropped segmentation of the right and left tibia, talus, calcaneus, and navicular.



(b) Sagittal view of the right foot

Figure 9: Cropped hindfoot CT scan with the tibia, talus, calcaneus, and navicular segmented for both legs. Part of the lower leg database by Fischer [42]

2.2.1.2 nnU-Net training

The first step of training is experiment planning and preprocessing the data. During this step, nnU-Net extract a dataset fingerprint with a set of dataset properties which is used to design U-Net configurations such as 2d or 3d_fullres, learning the segmentation slice-wise or by 3D structure, respectively. These configurations are used during training and validation to find the optimal segmentation model. Furthermore, the training/validation splits are determined for each of the five folds used for training. Each fold uses 18 training and 5 validation scans, randomly selected.

Multiple different trainings were performed to

understand the architecture of nnU-Net and find the optimal model, as shown in Table 1. The first training is not relevant for the goal of this chapter as only one bone label was used, but it was performed to become acquainted with the nnU-Net architecture, using the standard training scripts. The second training used all eight bone labels with the standard script. This resulted in a model which was not accurate with low training and validation Dice scores.

In order to improve training and validation Dice scores, the main training code was modified by tuning some hyperparameters and settings. The number of epochs was decreased from 1000 to 400. An epoch is when all the training data has passed the training algorithm and all model training iterations have run their cycle. The number of epochs determines how many cycles of model training are performed. The number of epochs was reduced to 400 as it was found that too many epochs resulted in the model overfitting and increased training time. The percentage of oversampling foreground pixels was increased from 0.33 to 0.7. This was done to increase the focus on the foreground, improving the level of detail in the segmentation. The initial learning rate was decreased from 1e-2 to 1e-3 as starting with a lower learning rate which decreases every epoch, decreases the odds of overfitting and improves prediction of new data. The largest increase in model accuracy was found after disabling mirroring. nnU-Net uses mirroring and data augmentation to mitigate large differences between images, but since this model should segment the bones of the right and left feet separately, mirroring would result in a model which segments both feet together, i.e. give the label "Tibia_R" to both the right and left tibia. For this reason, mirroring was disabled. This resulted in a modified training script (trainings 3 - 7 in Table 1) which showed vastly improved performance. The model was trained with four different numbers of epochs (400, 600, 800, and 1000) to test the influence of the number of epochs on the training time and Dice scores. It was found that the Dice scores did not change significantly whereas the training time for 400 epochs was much shorter. This meant that 400 epochs was chosen as the best number of epochs. One final training was performed using the 2D configuration as a com-

Table 1: nnU-Net different training settings and scores

Training nr	Label info ^a	Hyperparameters & settings ^b	Configuration	Training time ([hh]:mm:ss) ^c	Training Dice ^d	Validation Dice ^d
1	<i>Bones - 1</i> ^e	<i>Standard</i>	<i>2d</i>	20:07:54	0.9256	0.9234
2	Ankles - 8	Standard	3d_fullres	27:37:32	0.5470	0.4193
3	Ankles - 8^f	Modified - 400	3d_fullres	11:14:13	0.9027	0.8981
4	Ankles - 8	Modified - 600	3d_fullres	16:50:33	0.9011	0.8970
5	Ankles - 8	Modified - 800	3d_fullres	22:09:04	0.9018	0.8954
6	Ankles - 8	Modified - 1000	3d_fullres	27:36:03	0.9060	0.8995
7	Ankles - 8^f	Modified - 400	2d	08:22:32	0.9076	0.8997

^aAnkles corresponds to all 8 bones having a separate label; Bones is all bones combined into one label "bone"=1 and "background"=0.

^bStandard is the training python code from nnU-Net; Modified is the standard code but with mirroring disabled, the foreground oversampling increased, and the initial learning rate decreased. The number of epochs is shown on the right.

^cTrained using NVIDIA GeForce RTX 2080 Ti GPU.

^dMean Dice scores from the 5 folds used for training.

^eThis training is not relevant due to only using one label.

^fThese trained models are used in the ensemble for nnU-Net Ankle segmentation model.

parison to the 3D configuration. This model (training 7), was actually more accurate than the 3D model (training 3). Therefore, nnU-Net was tasked to find the best configuration and it determined an ensemble of 2D and 3D to be the best configuration due to the validation Dice scores of the combination being higher than of the individual configurations. This segmentation model will be referred to as "nnU-Net Ankle segmentation model".

A complete user manual on how to train the nnU-Net segmentation model can be found in Appendix D.

2.2.2 Segmentation of ankle CT scans with Infinity TAS implant

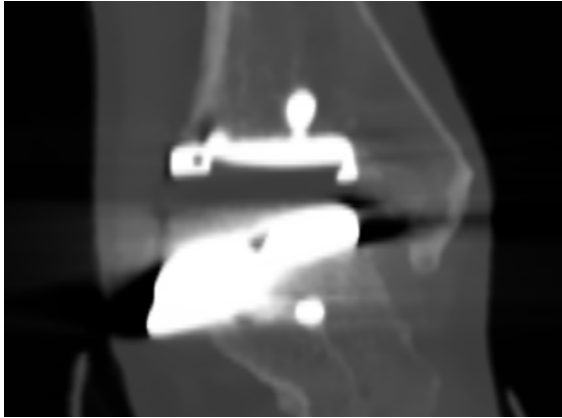
The nnU-Net Ankle segmentation model, trained in chapter 2.2.1, is able to predict the segmentation of an ankle CT scan accurately. However, segmentation of a TAA ankle CT scan has to take into account the metal implant, which the model has not been trained on. For that reason, a segmented implant scan was fed back into the model training so nnU-Net could learn the bone segmentation around the implant. There were only post-op ankle CT scans available with high enough resolution. One of those was fed back into the model training to have a sufficient number of test scans.

2.2.2.1 Scan preprocessing and MAR application

As explained in chapter 2.1.2, CT scans with a metal implant suffer from metal artefacts that distort the image and the grey value intensities of adjacent structures. In order to reduce the effect of the metal artefacts, the MAR method by Zhang [40] was adapted to be applied to ankle CT scans (Figure 10b). The code they developed was not available to use, so new MAR code was created based on the described process in the paper. The main difference is in the k-means clustering method, where the initial values for the centroids were set to -1000 HU for air, 0 HU for soft tissue, and +1000 for bone as this better represents the intensities in the CT scans used. Dividing bone into trabecular bone (+500 HU) and cortical bone (+1500 HU) was tried, but did not results in better artefact reduction. There are still some artefacts visible, but the grey value intensity of the bone has been restored (Figure 10b). This helps nnU-Net recognise the bone and more accurately predict the segmentation.

Another part of the preprocessing is a threshold to remove the metal implant from the CT scan. This ensures that nnU-Net does not mistake the high intensity of the implant with the intensity of bone. Cortical bone can show an intensity of up to 2000 HU, which is close to the 2500 HU of metal. Therefore, a threshold was

applied which set everything above 2500 HU to -1024 HU, which is the background intensity (Figure 10c).



(a) Original right ankle CT scan with the Infinity TAS implanted.



(b) Result of applying the proposed MAR method on a right ankle CT scan with the Infinity TAS implanted.



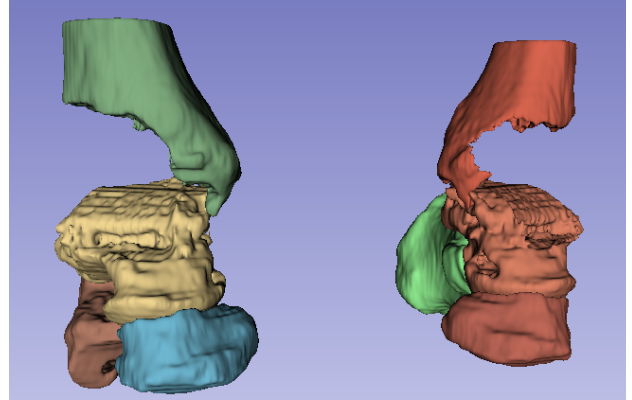
(c) Thresholded MAR CT scan.

Figure 10: Comparison of the same right ankle CT scan with the Infinity TAS, with and without applying MAR.

2.2.2.2 nnU-Net training feedback



(a) Sagittal view



(b) 3D view

Figure 11: Segmentation of CT scan with double Infinity TAS using nnU-Net Ankle segmentation model.

In order to train nnU-Net to recognise bone around the Infinity TAS it needed information about the location of the implant and the intensities of bone around it. The scan of Figure 10c was duplicated and mirrored to artificially create a CT scan with the Infinity TAS implanted in the right and left ankle. The nnU-Net Ankle segmentation model predicted the segmentation.

The result is a segmentation with a correct segmentation of the talus, calcaneus and navicular, but distal tibial bone not correctly segmented (Figure 11a). Figure 11 shows that the distal tibia is missing bone around where the implant is located. This is expected because nnU-Net does not know how to segment around the implant.

To combat this, the tibia segment was manually edited whereby additional in-painting was done to include bone around the implant (Fig-

ure 12). This improved segmentation was then exported as a labelmap, and the scan and labelmap were added to the training data for nnU-Net. The model was trained in the same way as nnU-Net Ankle segmentation model - 2D and 3D configuration with the modified script - and the training / validation split was such that the implant scan was in the training data for 4 of the 5 folds. The 2D training ran for 10,5 hours and the 3D training for 11,5 hours, slightly longer than the previous model. nnU-Net once again determined that an ensemble of 2D and 3D was the most optimal model, so this was saved. This new model is now referred to as "nnU-Net TAA segmentation model".

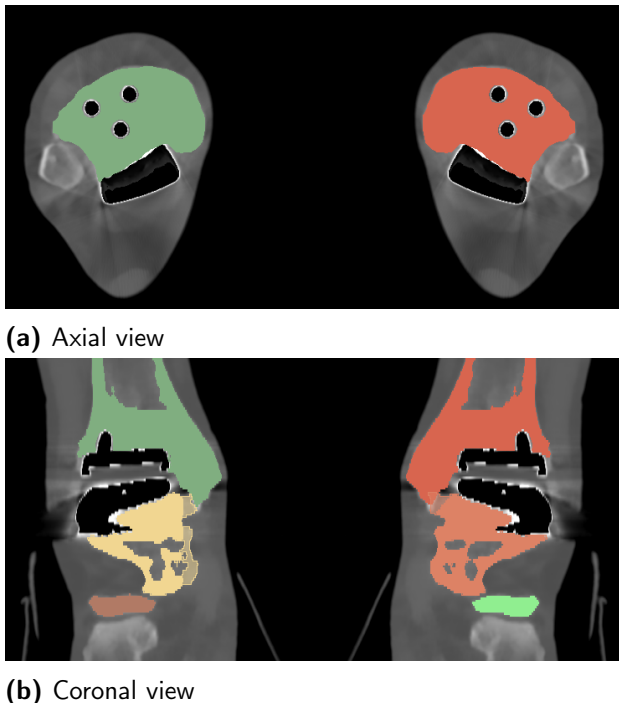


Figure 12: Tibia in-painted segmentation of a double Infinity TAS CT scan.

2.2.3 Accuracy testing

As mentioned in chapter 2.2.1.1, six CT scans were not used for training or optimisation (validation) of the nnU-Net model, as those were reserved for testing the performance of the nnU-Net Ankle segmentation model. The provided segmentations from the dataset were used as the ground truth. In order to test the performance of the nnU-Net TAA segmentation model, three ankle CT scans with the Infinity TAS implanted in one ankle were used, next to the six test

scans from the database. The three Infinity TAS CT scans were manually segmented to create a ground truth segmentation. In chapter 2.2.2.1, preprocessing implant CT scans with MAR was described as a useful step to improve segmentation due to the metal artefacts distorting the intensity of bone around the implant. However, it is not known whether this MAR application actually improves segmentation prediction.

Two tests were performed to evaluate the performance of the trained nnU-Net segmentation models. The first test evaluated the performance of nnU-Net Ankle, and the second test evaluated the performance of nnU-Net TAA and the influence of MAR.

For both nnU-Net Ankle and nnU-Net TAA, the validation data was used during the training process to determine the optimal model, which was an ensemble of 2D and 3D. The ensemble averages the prediction of 2D and 3D. The test data segmentations were predicted using nnU-Net Ankle and nnU-Net TAA for the conditions in Table 2

Table 2: Accuracy tests of nnU-Net Ankle and nnU-Net TAA

Test	Model	CT scans	Preprocessing
1	nnU-Net Ankle	6 test	None
2	nnU-Net TAA	6 test + 3 implant	MAR + 2500 HU threshold
3	nnU-Net TAA	6 test + 3 implant	2500 HU thresh-old

Prediction was run using the 2D model, then the 3D model, and then ensembling was run to average the predictions. The validation data is also used to determine what postprocessing should be applied on the predictions. This postprocessing implies removing all but the largest structure from a label, making it more accurate to the validation data. The postprocessing information is only saved for the configuration which nnU-Net determines as most optimal so it is only applied to the ensemble predictions.

The 2D, 3D, ensemble (ens), and ensemble postprocessed (ensPP) predicted labelmaps were saved, and using Matlab the Dice scores of the predictions with the ground truth were computed.

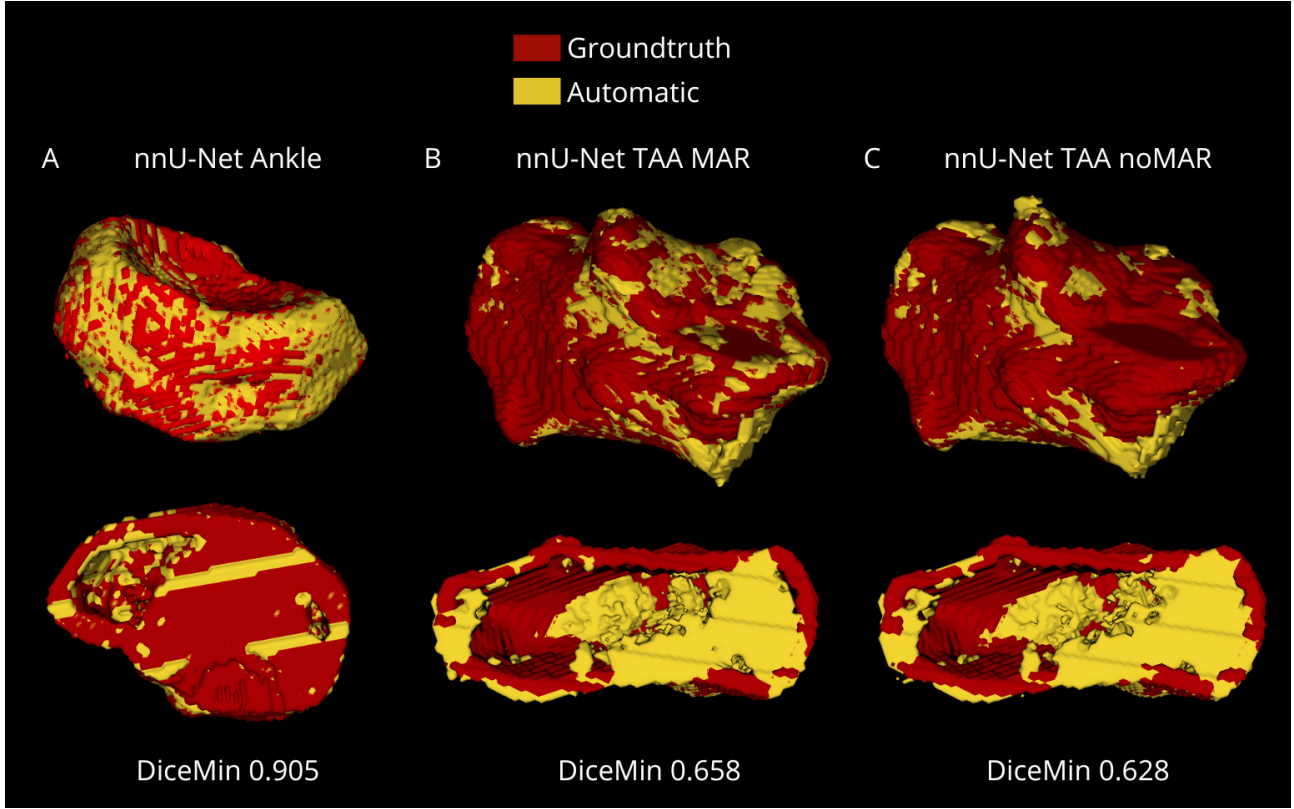


Figure 13: Accuracy of nnU-Net segmentation for (A) the test scans using nnU-Net Ankle, (B) the Infinity TAS CT scans with MAR using nnU-Net TAA, and (C) the Infinity TAS CT scans without MAR using nnU-Net TAA. Top shows the 3D view of the segmentation. Bottom shows a cross-section in the transverse plane.

2.3 Results

2.3.1 Accuracy of the nnU-Net Ankle segmentation model

The test Dice scores of the test scan segmentations were computed using Matlab with the segmentations from the Fischer database as ground truth. The 3D configuration had the highest test Dice with a mean(SD) of 0.931(0.014) (Figure 14). To test for significance, Mann-Whitney U tests were performed between the means of each configuration. No significant differences were found with a confidence interval of 95% or 90%.

Figure 22 in Appendix A.1 shows the Dice scores of the test scan segmentations per bone label.

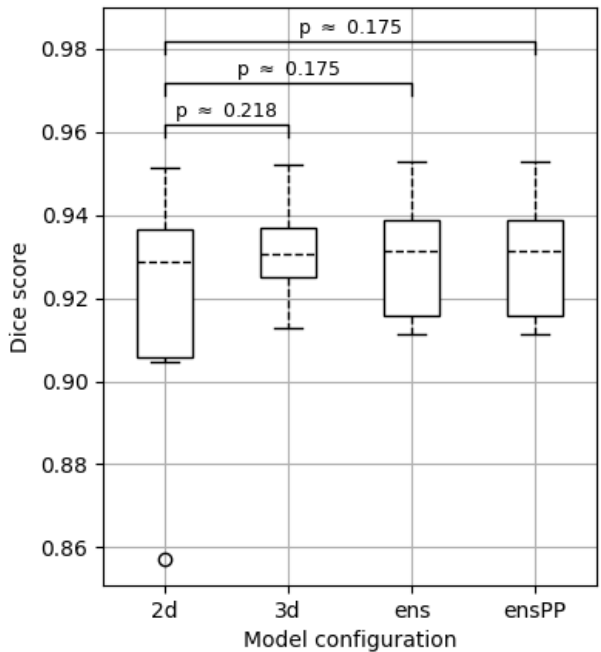


Figure 14: Test Dice scores of applied nnU-Net Ankle segmentation model per model configuration

2.3.2 Accuracy of the nnU-Net TAA segmentation model for a CT scan with Infinity TAS

The test Dice scores of the implant scan segmentations were computed using Matlab with the manual segmentations as ground truth. The 3D configuration with MAR had the highest Dice score with a mean(SD) of 0.819(0.097) (Figure 15). This is smaller than for the test scans by more than 0.1. To test for significance, Mann-Whitney U tests were performed between the means of MAR and noMAR within each configuration. No significant differences were found with a confidence interval of 95%, nor with a confidence interval of 90%.

Figure 23 in Appendix A.2 shows the Dice scores of the Infinity TAS implant scan segmentations with and without applying MAR before segmentation, per bone label. The Mann-Whitney U test found 6 (75%) significant differences between the same bone right versus left, with a confidence interval of 95%.

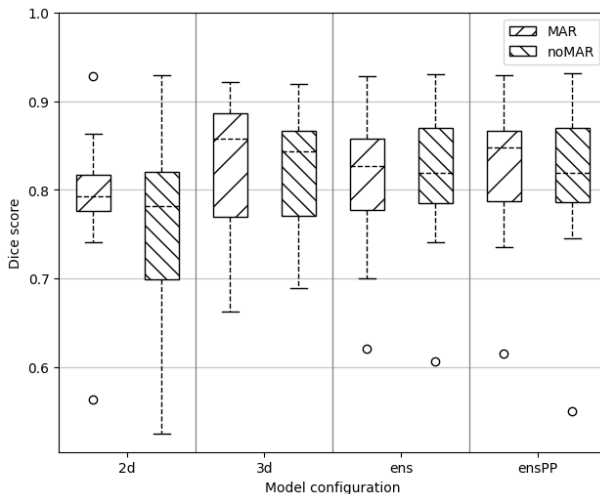
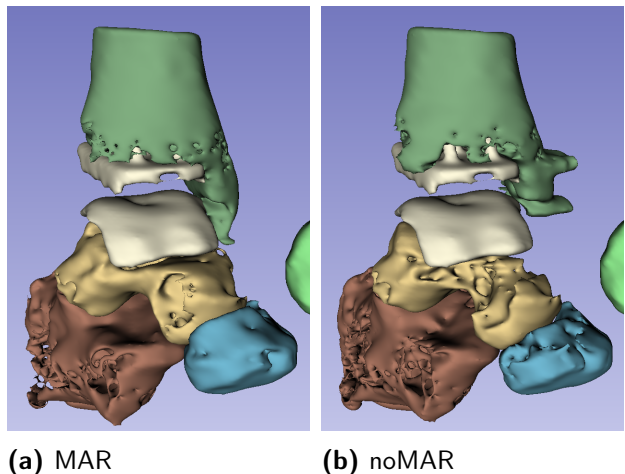


Figure 15: Dice scores of the applied nnU-Net TAA segmentation model on Infinity TAS CT scans with and without MAR applied, per model configuration

A visual comparison of the right foot of a segmentation of an Infinity TAS CT scan using the 3D configuration is shown in Figure 16. In both MAR and noMAR, holes are visible in all four bones, around the implant where errors are expected, but also in the calcaneus and navicular where there is no scattering of the metal implant. In noMar, the effects of metal artefacts are visible at the medial tibia where the artefacts are

segmented as tibia, but also in the talus where bone is missing anterior to the talar dome.



(a) MAR (b) noMAR

Figure 16: 3D views of the right foot of the 3D configuration segmentation an implant CT scan, showing the difference between applying MAR and not applying MAR.

2.4 Discussion

The first goal of this chapter was to develop an nnU-Net segmentation model which accurately segments ankle CT scans. The second goal was to adjust and further train the model to accurately segment Infinity TAS CT scans and determine the influence of applying MAR before segmentation on the accuracy of the segmentation.

2.4.1 Major findings testing the accuracy of the nnU-Net Ankle segmentation model

The mean test Dice scores do not differ significantly at a 5%, or even a 10% confidence interval, between the model configurations. Figure 14 shows that the 3d configuration does have a higher precision than the other configurations, meaning that predictions lie closer together. The outlier in 2d is caused by an unexpectedly low Dice of 0.55 for Navicular_R in scan 25. Removing this outlier would increase the mean of 2d, resulting in even higher p-values. Therefore, it was deemed not necessary.

In a study of Sushmitha et al. a Res U-Net architecture is trained to segment vertebrae. Their proposed method obtained Dice scores between 0.814 and 0.922 [43], meaning that our nnU-Net Ankle segmentation model performs better.

This is consistent with what Isensee et al. found in their paper about their nnU-Net architecture. They found that nnU-Net outperforms most specialised DL pipelines for segmentation, in terms of Dice scores [35]. The nnU-Net Ankle segmentation model obtained similar Dice scores as the nnU-Net models used by Kok et al. and by Zhang et al. [37, 38].

When comparing the bone labels, several significant differences were found at a 99% confidence interval. This means that the segmentation by nnU-Net Ankle is not equally accurate across bone labels. Segmentation of the right navicular obtained the lowest Dice score on average, but still the groundtruth and automatic segments correspond a lot (Figure 13).

2.4.2 Major findings testing the influence of MAR on the nnU-Net TAA segmentation model

The test Dice scores do not differ significantly between MAR and noMAR, nor between the configurations, at a 95%, or even a 90% confidence interval. This means that applying MAR before segmentation does not influence the accuracy of segmentation. Appendix A.2 Figure 23 shows that the ankle without the implant is segmented much more accurately than with the implant, apart from the Navicular. Due to the scattering in the image caused by the implant, it is not surprising that the Tibia and Talus with the implant are not segmented as accurately by the model as without. However, it is surprising that Calcaneus_R is segmented this inaccurately, because the implant is not positioned near the Calcaneus, nor are there any issues regarding grey value intensity visible in the CT scans. To check whether this was just a problem with the new nnU-Net TAA segmentation model, the old nnU-Net Ankle segmentation predicted the same 3 CT scans and had even worse results with the Calcaneus. Although the right calcaneus obtained low Dice scores for both MAR and noMAR, the outer shape of the groundtruth and automatic segments do look alike, but most differences are found on the inside of the segment (Figure 13, top). The automatic segmentations segmented a lot of bone inside the calcaneus, whereas the groundtruth only segmented the cortical shell (Figure 13, bottom).

In Appendix A.2, Figure 24, the nnU-Net TAA segmentation model was also applied to the same six test scans as for Chapter 2.2.3. This was done to evaluate the difference in segmentation of each bone between CT scans without implant and with implant. Significant differences were found between the Test Scans and MAR and noMAR, for each bone label, apart from Navicular_R. This suggests that the nnU-Net TAA segmentation model can still accurately predict the segmentation of ankle CT scans, still struggles with implant CT scans. This can also be seen in Table 10, which shows that there are no significant differences between the predicted segmentations of nnU-Net Ankle and nnU-Net TAA, with a confidence interval of 95%. However, it is interesting that even the left ankle (without implant) is segmented significantly less accurate than the Test Scans. This suggests that either more pre-processing should have been performed on the CT scans to increase the similarity with the training data, or the quality of the CT scans was poorer, leading to less accurate segmentation. Furthermore, nnU-Net uses contextual information during segmentation, which means that a poor segmentation of one bone could lead to poor segmentation of neighbouring bones [44]. It is likely that the poor segmentation of the right calcaneus and tibia is caused by a poorer segmentation of the right talus.

2.4.3 Visual comparison of Infinity TAS CT scan segmentation with and without MAR

Appendix A.3 Figure 25 shows the complete visual comparison of Figure 16, with the 2d and ensPP configurations and the left feet included. Looking at the right Calcaneus (bottom left, brown) in each of the images, it is clear to see why such low Dice scores were recorded in Table 9 for Calcaneus_R.

This visual comparison shows that the 3d configuration produces the most accurate segmentation in terms of the shape of the bones. The ensemble configurations (ens and ensPP) take the average of 2d and 3d, and because the 2d configuration produces visually worse segmentations than 3d, the 3d configuration should be used for further application.

2.4.4 Limitations

The low number of available CT scans of ankles with the Infinity TAS (1 for training and 3 for testing) caused some issues with training the nnU-Net TAA segmentation model and evaluating its performance. One of nnU-Net's strengths is that it is able to be trained on small datasets and still achieve high accuracy. However, the addition of only one segmented CT scan with a double implant might not have been enough to train the model on how to segment around the Infinity TAS. Furthermore, only having 3 Infinity TAS test scans creates difficulties in evaluating the accuracy of the nnU-Net TAA segmentation model, especially evaluating statistically significant differences between configurations, or between bone labels.

The MAR algorithm which was adapted from Zhang et al.'s proposed MAR method did not

work perfectly and still left dark streaks around the implant. This was expected as MAR methods are under much development and are still not very effective [45]. However, promising results have been reported with combining MAR with photon-counting CT.

2.5 Conclusion

The nnU-Net Ankle segmentation model shows high prediction accuracy with no significant differences between the different configurations. There are significantly different Dice scores for the predicted bone labels, but all bone labels are predicted very accurately. The nnU-Net TAA segmentation model shows high prediction accuracy for the same CT scans as nnU-Net Ankle, but lower accuracy for predicting Infinity TAS implanted CT scans.

3 Analysis of hindfoot range of motion with 3D registration

3.1 Introduction

To obtain the range of motion of hindfoot joints, 3D registration can be performed. This entails virtually moving one object towards another object and computing the translation and rotation, or transformation, to perform that movement. In this chapter, Bayesian Coherent Point Drift 3D registration is adapted for rigid registration of hindfoot bone models. This algorithm is then used to compute the 3D registration of separate hindfoot joints, and the robustness of the algorithm is tested.

3.1.1 Volume merge

A 3D registration method which has been verified and used for range of motion research is the volume merge method by Ochiai et al [46]. This method takes three-dimensional digital models of segmented bone, converted into point cloud data, and computes the transformation between two positions of the same bone. The bone is virtually rotated and translated towards the same bone in a different position until the moving bone merges with the target bone (Figure 17).

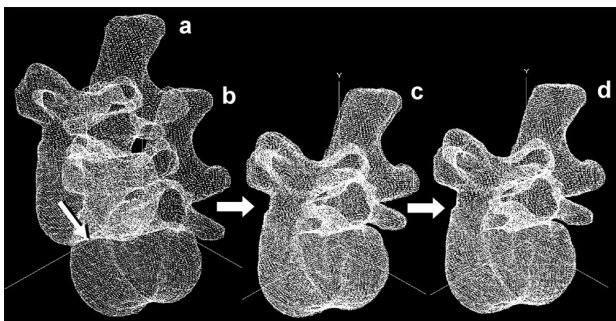


Figure 17: The volume merge method: Vertebral body in the neutral position (a) was virtually rotated and translated toward the rotated position (b) using values calculated by an Eigen vector method (c). Further rotation and translation of c was conducted with 0.1° and 0.1 mm increments, respectively, until the maximized volume merging was determined (d) [46].

This method was validated with a phantom study and they found that the mean absolute error was

less than 0.1 mm and 0.2° for translation and rotation, respectively. This volume merge method has been verified and has therefore been used in multiple hindfoot range of motion studies [2, 47, 48].

3.1.2 Bayesian Coherent Point Drift

The Bayesian Coherent Point Drift (BCPD) algorithm, created by Hirose [49], is an open-source 3D-registration implementation which can perform both rigid and non-rigid registration. It is based on the Coherent Point Drift (CPD), which is a state-of-the-art non-rigid registration algorithm. Coherent Point Drift is a probabilistic method for point set registration that models one dataset as centroids of a Gaussian Mixture Model (GMM) and aligns them to the other using maximum likelihood estimation [50]. Unlike traditional methods, CPD enforces coherence by ensuring that points move collectively, leading to smooth transformations [50]. For rigid registration, it optimizes transformation parameters directly, while for non-rigid cases, it regularizes deformations using a motion coherence constraint [50]. CPD has high registration performance and is scalable to large point sets. This is due to convergence depending on a soft-matching method, meaning that not every point should match one-to-one [49]. BCPD expands on this by using a Bayesian setting which is advantageous due to convergence being guaranteed, a possible combination of rigid and non-rigid CPD, and intuitive parameter tuning [49].

Bayesian Coherent Point Drift is particularly useful for the 3D registration of bone models, where rigid transformations are required to achieve accurate alignment [49]. Given that bone structures may undergo slight deformations due to natural anatomical variations, injury, or scanning artifacts, BCPD's ability to model smooth, coherent deformations while preserving local structure makes it an ideal choice. The Bayesian formulation allows for robust outlier handling, which is essential when dealing with medical scans where noise, partial occlusions, or missing data can affect registration accuracy [49]. Additionally, the soft-matching approach of

Table 3: BCPD model parameters and settings

Parameter	Value	Explanation
-w (Omega)	0.1	Outlier probability $\in (0, 1)$.
-b (Beta)	2.0	The length scale of the Gaussian kernel used for smoothing in the motion coherence model.
-l (Lambda)	1e9	Controls the length of deformation vectors, where smaller Lambda is longer deformation vectors. For rigid registration, Lambda should be large.
-g (Gamma)	0.5	Defines the randomness of point matching at the start of optimization. A higher Gamma is more tolerant of mismatches, in case of outliers in the point clouds.
-J	300	#Nystrom samples for computing G, the Gram matrix of pairwise similarities.
-K	70	#Nystrom samples for computing P, the uncertainty matrix.
-f	0.3	The value of sigma where the KD tree search is turned on.
-D	b, 20000, 0.02	Downsampling. b=apply for both datasets; number of points extracted by downsampling; voxel size of downsampling.
-u	y	Normalisation of both models using the location and scale of the source data, model Y. Normalisation improves numerical stability by making sure that both models have the same scale.
-c	1e-6	Convergence tolerance. Determines until when convergence should be optimized.
-n	500	The maximum number of iterations.

BCPD ensures that corresponding points do not need to be strictly one-to-one, making it more adaptable to variations in bone morphology and partial data sets, such as those obtained from CT or MRI scans [49].

BCPD employs multiple acceleration methods to speed up the registration process [49]. The first is the Nyström method which is used to approximate large kernel matrices efficiently by reducing the number of points. Another acceleration method is the k-dimensional tree (KD-tree) search. A KD-tree organises points hierarchically which means that nearest-neighbour searching is only done for points close to each other, speeding up the process of computing distances. The third is downsampling. By downsampling the number of data points, fewer computations have to be performed, speeding up convergence.

3.2 Methods

3.2.1 Adapting BCPD

The BCPD Github repository consists of the base code which is the backbone of the computations, and several demo scripts which are used to run the computations. The complete repository was downloaded and the demo scripts for rigid registration were used as a template to base the BCPD 3D registration method on.

The registration of BCPD is controlled by sev-

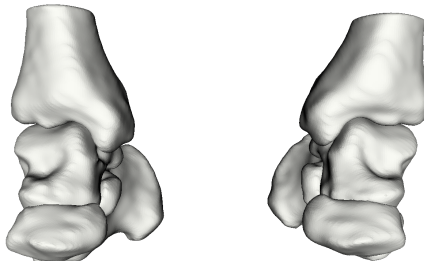


Figure 18: STL model of the ankle. Created by combining all segments into one.

eral user-determined parameters (Table 3). In order to find the optimal parameters for hindfoot 3D registration using BCPD, three parameters were varied and the best were used. The number of points used for downsampling was tried for 10000, 20000, and 30000. Gamma was tried for 0.1, 0.5, 1.0 and 2.0. Beta was tried for 0.5, 1.0, 2.0, and 5.0. These three parameters were varied as they influence the accuracy of registration more than the other parameters which were set as standard settings. Chapter 3.3.1 explains why the values in Table 3 were used.

To this end, the bone segments of the first 20 CT scan from the Fischer database [42] were exported as one STL model (Figure 18), resulting in 20 bone models. A Matlab script was written which applied an arbitrarily chosen prescribed transformation to the STL models and computed the 3D registration.

For all 48 combinations of parameters, the following process was applied:

1. The STL model was converted into point cloud data and transformed with a rotation of $3^\circ \alpha$, $14^\circ \beta$ and $-20^\circ \gamma$ (axes z, y, and x, respectively), and a translation of 14 mm x, -45 mm y and 7.5 mm z.
2. BCPD 3D registration of the transformed point cloud over the original point cloud.
3. The translation output was denormalised (Appendix B.1.1) and the translation vector $\vec{t} = (x, y, z)$ was obtained.
4. The rotation vector $\vec{r} = (\alpha, \beta, \gamma)$ with Euler angles was obtained from the rotation matrix R (Appendix B.1.2).
5. The translation and rotation along each axis was calculated.

The mean absolute error was used to determine the best combination of parameters. The mean absolute error is computed using Equation 2 [51], where y_i is the prescribed translation or rotation value for bone i , and y_r is the translation or rotation value computed by the registration. The absolute value of the difference of y_i and y_r is summed for each instance and then the mean is computed by dividing by the total number of bones N .

$$MAE = \frac{1}{N} \sum_{i=1}^N |y_i - y_r| \quad (2)$$

3.2.2 3D registration of separate bones for joint range of motion

For joint 3D registration, each segment of the Fischer database was exported as a separate STL model. This resulted in 8 STL models per segmentation: TibiaR, TibiaL, TalusR, TalusL, CalcaneusR, CalcaneusL, NavicularR, and NavicularL. Separate translations and rotations were prescribed to each bone, see Table 4 and Table 5.

They are derived from the hindfoot ROM found by Imai et al. [2], with the tibia held stationary. Both dorsiflexion and plantarflexion motion were simulated in this test. 3D registration was performed and the translation and rotation vectors of the bones were obtained. The

translation and rotation vectors of the joints were computed by subtracting the vectors of one bone from the vectors of the other: $\vec{t}_{TT} = \vec{t}_{tal} - \vec{t}_{tib}$ and $\vec{r}_{TT} = \vec{r}_{tal} - \vec{r}_{tib}$, with TT=tibiotalar joint, tal=talus, and tib=tibia. This was also done for talocalcaneal = calcaneus - talus; and talonavicular = navicular - talus.

Table 4: Prescribed translations for each bone.

A Dorsiflexion of the ankle			
Bone	x ^a (in mm)	y ^b (in mm)	z ^c (in mm)
Tibia	0	0	0
Talus	-0.4	1.9	1.5
Calcaneus	-0.4	-5.9	-2.8
Navicular	-3.7	-1.4	9.2

B Plantarflexion of the ankle			
Bone	x ^a (in mm)	y ^b (in mm)	z ^c (in mm)
Tibia	0	0	0
Talus	-0.6	4.2	-3.5
Calcaneus	3.2	17.2	15.5
Navicular	-5.6	18.8	-16.6

^aMovement along the x-axis. This corresponds with medial (+) and lateral (-) motion.

^bMovement along the y-axis. This corresponds with posterior (+) and anterior (-) motion.

^cMovement along the z-axis. This corresponds with proximal (+) and distal (-) motion.

Table 5: Prescribed rotation angles for each bone.

A Dorsiflexion of the ankle			
Bone	α^a (in °)	β^b (in °)	γ^c (in °)
Tibia	0	0	0
Talus	15.9	5.2	7.3
Calcaneus	16.7	4.3	6.5
Navicular	17.2	3.2	7.4

B Plantarflexion of the ankle			
Bone	α^a (in °)	β^b (in °)	γ^c (in °)
Tibia	0	0	0
Talus	-41.3	-14.1	3.4
Calcaneus	-42.0	-14.1	2.5
Navicular	-48.1	-13.2	-0.2

^aAngle α is along the z-axis of rotation. This motion corresponds with dorsiflexion (+) and plantarflexion (-).

^bAngle β is along the y-axis of rotation. This motion corresponds with abduction (+) and adduction (-).

^cAngle γ is along the x-axis of rotation. This motion corresponds with eversion (+) and inversion (-).

3.2.3 Robustness test

The final test that was performed for the 3D registration was to test robustness. The complete hindfoot registration and joint registration tests used a single segment model which was digitally transformed into another position. However, if the registration is to be performed for real life ankle ROM, the models are from separate segments from separate CT scans from the same patient. Unfortunately, it was not possible to obtain multiple CT scans from the same patient. However, during testing of the nnU-Net Ankle segmentation model and the nnU-Net TAA segmentation model in chapter 2, multiple segmentations were made of the same CT scan (2D, 3D, ens, and ensPP). These segmentations were used to test the robustness of the BCPD 3D registration algorithm as each segmentation model differed in small structural details.

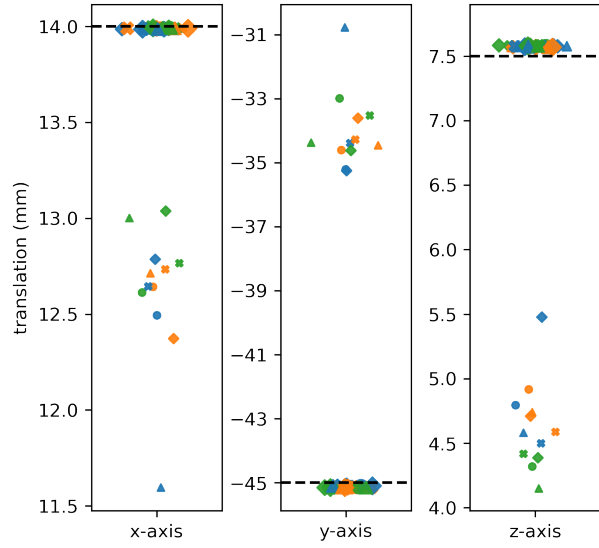
For this test, no transformations were prescribed, and the results should reflect that. The translation and rotation vectors should be $\vec{t} = (0, 0, 0)$ and $\vec{r} = (0, 0, 0)$. The registration was performed between each configuration of each scan, resulting in 6 registration processes per scan: 2d to 3d, 2d to ens, 2d to ensPP, 3d to ens, 3d to ensPP, and ens to ensPP. The translation and rotation vectors were computed.

Established and validated bone 3D registration methods such as the Volume Merge are accurate with a mean absolute translation error of 0.1 mm and a mean absolute rotation error of 0.2°. The BCPD algorithm is deemed "robust" if the mean absolute errors for the respective motion are smaller than 0.1 mm and 0.2°.

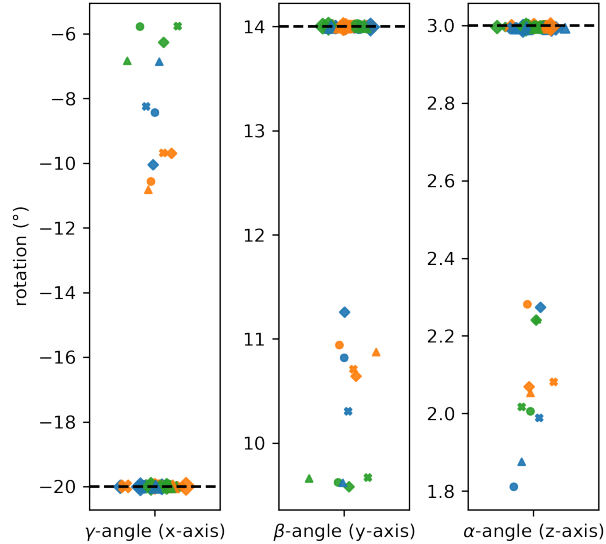
3.3 Results

3.3.1 Parameter search

The parameter search was performed using 20 ankle bone models which were 3D registered from a neutral position to a prescribed transformed position, for 48 combinations of values for the number of points used for downsampling, Gamma, and Beta. The mean absolute error was computed for each combination of parameters in all three axes of translation and rotation. The combination of parameters with the smallest mean absolute error in both translation and rotation is D=20000, Gamma=0.5, and Beta=1.0. The mean absolute



(a) Mean translations of every combination



(b) Mean rotations of every combination

Figure 19: Scatterplots of the mean translations and rotations for all 48 combinations. The black striped line is the prescribed value of the axis. D = number of points used for downsampling.

translation errors are 0.0139 mm, 0.1661 mm, and 0.0737 mm in the x, y, and z-axis, respectively. The mean absolute rotation errors are 0.0239°, 0.0093°, and 0.0132°, for angles γ in the x-axis, β in the y-axis, and α in the z-axis, respectively.

Unpaired t-tests were performed to test for

significant differences between the mean absolute errors in the translational and rotational axes. The null hypothesis stated that there were no significant differences between the mean absolute errors of the axes. The mean absolute transla-

tion errors of all axes differ significantly from each other, with a confidence interval of 95%. The mean absolute rotation errors of the x and z-axis, and the x and y-axis differ significantly from each other, with a confidence interval of 95%.

Table 6: Joint translation results

A Dorsiflexion of the ankle								
Joint	x (mm)		y (mm)		z (mm)		Ref	MAE
	Mean	± SD	Mean	± SD	Mean	± SD		
TibioTalar_L	-0.37	± 0.049	-0.4	1.90 ± 0.020	1.9	1.55 ± 0.115	1.5	0.0359
TibioTalar_R	-0.38	± 0.037	-0.4	1.90 ± 0.016	1.9	1.51 ± 0.063	1.5	0.0270
TaloCalcaneal_L	-0.01	± 0.017	0.0	-7.91 ± 0.066	-7.8	-4.30 ± 0.012	-4.3	0.0460
TaloCalcaneal_R	0.06	± 0.061	0.0	-7.82 ± 0.070	-7.8	-4.28 ± 0.021	-4.3	0.0512
TaloNavicular_L	-3.31	± 0.017	-3.3	-3.32 ± 0.010	-3.3	7.70 ± 0.013	7.7	0.0139
TaloNavicular_R	-3.30	± 0.008	-3.3	-3.30 ± 0.010	-3.3	7.71 ± 0.010	7.7	0.0080

B Plantarflexion of the ankle								
Joint	x (mm)		y (mm)		z (mm)		Ref	MAE
	Mean	± SD	Mean	± SD	Mean	± SD		
TibioTalar_L	-0.57	± 0.051	-0.6	4.21 ± 0.031	4.2	-3.46 ± 0.114	-3.5	0.0379
TibioTalar_R	-0.58	± 0.046	-0.6	4.22 ± 0.021	4.2	-3.50 ± 0.061	-3.5	0.0329
TaloCalcaneal_L	4.05	± 0.148	3.8	13.79 ± 0.630	13.0	19.03 ± 0.060	19.0	0.3636
TaloCalcaneal_R	3.80	± 0.113	3.8	14.04 ± 0.647	13.0	19.08 ± 0.074	19.0	0.4047
TaloNavicular_L	-5.09	± 0.112	-5.0	15.11 ± 0.512	14.6	-13.16 ± 0.078	-13.1	0.2252
TaloNavicular_R	-5.24	± 0.134	-5.0	15.32 ± 0.501	14.6	-13.18 ± 0.077	-13.1	0.3356

Table 7: Joint rotation results

A Dorsiflexion of the ankle								
Joint	γ -angle (°)		β -angle (°)		α -angle (°)		Ref	MAE
	Mean	± SD	Ref	Mean	± SD	Ref	Mean	± SD
TibioTalar_L	7.31	± 0.092	7.3	5.33 ± 0.276	5.2	16.02 ± 0.554	15.9	0.1777
TibioTalar_R	7.28	± 0.119	7.3	5.26 ± 0.264	5.2	15.89 ± 0.568	15.9	0.1680
TaloCalcaneal_L	-0.99	± 0.227	-0.8	-0.82 ± 0.346	-0.9	0.96 ± 0.227	0.8	0.2495
TaloCalcaneal_R	-1.03	± 0.362	-0.8	-1.22 ± 0.392	-0.9	0.80 ± 0.321	0.8	0.3509
TaloNavicular_L	0.11	± 0.051	0.1	-2.15 ± 0.254	-2.0	1.40 ± 0.210	1.3	0.0970
TaloNavicular_R	0.11	± 0.089	0.1	-2.05 ± 0.265	-2.0	1.41 ± 0.212	1.3	0.0886

B Plantarflexion of the ankle								
Joint	γ -angle (°)		β -angle (°)		α -angle (°)		Ref	MAE
	Mean	± SD	Ref	Mean	± SD	Ref	Mean	± SD
TibioTalar_L	3.39	± 0.123	3.4	-14.10 ± 0.245	-14.1	-40.97 ± 0.746	-41.3	0.2298
TibioTalar_R	3.36	± 0.108	3.4	-14.17 ± 0.202	-14.1	-41.06 ± 0.679	-41.3	0.1950
TaloCalcaneal_L	-1.13	± 0.284	-0.9	0.33 ± 0.394	0.0	-0.68 ± 0.346	-0.7	0.3168
TaloCalcaneal_R	-0.60	± 0.190	-0.9	0.39 ± 0.318	0.0	-0.66 ± 0.299	-0.7	0.3184
TaloNavicular_L	-3.57	± 0.086	-3.6	0.88 ± 0.222	0.9	-6.91 ± 0.257	-6.8	0.0900
TaloNavicular_R	-3.57	± 0.080	-3.6	0.99 ± 0.207	0.9	-6.94 ± 0.256	-6.8	0.0886

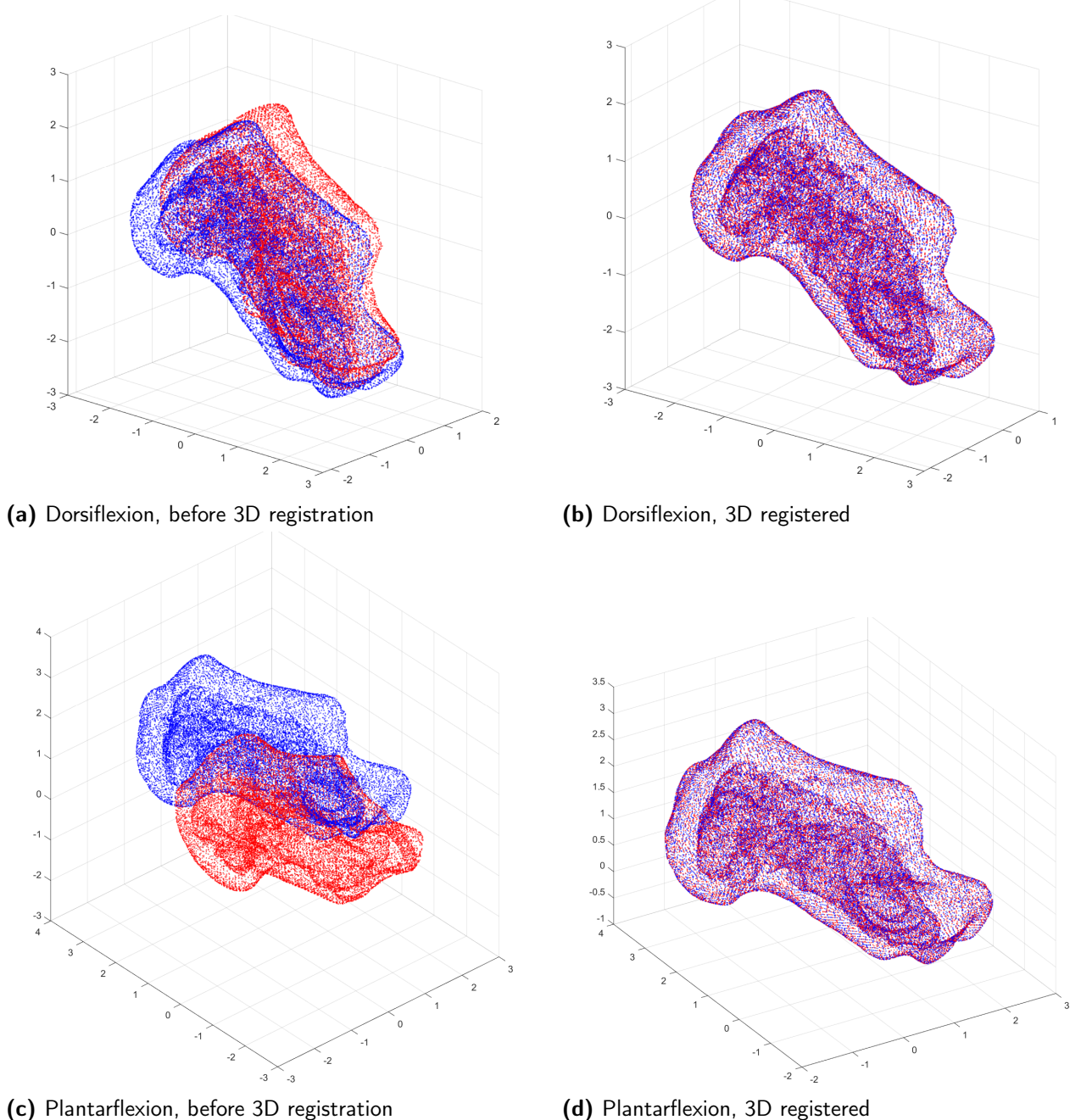


Figure 20: 3D registration of the left calcaneus in dorsiflexion and plantarflexion.

3.3.2 Accuracy of joint 3D registration

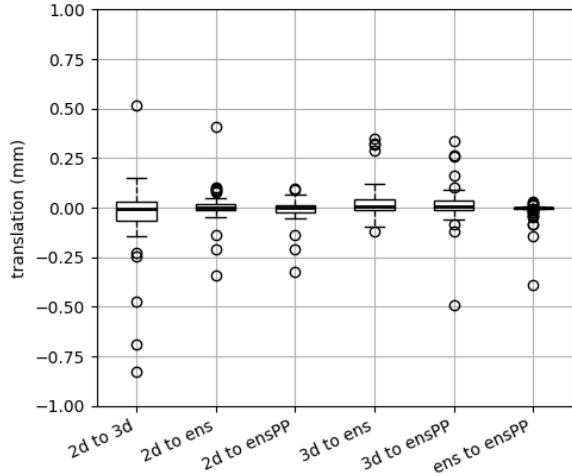
3D registration for hindfoot joints was tested by prescribing physiological translations and rotations to the bone models, 3D registering the bone models, and deriving the joint translation and rotation. The results of the test are shown in Tables 6 and 7. The smallest mean absolute translation error in plantarflexion is a factor 4.1 larger than in dorsiflexion (0.0080 mm dorsiflexion, 0.0329 mm plantarflexion), whereas the largest mean abso-

lute translation error in plantarflexion is a factor 7.9 larger than in dorsiflexion (0.0512 mm dorsiflexion, 0.4047 mm plantarflexion).

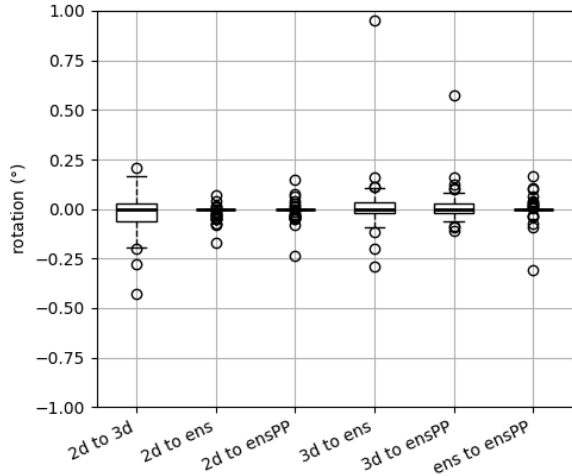
The smallest mean absolute rotation error in plantarflexion the same as in dorsiflexion (0.0886° dorsiflexion, 0.0886° plantarflexion), whereas the largest mean absolute rotation error in plantarflexion is a factor 1.1 smaller than in dorsiflexion (0.3509° dorsiflexion, 0.3184° plantarflexion).

The mean absolute translation errors are com-

parable with those found for the parameter search with the y-axis of plantarflexion showing the greatest error (Table 11). Interestingly, the mean absolute rotation errors are larger than for the parameter search, in both dorsiflexion and plantarflexion.



(a) Mean computed translations



(b) Mean computed rotations

Figure 21: Robustness test: BCPD mean computed translations and rotations for each model configuration combination.

3.3.3 Robustness test

The robustness test was performed to determine whether the BCPD 3D registration algorithm could register differently segmented bone models from the same CT scan with mean absolute errors smaller than 0.1mm in translation and 0.2° in rotation. The mean computed translations and rotations of the 3D registration robustness test are shown in Figure 21. The mean absolute

translation errors are 0.0462 mm, 0.0546 mm, and 0.1051 mm in the x, y, and z-axes, respectively. The mean absolute rotation errors are 0.0625°, 0.0491°, and 0.0708°, for angles γ in the x-axis, β in the y-axis, and α in the z-axis, respectively.

3.4 Discussion

The first goal of this chapter was to adapt the BCPD algorithm for rigid registration of the hindfoot and this was done by performing a parameter search using the complete hindfoot for registration. The second goal was to test the accuracy of 3D registration of separate joints. The third goal was to test the robustness of the algorithm.

3.4.1 Major findings for the parameters search

Translation along the x-axis has the smallest mean absolute error. The mean absolute translation errors in the y and z-axis a factor 11.9 and 5.3 larger. The significant differences between the mean absolute errors of the axes mean that the null hypothesis is rejected. Translation in the y-axis is computed with more error than in the x-axis and in the z-axis, and translation in the z-axis is computed with more error than in the x-axis. The CT scans from which the bone models originate have a different resolution in the z-axis than in the x and y-axis. This resolution was not used to scale the 3D models as that would create large differences in mean absolute error between the axes. The z-axis would have a much larger mean absolute translation error due to the scale of the z-axis being on average half of x and y. However, for real-life range of motion research, the translation vector should be scaled with the resolution of the CT scan to convert the distances from voxel spacings to millimetres.

Rotation along the y-axis (β) has the smallest mean absolute error. The mean absolute rotation errors in the x and z-axis (γ and α respectively) are a factor 2.6 and 1.4 higher. The significant differences between the mean absolute rotation errors of the x and y-axis, and between the x and z-axis mean that the null hypothesis is rejected. Rotation in the x-axis is computed with more error than in the y-axis and z-axis.

In the study by Ochiai et al. about the vol-

ume merge, the mean absolute translation error was less than 0.1 mm in x-direction and z-direction [46]. The mean absolute rotation error was less than 0.2° about x-axis and z-axis [46]. This means that the BCPD 3D registration of the complete hindfoot is more accurate in translation in the x-direction but less in the z-direction, and more accurate in rotation in all axes than the volume merge method.

3.4.2 Major findings testing the accuracy of 3D registration of separate joints

The TibioTalar joint translation is computed with the smallest mean absolute error in plantarflexion. This makes sense because only the talus was translated with the tibia remaining stationary. For the TaloCalcaneal and TaloNavicular joints, both bone models in the joint were translated. This adds another level of uncertainty to the 3D registration, causing the higher errors.

The large difference in mean absolute translation errors between dorsiflexion and plantarflexion for every joint apart from the TibioTalar joint is ambiguous. The prescribed translations in plantarflexion were larger than in dorsiflexion (Table 4), but not a factor 7.9. Figure 20 shows that the distances in plantarflexion are larger, but convergence still happens with a good fit.

The mean absolute rotation errors are comparable for each joint and between dorsiflexion and plantarflexion. It is interesting that similar differences between dorsiflexion and plantarflexion as for translation were not found for rotation.

3.4.3 Major findings of the robustness test

The goal of the robustness test was to check if different segmentation models from the same bone from the same scan (and thus the same patient) could still be accurately registered. Figure 21a and b show that both translation and rotation are computed about 0 mm and 0°, respectively. The mean absolute translation errors are smaller than 0.1 mm, which means that BCPD 3D registration is robust in translation.

The mean absolute rotation errors are all smaller than 0.1°. The BCPD 3D registration algorithm is robust enough to handle different segmentation models of the same patient.

3.4.4 Limitations

Several limitations within this chapter must be acknowledged. First, the study was constrained by the unavailability of multiple CT scans from the same patient. Consequently, rigid transformations had to be artificially applied to a single segmented bone model to simulate relative joint motion. While this approach allowed for controlled experimentation, it does not fully replicate the anatomical variability and physiological motion patterns present in real-world data, thereby limiting the real-world validity of the results.

Second, the absence of a physical phantom for imaging precluded the possibility of ground-truth validation under controlled conditions. This phantom should represent a single bone which could be moved with a known translation and rotation prior to being scanned. The addition of a phantom experiment provides a step between the digital validation performed in this chapter and cadaver testing.

Lastly, the implementation of the Bayesian Coherent Point Drift (BCPD) algorithm was hindered by insufficient documentation and a lack of clarity regarding parameter definitions on the GitHub repository. This meant that the optimisation of the BCPD parameters was a rigorous trial-and-error process rather than being based on theory.

3.4.5 Future work

In this chapter, the BCPD 3D registration was tested and validated by prescribing a transformation to a point cloud bone model and registering the same model from the same scan. However, in reality a CT scan would be made for each position of the foot, and then the bone model from scan 1 would be registered over the bone model from scan 2. These scans are different, have a different segmentation, and the applied translation and rotation are not prescribed. Therefore, to test the methodology described in chapter 2 and 3, a cadaver study should be performed. At least two lower leg (knee to toe) cadavers would be needed to study the use of the 3D Foot Plate with both feet in the CT scan. 5 CT scans would be made of the cadavers, using the 3D Foot Plate to place the feet in neutral position, extreme dorsiflexion, extreme plantarflexion, extreme eversion, and extreme inversion. This would be done with

and without the Infinity TAS implanted. This study would serve as a verification of the complete methodology prior to performing the research of the METC application in chapter 4.

3.5 Conclusion

The BCPD 3D registration algorithm shows comparable translation errors and smaller rotation errors than existing point cloud 3D registration algorithms. BCPD 3D registration is prone to

errors caused by differences in scale of the x, y, and z coordinates of digital bone models. 3D registration of bones to compute joint translation is prone to errors due to large translations. The BCPD 3D registration is able to compute the 3D registration of differently segmented digital models of the same patient with mean absolute translation errors smaller than 0.1 mm and mean absolute rotation errors smaller than 0.2°, making it robust.

4 Development of an METC application for medical hindfoot ROM analysis

4.1 Introduction

To study the influence of gutter impingement of the Infinity TAS on ankle and hindfoot range of motion, research should be performed with human subjects who have received the Infinity TAS as treatment for end-stage ankle arthritis. This research will be performed at the MUMC+ in collaboration with the department of Orthopaedic Surgery and the department of Radiology.

4.2 Research protocol

The research described in this chapter will be performed after the finalisation of this thesis and will therefore apply the methods of chapters 2 and 3 to study the range of motion of the hindfoot after total ankle arthroplasty.

4.2.1 Objectives

The objective of the study is to determine quantitatively, via a 3D CT-stress test, how impingement of the Infinity Total Ankle System (TAS) influences the range of motion of the hindfoot.

The secondary objectives are as follows:

- Determine whether the range of motion of the hindfoot is influenced by a change in the surgical placement of the Infinity TAS to prevent gutter impingement,
- Determine the influence of the Infinity TAS on the range of motion of the hindfoot as compared to the healthy contralateral ankle,
- Determine whether there is loosening of the Infinity TAS components.

4.2.2 Study design

The research is a case-control study comparing the hindfoot range of motion between patients with impingement of the Infinity TAS and patients without impingement. The study will involve human subjects with a history of ankle arthritis and who have had arthroplasty with the

Infinity TAS. To this end, patients with a single-sided implant and otherwise healthy contralateral ankle will be asked to participate in the study. The inclusion criteria for the study are:

- Implantation of the Infinity Total Ankle System: to ensure focus on this specific implant.
- At least 1-year post-surgery to allow for acquaintance with the implant and sufficient integration of the implant.
- Half of subjects must present clinical and/or radiographic evidence of gutter impingement.
- Other half of subjects must not have clinical or radiographic evidence of gutter impingement.
- Subject must provide informed consent to participate.

The exclusion criteria include inability to travel to MUMC+ and previous revision surgery of the Infinity TAS.

The in- and exclusion criteria were based on academic and medical relevance to the study and feasibility for the patients to participate.

The sample size of the study is based on meta-analysis by Hermus et al. [52]. The incidence of impingement for implanted Infinity TASs is approximately 6%. Given that approximately 50 TAA surgeries have been performed at the MUMC+ since 2017, this gives an initial sample size of 3. However, a sample size of 3 may not provide sufficient precision or statistical power for meaningful conclusions due to being highly susceptible to variability. An increased sample size of 10 improves robustness of the study and ensures more reliable results for the impingement cases. As the number of subjects in both groups should be equal, 10 patients without impingement will be included, giving a total number of 20 subjects.

4.2.2.1 CT acquisition

The study requires CT scans of the foot in five different positions: neutral, extreme dorsiflexion, extreme plantarflexion, extreme eversion, and extreme inversion. The 3D Foot Plate, described in Chapter 1.6, is used to place and hold the foot in the required position during CT acquisition. CT scan acquisition is performed with the protocol in Appendix C, C1: Research Protocol, APPENDIX A: Computer Tomography Protocol. The subjects will be exposed to a total radiation dose of 0.55 mSv on their ankles which is a low risk level. The subjects will be scanned during a maximum of 20 minutes which includes changing the foot position between scans.

4.2.2.2 CT segmentation and 3D registration

The CT scans are segmented with the nnU-Net TAA segmentation model for the bones and manual segmentation with a 2500 HU threshold of the implant components (chapter 2.2.2). 3D registration is performed on each joint (chapter 3.2.2) for each of the three secondary objectives: impingement vs. no impingement, Infinity TAS vs. contralateral ankle, and implant component vs. attached bone. In case the data is normally distributed, unpaired t-test will be performed for the impingement vs. no impingement study parameters. For the other two test groups, paired t-tests will be performed as they concern different conditions within the same group of subjects. In case the data is not normally distributed, Mann-Whitney U tests are performed for the first study parameters, and Wilcoxon signed-rank tests are performed for the two other groups. A complete overview of the studied parameters can be found in Appendix C, C1: Research Protocol, 9. STATISTICAL ANALYSIS.

4.3 METC application process

As human subjects will take part in the research, a research application conforming to the Medical Research Involving Human Subjects Act (WMO) must be created and submitted to the Medical Research Ethics Committee (Medisch-ethische Toetsingscommissie, or METC, in Dutch). In order to carry out this research, several documents should be submitted to gain approval from the

METC. The information about what these documents should include is provided by the Central Committee on Research Involving Human Subjects (Centrale Commissie Mensgebonden Onderzoek, or CMMO, in Dutch).

- A1: Letter of correspondence. Addressed to the members of the METC, introducing the application.
- B1: ABR form. Includes information regarding the type of research that is to be performed.
- C1: Research protocol. The research protocol describes the whole research process, study population, the use of medical devices, safety and risk analysis, and ethical considerations. The complete C1 Research protocol can be found in Appendix ??.
- D2: IMDD. In case a new investigational medical device is used, the IMDD, information about the device's use and risk analysis, should be included.
- E1/E2: Patient information and participation permission form. This is sent to patients who fall under the set study population criteria, asking them to participate in the study.
- F1: Questionnaires. Patients could be presented with questionnaires regarding their quality of life and experience with the Infinity TAS.
- G1: Insurance certificate. This includes the hospital's insurance and patient insurance.
- H: CV's of independent expert and coordinating investigator.
- I3: CV's of participating investigators
- K6: Letter of approval of radiation use by the Radiation Protection Unit (Stralingsbeschermingseenheid, or SBE, in Dutch).

Through the course of seven months, the research methodology was developed and the METC application was written. The first meeting in the MUMC+ with surgeons Joris Hermus and Martijn Poeze took place on 23-08-2024. After this meeting, writing the C1 research protocol

started and the research methodology was developed.

On 17-12-2024, the complete application was sent to the Orthopaedics Trial Office for feedback and submission to the METC. Unfortunately, as of now, the application has not been submitted to the METC.

4.4 Limitations throughout the application process

This chapter, although short, enveloped a long process of writing and improving the METC application. At the start of the process, there was hope of the application being submitted in late October, and approved in early to late January. If that was achieved, one or two patients could have participated in the study, and their hind-foot ROM could have been analysed within this thesis. Unfortunately, this did not happen due to a number of reasons.

As this research will be performed at the MUMC+, various agreements needed to be made with people from both the department of Orthopaedic Surgery and the department of Radiology. The doctors, naturally, have a very busy schedule which creates difficulties when making appointments, which slows down the process. However, a more pro-active approach should have been applied to make sure that this was not as much of a limiting factor.

Furthermore, due to strict rules by the CCMO

about research involving human subjects, every document in the application should be carefully written to avoid being turned down by the METC.

Once the research protocol was finished, the department of Radiology had to give permission to make CT scans of patients with the calculated radiation dose. This required a quotation from the Imaging department about the costs of the CT scans, and a research number provided by the Orthopaedics Trial Office. However, due to a large workload for both parties, more than a month passed between the quotation request and receiving the letter for the approval of radiation on subjects.

4.5 Next steps

Once the METC have approved the research, the first step is to invite patients who comply with the inclusion criteria to participate in the study. As soon as the participating patients are known, appointments for the CT scans should be made in collaboration with Radiology, and patients can be scanned according to the scan protocol in chapter 4.2.2.1. Then, study parameters are computed according to chapter 4.2.2.2.

This research aims to expand the knowledge about the workings of the Infinity TAS and how quality of life and performance of the implant can be improved through improved surgery.

References

- [1] S. Angin and I. Demirbüken, “Ankle and foot complex,” in *Comparative Kinesiology of the Human Body: Normal and Pathological Conditions*, pp. 411–439, Academic Press, 2020.
- [2] K. Imai, D. Tokunaga, R. Takatori, K. Ikoma, M. Maki, H. Ohkawa, A. Ogura, Y. Tsuji, N. Inoue, and T. Kubo, “In vivo three-dimensional analysis of hindfoot kinematics,” *Foot and Ankle International*, vol. 30, pp. 1094–1100, 11 2009.
- [3] “Tarsal Coalition - OrthoInfo - AAOS.”
- [4] M. Glazebrook, T. Daniels, A. Younger, C. J. Foote, M. Penner, K. Wing, J. Lau, R. Leighton, and M. Dunbar, “Comparison of health-related quality of life between patients with end-stage ankle and hip arthroscopy,” *The Journal of bone and joint surgery. American volume*, vol. 90, no. 3, pp. 499–505, 2008.
- [5] A. Barg, G. I. Pagenstert, T. Hügle, M. Gloyer, M. Wiewiorski, H. B. Henninger, and V. Valderrabano, “Ankle osteoarthritis: Etiology, diagnostics, and classification,” 2013.
- [6] V. Valderrabano, M. Horisberger, I. Russell, H. Dougall, and B. Hintermann, “Etiology of ankle osteoarthritis,” *Clinical Orthopaedics and Related Research*, vol. 467, no. 7, pp. 1800–1806, 2009.
- [7] C. L. Saltzman, M. L. Salamon, G. M. Blanchard, T. Huff, A. Hayes, J. A. Buckwalter, and A. Amendola, “Epidemiology of Ankle Arthritis: Report of a Consecutive Series of 639 Patients from a Tertiary Orthopaedic Center,” *The Iowa Orthopaedic Journal*, vol. 25, p. 44, 2005.
- [8] M. Horisberger, V. Valderrabano, and B. Hintermann, “Posttraumatic ankle osteoarthritis after ankle-related fractures,” *Journal of Orthopaedic Trauma*, vol. 23, pp. 60–67, 1 2009.
- [9] M. T. Gross, V. S. Mercer, and F. C. Lin, “Effects of foot orthoses on balance in older adults,” *Journal of Orthopaedic and Sports Physical Therapy*, vol. 42, no. 7, pp. 649–657, 2012.
- [10] G. H. Saito, A. E. Sanders, C. de Cesar Netto, M. J. O’Malley, S. J. Ellis, and C. A. Demetracopoulos, “Short-Term Complications, Reoperations, and Radiographic Outcomes of a New Fixed-Bearing Total Ankle Arthroplasty,” *Foot and Ankle International*, vol. 39, pp. 787–794, 7 2018.
- [11] S. Fuchs, C. Sandmann, A. Skwara, and C. Chylarecki, “Quality of life 20 years after arthrodesis of the ankle. A study of adjacent joints,” *The Journal of bone and joint surgery. British volume*, vol. 85, pp. 994–998, 9 2003.
- [12] A. L. Lenz, J. A. Nichols, K. E. Roach, K. B. Foreman, A. Barg, C. L. Saltzman, and A. E. Anderson, “Compensatory Motion of the Subtalar Joint Following Tibiotalar Arthrodesis: An in Vivo Dual-Fluoroscopy Imaging Study,” *The Journal of Bone and Joint Surgery. American Volume*, vol. 102, p. 600, 4 2020.
- [13] C. A. Demetracopoulos, J. P. Halloran, P. Maloof, S. B. Adams, and S. G. Parekh, “Total ankle arthroplasty in end-stage ankle arthritis,” *Current Reviews in Musculoskeletal Medicine*, vol. 6, pp. 279–284, 7 2013.
- [14] H. G. Jung, S. H. Lee, M. H. Shin, D. O. Lee, J. S. Eom, and J. S. Lee, “Anterior Heterotopic Ossification at the Talar Neck after Total Ankle Arthroplasty,” *Foot and Ankle International*, vol. 37, pp. 703–708, 7 2016.
- [15] R. M. Queen, J. C. De Biassio, R. J. Butler, J. K. DeOrio, M. E. Easley, and J. A. Nunley, “Changes in pain, function, and gait mechanics two years following total ankle arthroplasty performed with two modern fixed-bearing prostheses,” *Foot and Ankle International*, vol. 33, pp. 535–542, 7 2012.

- [16] J. Kim and C. Demetracopoulos, "Outcomes of Total Ankle Arthroplasty After Reoperation due to Gutter Impingement," *Foot and ankle clinics*, vol. 29, pp. 111–122, 3 2024.
- [17] Stryker, "Infinity."
- [18] S. B. Mani, H. Do, E. Vulcano, M. V. Hogan, S. Lyman, J. T. Deland, and S. J. Ellis, "Evaluation of the foot and ankle outcome score in patients with osteoarthritis of the ankle," *The bone & joint journal*, vol. 97-B, pp. 662–667, 5 2015.
- [19] V. Valderrabano, B. Hintermann, B. M. Nigg, D. Stefanyshyn, and P. Stergiou, "Kinematic Changes after Fusion and Total Replacement of the Ankle Part 1: Range of Motion," *Foot and Ankle International*, vol. 24, no. 12, pp. 881–887, 2003.
- [20] M. Sokolowski, N. Krähenbühl, C. Wang, L. Zwicky, C. Schweizer, T. Horn Lang, and B. Hintermann, "Secondary Subtalar Joint Osteoarthritis Following Total Ankle Replacement," *Foot and Ankle International*, vol. 40, pp. 1122–1128, 10 2019.
- [21] M. A. Prissel, J. L. Daigre, M. J. Penner, and G. C. Berlet, "INFINITY® total ankle system," *Primary and Revision Total Ankle Replacement: Evidence-Based Surgical Management*, pp. 75–87, 1 2015.
- [22] C. J. Van Bergen, G. J. Tuijthof, M. Maas, I. N. Sierevelt, and C. N. Van Dijk, "Arthroscopic accessibility of the talus quantified by computed tomography simulation," *The American journal of sports medicine*, vol. 40, pp. 2318–2324, 10 2012.
- [23] J. A. Nichols, K. E. Roach, N. M. Fiorentino, and A. E. Anderson, "Subject-Specific Axes of Rotation Based on Talar Morphology Do Not Improve Predictions of Tibiotalar and Subtalar Joint Kinematics," *Annals of Biomedical Engineering*, vol. 45, pp. 2109–2121, 9 2017.
- [24] L. Beimers, G. J. Maria Tuijthof, L. Blankevoort, R. Jonges, M. Maas, and C. N. van Dijk, "In-vivo range of motion of the subtalar joint using computed tomography," *Journal of biomechanics*, vol. 41, no. 7, pp. 1390–1397, 2008.
- [25] E. Masih, "OPEN-SOURCE APPROACH FOR MEDICAL DEVICES WITHOUT BUSINESS CASE: Offering the 3D Foot Plate open source and expert opinion on MDR compliance for open-source medical devices," Master's thesis, University of Twente, 2024.
- [26] S. Minaee, Y. Boykov, F. Porikli, A. Plaza, N. Kehtarnavaz, and D. Terzopoulos, "Image Segmentation Using Deep Learning: A Survey," *IEEE Transactions on Pattern Analysis and Machine Intelligence*, vol. 44, pp. 3523–3542, 7 2022.
- [27] "Materialise Mimics," 12 2024.
- [28] "3D Slicer image computing platform," 1 2025.
- [29] M. Hershman, B. Yousefi, L. Serletti, M. Galperin-aizenberg, L. Roshkovan, J. M. Luna, J. C. Thompson, C. Aggarwal, E. L. Carpenter, D. Kontos, and S. I. Katz, "Impact of interobserver variability in manual segmentation of non-small cell lung cancer (Nsclc) applying low-rank radiomic representation on computed tomography," *Cancers*, vol. 13, p. 5985, 12 2021.
- [30] D. S. Carmo, A. A. Pezzulo, R. A. Villacreses, M. L. Eisenbeisz, R. L. Anderson, S. E. V. Dorin, L. Rittner, R. A. Lotufo, S. E. Gerard, J. M. Reinhardt, and A. P. Comellas, "Manual segmentation of opacities and consolidations on CT of long COVID patients from multiple annotators," *Scientific Data*, vol. 12, p. 402, 3 2025.

- [31] N. Karunananayake, L. Lu, H. Yang, P. Geng, O. Akin, H. Furberg, L. H. Schwartz, and B. Zhao, “Dual-Stage AI Model for Enhanced CT Imaging: Precision Segmentation of Kidney and Tumors,” *Tomography*, vol. 11, p. 3, 1 2025.
- [32] S. Ghosh, N. Das, I. Das, and U. Maulik, “Understanding deep learning techniques for image segmentation,” *ACM Computing Surveys*, vol. 52, 7 2019.
- [33] M. E. Rayed, S. M. Islam, S. I. Niha, J. R. Jim, M. M. Kabir, and M. F. Mridha, “Deep learning for medical image segmentation: State-of-the-art advancements and challenges,” *Informatics in Medicine Unlocked*, vol. 47, p. 101504, 1 2024.
- [34] O. Ronneberger, P. Fischer, and T. Brox, “U-Net: Convolutional Networks for Biomedical Image Segmentation,” *Lecture Notes in Computer Science (including subseries Lecture Notes in Artificial Intelligence and Lecture Notes in Bioinformatics)*, vol. 9351, pp. 234–241, 2015.
- [35] F. Isensee, P. F. Jaeger, S. A. Kohl, J. Petersen, and K. H. Maier-Hein, “nnU-Net: a self-configuring method for deep learning-based biomedical image segmentation,” *Nature Methods 2020 18:2*, vol. 18, pp. 203–211, 12 2020.
- [36] A. S. Sandhu, “Calculating the Sørensen–Dice Coefficient: A Simplified Guide,” *Medium*, 11 2023.
- [37] J. Kok, Y. M. Shcherbakova, T. P. Schlösser, P. R. Seevinck, T. A. van der Velden, R. M. Castelein, K. Ito, and B. van Rietbergen, “Automatic generation of subject-specific finite element models of the spine from magnetic resonance images,” *Frontiers in Bioengineering and Biotechnology*, vol. 11, 2023.
- [38] F. Zhang, L. Zheng, C. Lin, L. Huang, Y. Bai, Y. Chen, and X. Luo, “A comparison of U-Net series for teeth segmentation in CBCT images,” <https://doi.org/10.1117/12.3006464>, vol. 12926, pp. 810–815, 4 2024.
- [39] E. Meyer, R. Raupach, M. Lell, B. Schmidt, and M. Kachelrieß, “Frequency split metal artifact reduction (FSMAR) in computed tomography,” *Medical physics*, vol. 39, no. 4, pp. 1904–1916, 2012.
- [40] S. Zhang, B. Jiang, and H. Shi, “A metal artifact reduction method with bone segmentation for CBCT images,” in *Journal of Physics: Conference Series*, vol. 2024, IOP Publishing Ltd, 9 2021.
- [41] M. C. M. Fischer, “Database of segmentations and surface models of bones of the entire lower body created from cadaver CT scans,” *Scientific Data*, vol. 10, 11 2023.
- [42] M. C. M. Fischer, “VSDFullBodyBoneReconstruction: Segmentations and surface models of bones of the entire lower body created from cadaver CT scans from the VSDFullBody collection,” 8 2023.
- [43] Sushmitha, M. Kanthi, V. Kedlaya K, T. Parupudi, S. N. Bhat, and S. G. Nayak, “Identification of Vertebrae in CT Scans for Improved Clinical Outcomes Using Advanced Image Segmentation,” *Signals 2024, Vol. 5, Pages 869-882*, vol. 5, pp. 869–882, 12 2024.
- [44] S. On, J. Ock, M. Bae, J. W. Park, S. H. Baek, S. Ham, and N. Kim, “Improving accuracy for inferior alveolar nerve segmentation with multi-label of anatomical adjacent structures using active learning in cone-beam computed tomography,” *Scientific Reports 2025 15:1*, vol. 15, pp. 1–10, 3 2025.
- [45] J. A. Anhaus, M. Heider, P. Killermann, C. Hofmann, and A. H. Mahnken, “A New Iterative Metal Artifact Reduction Algorithm for Both Energy-Integrating and Photon-Counting CT Systems,” *Investigative Radiology*, vol. 59, pp. 526–537, 7 2024.

- [46] R. S. Ochiai, N. Inoue, S. M. Renner, E. P. Lorenz, T.-H. Lim, G. B. J. Andersson, and H. S. An, “Three-Dimensional In Vivo Measurement of Lumbar Spine Segmental Motion,” Tech. Rep. 18, 2006.
- [47] K. Imai, K. Ikoma, M. Maki, M. Kido, Y. Tsuji, R. Takatori, D. Tokunaga, N. Inoue, and T. Kubo, “Features of hindfoot 3D kinetics in flat foot in ankle-joint maximal dorsiflexion and plantarflexion,” *Journal of Orthopaedic Science*, vol. 16, no. 5, pp. 638–643, 2011.
- [48] M. Kido, K. Ikoma, K. Imai, M. Maki, R. Takatori, D. Tokunaga, N. Inoue, and T. Kubo, “Load response of the tarsal bones in patients with flatfoot deformity: In vivo 3D study,” *Foot and Ankle International*, vol. 32, pp. 1017–1022, 11 2011.
- [49] O. Hirose, “A Bayesian Formulation of Coherent Point Drift,” *IEEE Transactions on Pattern Analysis and Machine Intelligence*, vol. 43, pp. 2269–2286, 7 2020.
- [50] A. Myronenko and X. Song, “Point set registration: Coherent point drifts,” *IEEE Transactions on Pattern Analysis and Machine Intelligence*, vol. 32, no. 12, pp. 2262–2275, 2010.
- [51] T. Nečasová, N. Burgos, and D. Svoboda, “Validation and evaluation metrics for medical and biomedical image synthesis,” in *Biomedical Image Synthesis and Simulation: Methods and Applications*, pp. 573–600, Elsevier, 1 2022.
- [52] J. P. Hermus, J. A. Voesenek, E. H. van Gansewinkel, M. A. Witlox, M. Poeze, and J. J. Arts, “Complications following total ankle arthroplasty: A systematic literature review and meta-analysis,” *Foot and Ankle Surgery*, vol. 28, pp. 1183–1193, 12 2022.

Appendices

Appendix A Results of the nnU-Net segmentation tests

A.1 nnU-Net Ankle segmentation model, accuracy

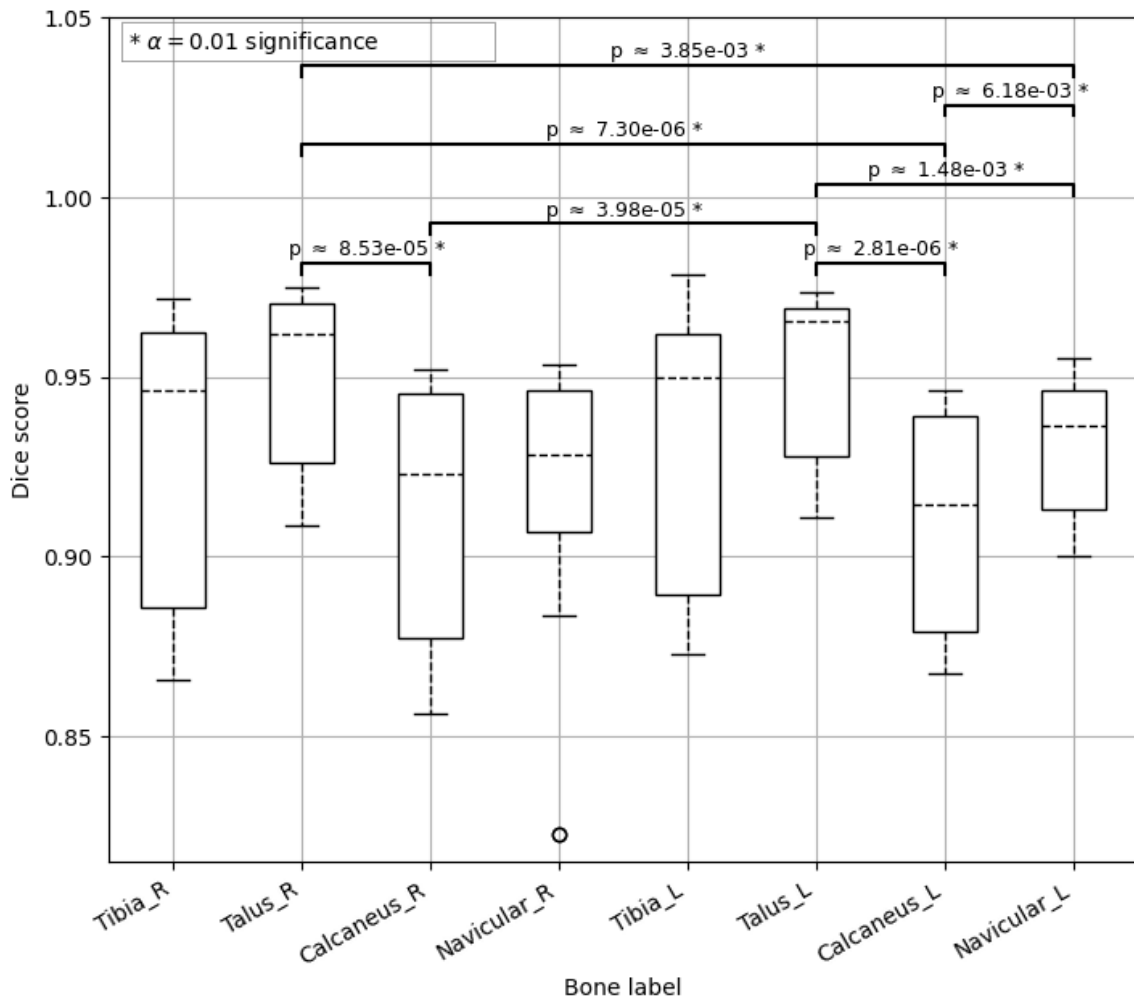


Figure 22: Test Dice scores of applied nnU-Net Ankle segmentation model per bone label

Table 8: nnU-Net Ankle segmentation model test Dice scores per bone label

Bone label	Mean	St.Dev	Median
Tibia_R	0.930	0.040	0.947
Talus_R	0.950	0.024	0.962
Calcaneus_R	0.912	0.037	0.923
Navicular_R	0.905	0.084	0.928
Tibia_L	0.933	0.038	0.950
Talus_L	0.952	0.024	0.965
Calcaneus_L	0.910	0.030	0.914
Navicular_L	0.931	0.019	0.936

A.2 nnU-Net TAA segmentation model, influence of MAR

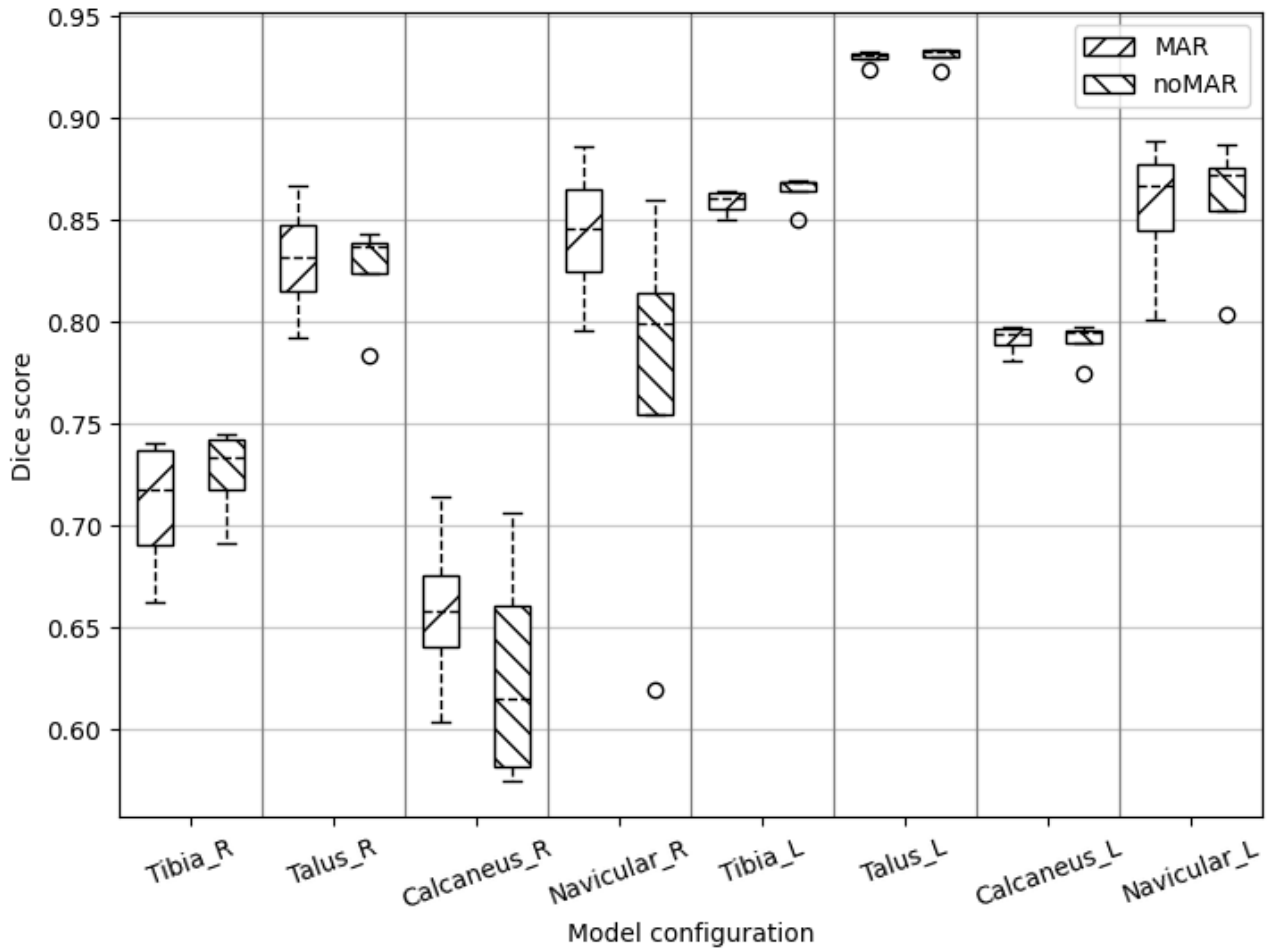


Figure 23: Test Dice scores of the applied nnU-Net TAA segmentation model per bone label, for MAR versus no MAR applied.

Table 9: nnU-Net TAA segmentation model test Dice scores per bone label, with and without MAR applied

Bone label	MAR		no MAR		U-statistic	p-value
	Mean \pm SD	(range)	Mean \pm SD	(range)		
Tibia_R	0.710 \pm 0.036	(0.66-0.74)	0.726 \pm 0.024	(0.69-0.75)	5.000	0.4857
Talus_R	0.831 \pm 0.032	(0.79-0.87)	0.825 \pm 0.028	(0.78-0.84)	9.000	0.8857
Calcaneus_R	0.658 \pm 0.045	(0.60-0.71)	0.628 \pm 0.061	(0.57-0.71)	12.000	0.3429
Navicular_R	0.843 \pm 0.038	(0.80-0.89)	0.769 \pm 0.104	(0.62-0.86)	11.000	0.4678
Tibia_L	0.859 \pm 0.006	(0.85-0.86)	0.864 \pm 0.009	(0.85-0.87)	4.000	0.3429
Talus_L	0.930 \pm 0.004	(0.92-0.93)	0.931 \pm 0.005	(0.92-0.93)	5.000	0.4857
Calcaneus_L	0.792 \pm 0.008	(0.78-0.80)	0.791 \pm 0.011	(0.77-0.80)	8.000	1.0000
Navicular_L	0.856 \pm 0.039	(0.80-0.89)	0.859 \pm 0.037	(0.80-0.89)	8.000	1.0000

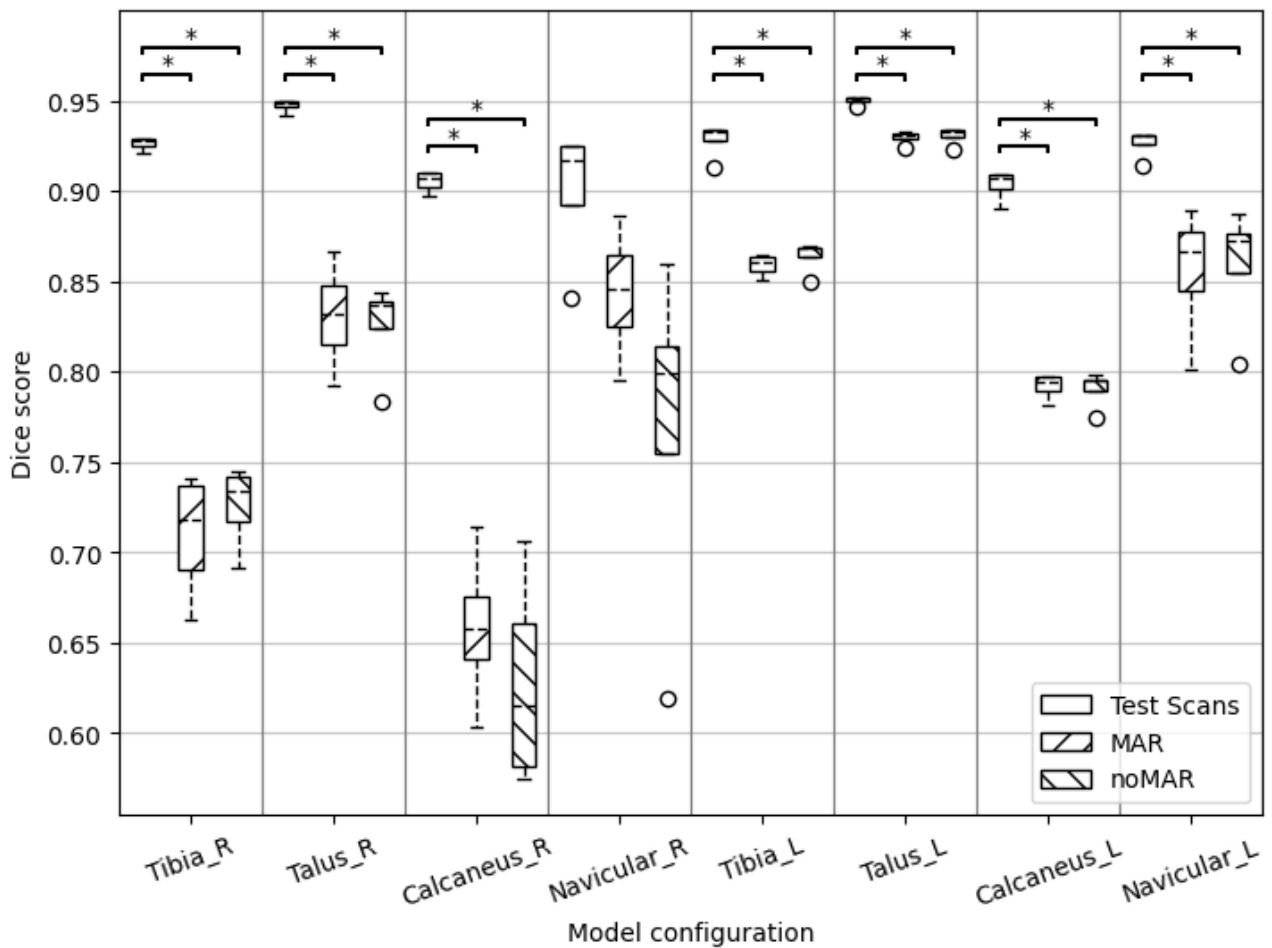


Figure 24: Test Dice scores of the nnU-Net TAA segmentation model applied on 6 non-implant CT scans, and 3 implant CT scans with and without MAR applied. Ordered per bone label.

Table 10: nnU-Net Ankle segmentation model vs nnU-Net TAA segmentation model test Dice scores per bone label

Bone label	nnU-Net Ankle		nnU-Net TAA		U-statistic	p-value
	Mean \pm SD	(range)	Mean \pm SD	(range)		
Tibia_R	0.930 \pm 0.040	(0.87-0.97)	0.926 \pm 0.040	(0.86-0.97)	14.000	0.1143
Talus_R	0.950 \pm 0.024	(0.91-0.97)	0.947 \pm 0.026	(0.90-0.97)	12.000	0.3094
Calcaneus_R	0.912 \pm 0.037	(0.86-0.95)	0.905 \pm 0.038	(0.85-0.95)	12.000	0.1143
Navicular_R	0.905 \pm 0.084	(0.55-0.95)	0.900 \pm 0.109	(0.41-0.95)	9.000	0.8839
Tibia_L	0.933 \pm 0.038	(0.87-0.98)	0.928 \pm 0.040	(0.85-0.98)	10.000	0.6857
Talus_L	0.952 \pm 0.024	(0.91-0.97)	0.950 \pm 0.024	(0.91-0.97)	14.000	0.1102
Calcaneus_L	0.910 \pm 0.030	(0.87-0.95)	0.903 \pm 0.030	(0.86-0.94)	14.000	0.1102
Navicular_L	0.931 \pm 0.019	(0.90-0.96)	0.927 \pm 0.021	(0.89-0.96)	13.000	0.1913

A.3 Visual comparison of Infinity TAS CT scan segmentation with and without MAR

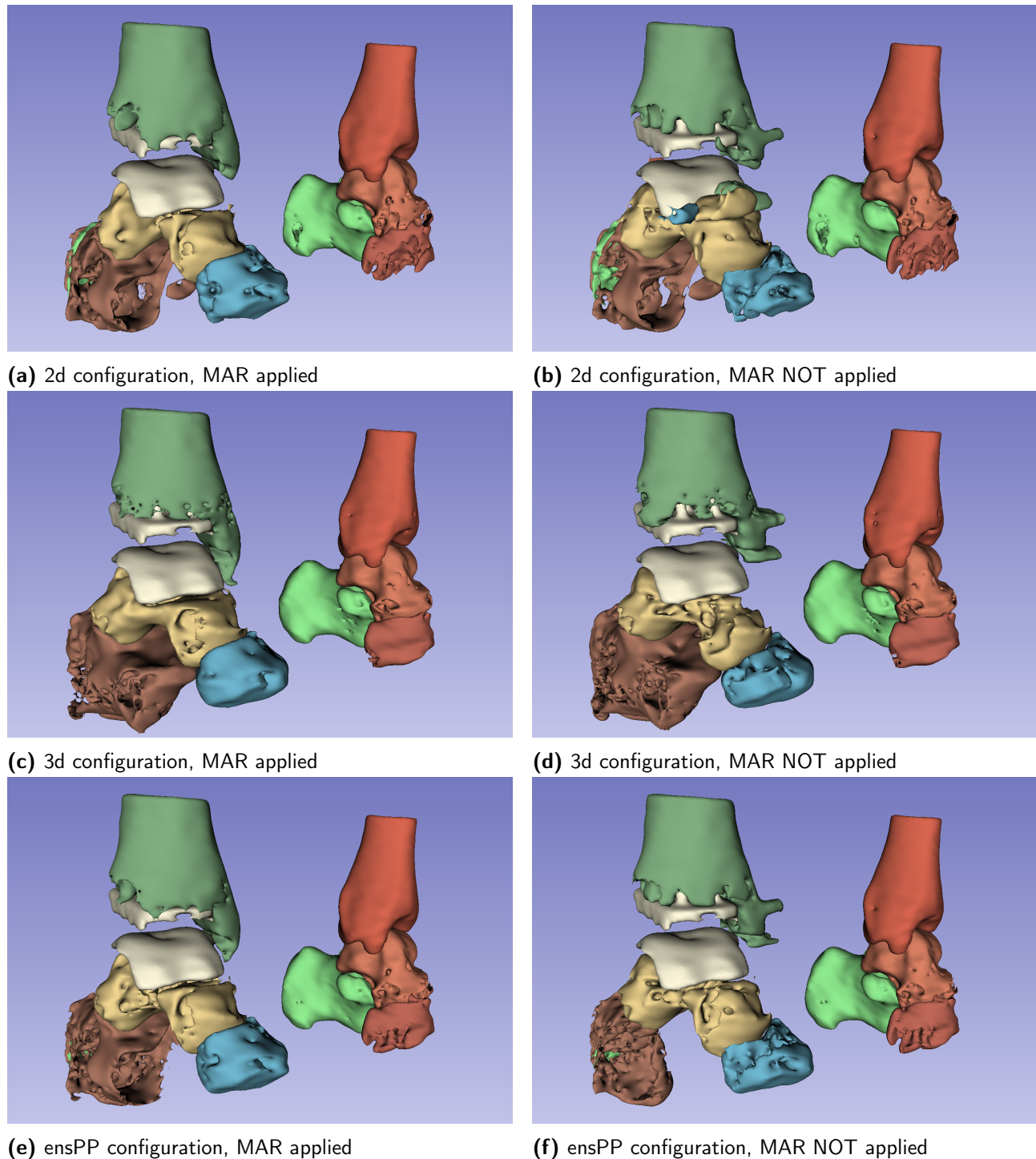


Figure 25: 3D view of the segmentation of scan InfinityTAS_001, showing the difference between applying MAR and not applying MAR, and between model configurations.

Appendix B 3D registration

B.1 Equations for postprocessing of 3D registration results

B.1.1 Denormalisation of the translation vector

During 3D registration, the target and source models (X and Y) are normalised with the location and scale of model Y to ensure equal scale of the models. To obtain the correct translation vector, the output translation was denormalised. Three translation outputs are generated with the 3D registration: $\overrightarrow{t_{norm}}$, \overrightarrow{Y} , and $\overrightarrow{Y_{norm}}$, being the normalised translation vector, a tensor with the (x,y,z)-coordinates of each point of the registered shape, and a tensor with the normalised (x,y,z)-coordinates of each point of the registered shape, respectively. To denormalise the translation vector, a scaling vector was computed by comparing the magnitudes of y and $\overrightarrow{Y_{norm}}$. To this end, the standard deviations were computed:

$$\overrightarrow{\sigma_{normY}} = \sqrt{\frac{1}{N} \sum_{i=1}^N (\overrightarrow{Y_{norm_i}} - \overrightarrow{\mu})^2} \quad (3)$$

$$\overrightarrow{\sigma_y} = \sqrt{\frac{1}{N} \sum_{i=1}^N (\overrightarrow{y_i} - \overrightarrow{\mu})^2} \quad (4)$$

with $\overrightarrow{\sigma_{normY}}$ the standard deviation of each axis of $\overrightarrow{Y_{norm}}$, and $\overrightarrow{\sigma_y}$ the standard deviation of each axis of \overrightarrow{y} .

The scaling vector \vec{S} is defined as:

$$\vec{S} = \frac{\overrightarrow{\sigma_y}}{\overrightarrow{\sigma_{normY}}} \quad (5)$$

and the denormalised translation vector t is computed:

$$\overrightarrow{t} = \overrightarrow{t_{norm}} \cdot \vec{S}^T \quad (6)$$

B.1.2 Derivation of the rotation vector

The rotation matrix for dorsiflexion/plantarflexion, abduction/adduction, and eversion/inversion (angles α , β , γ , respectively) is this:

$$R = R_z(\alpha)R_y(\beta)R_x(\gamma) = \begin{bmatrix} \cos \alpha \cos \beta & \cos \alpha \sin \beta \sin \gamma - \sin \alpha \cos \gamma & \cos \alpha \sin \beta \cos \gamma + \sin \alpha \sin \gamma \\ \sin \alpha \cos \beta & \sin \alpha \sin \beta \sin \gamma + \cos \alpha \cos \gamma & \sin \alpha \sin \beta \cos \gamma - \cos \alpha \sin \gamma \\ -\sin \beta & \cos \beta \sin \gamma & \cos \beta \cos \gamma \end{bmatrix} \quad (7)$$

In order to derive the individual Euler angles, the following equations were used. β was derived first, see Equation 8.

$$\beta = -\arcsin(r_{31}) \quad (8)$$

Then, α and γ were computed, see Equation 9 and 10.

$$\alpha = \begin{cases} \arctan 2(-r_{23}, r_{22}), & \text{if } \cos \beta = 0 \\ \arcsin\left(\frac{r_{21}}{\cos \beta}\right), & \text{otherwise} \end{cases} \quad (9)$$

$$\gamma = \begin{cases} 0, & \text{if } \cos \beta = 0 \\ \arcsin\left(\frac{r_{32}}{\cos \beta}\right), & \text{otherwise} \end{cases} \quad (10)$$

B.2 Joint 3D registration, accuracy

Table 11: Joint mean absolute errors

A		Mean absolute translation errors					
Joint		Dorsiflexion			Plantarflexion		
		x (mm)	y (mm)	z (mm)	x (mm)	y (mm)	z (mm)
TibioTalar_L		0.0306	0.0137	0.0635	0.0359	0.0206	0.0572
TibioTalar_R		0.0258	0.0096	0.0456	0.0309	0.0235	0.0444
TaloCalcaneal_L		0.0171	0.1115	0.0094	0.2507	0.7976	0.0425
TaloCalcaneal_R		0.0729	0.0581	0.0225	0.0888	1.0394	0.0857
TaloNavicular_L		0.0162	0.0162	0.0092	0.0920	0.5132	0.0704
TaloNavicular_R		0.0067	0.0080	0.0101	0.2430	0.7159	0.0840

B		Mean absolute rotation errors					
Joint		Dorsiflexion			Plantarflexion		
		γ -angle ($^{\circ}$)	β -angle ($^{\circ}$)	α -angle ($^{\circ}$)	γ -angle ($^{\circ}$)	β -angle ($^{\circ}$)	α -angle ($^{\circ}$)
TibioTalar_L		0.0623	0.1789	0.2918	0.0748	0.1284	0.4861
TibioTalar_R		0.0787	0.1408	0.2846	0.0734	0.1049	0.4067
TaloCalcaneal_L		0.2536	0.2918	0.2030	0.3057	0.4000	0.2447
TaloCalcaneal_R		0.3636	0.4377	0.2514	0.3070	0.4000	0.2483
TaloNavicular_L		0.0268	0.1540	0.1102	0.0430	0.0969	0.1300
TaloNavicular_R		0.0394	0.1202	0.1158	0.0353	0.1022	0.1379

B.3 3D registration robustness

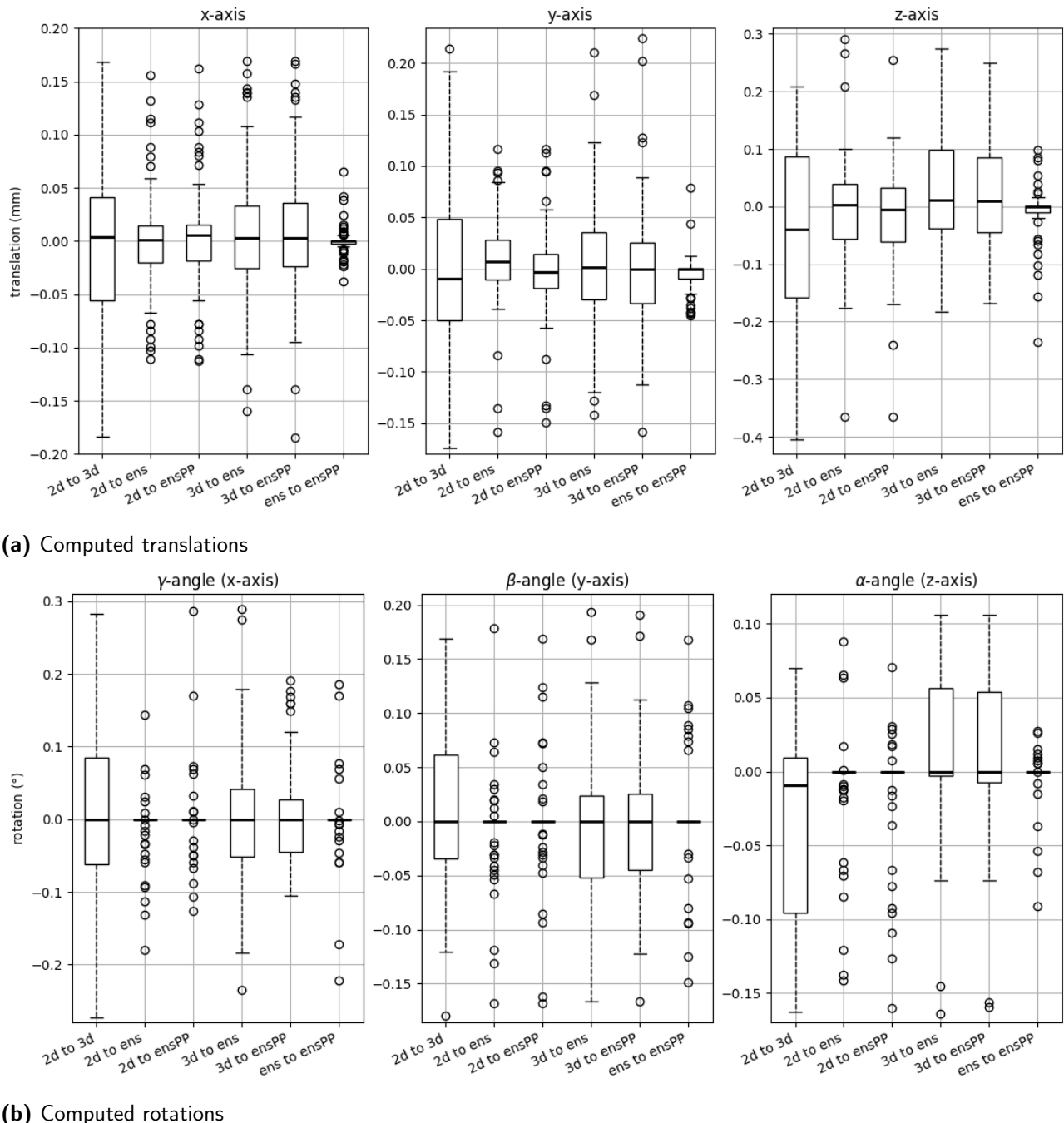


Figure 26: BCPD computed translations and rotations of the left and right ankle.

Appendix C METC application

B1: ABR Form (Dutch)

Formulier voor medisch-ethische beoordeling en registratie

ABR-formulier, versie april 2014

Het is raadzaam de ingevoerde gegevens tijdens het invullen van dit formulier tussentijds regelmatig op te slaan. Dit voorkomt eventueel verlies van gegevens bij een verbreking van de internetverbinding.

A. Sectie - Openbaar maken kerngegevens en resultaten medisch-wetenschappelijk onderzoek in het CCMO-register

- A1. De antwoorden op de vragen gemarkeerd met een wereldbol en de samenvatting van het ABR- formulier, start- en einddatum onderzoek en status onderzoeks dossier worden openbaar gemaakt in het CCMO-register nadat de METC een besluit heeft genomen over het onderzoek. Zie voor meer informatie de toelichting .
- A2. De samenvatting met resultaten van het onderzoek worden twaalf maanden na einde onderzoek openbaar gemaakt in het CCMO-register. Dit betreft zowel de publiekssamenvatting als de wetenschappelijke samenvatting. Zie voor meer informatie de toelichting .

NB: de knop ‘de verrichter verleent de CCMO toestemming voor de bovengenoemde openbaarmaking’ is standaard aangevinkt, maar niet zichtbaar. Indien bezwaar uitgevinkt.

B. Sectie - Administratief

- B1. Betreft het onderzoek met geneesmiddelen (inclusief gentherapie, somatische celtherapie, weefselmanipulatie producten, GGO's, zie verder toelichting) als bedoeld in de Wet medisch-wetenschappelijk onderzoek met mensen (WMO)?
- ja
 nee

- B1a. Wilt u informatie importeren van het EudraCT XML bestand?

- ja
 nee

- B1b. Wat is het EudraCT-nummer van dit onderzoeks dossier?

..... <eudraact-number>

- B2. Houdt het onderzoek verband met een eerder door een erkende METC of door de CCMO beoordeelde studie of is het onderzoek reeds eerder bij een erkende METC ter beoordeling voorgelegd?
- ja, het onderzoek houdt verband met – of is het vervolg op – een eerder beoordeelde studie

- ja, het onderzoek is eerder ter beoordeling aan een erkende METC of de CCMO voorgelegd (stuur kopie besluit mee)
 nee

B2a. Zo ja, door welke commissie?

METC Amsterdam UMC

B2b. Zo ja, geef het registratienummer van de eerder beoordeelde studie:

NL47339.018.14

B3. Wat is het protocol nummer van de opdrachtgever/sponsor (indien van toepassing)?

B4. Is het protocol (nog) in een ander openbaar trial register geregistreerd?

- ja
 nee

B4a. Zo ja, onder welk identificatienummer is het onderzoek geregistreerd, bijv ISRCTN, NCT nummer of UTM nummer

.....<ISRCTN-number/>

B5. a. Naam indiener/contactpersoon voor de oordelende toetsingscommissie

Achternaam indiener/contactpersoon: Hermus

Titel en voorletters: Drs J.P.

Tussenvoegsel:

b. Organisatie/Bedrijf: Maastrichts Universitair Medisch Centrum +

Afdeling: Orthopedische Chirurgie

Adres:

Straat en huisnummer: P. Debyelaan 25

Postcode en plaats: 6229 HX Maastricht

Land: Nederland

c. Intern adres:

Telefoon: +31 43 3875433

Fax:

E-mail: j.hermus@mumc.nl

B6. Is de indiener werkzaam bij de opdrachtgever/sponsor (verrichter) van het onderzoek?

ja (ga naar vraag C1)

nee

C. Onderzoek

C1. Volledige titel van het onderzoek C1a. in het Engels:

Influence of impingement of Infinity total ankle system on hindfoot range of motion

C1b. in het Nederlands:

De invloed van inklemming van het Infinity totale enkelsysteem op achtervoet bewegingsvrijheid

C2. Verkorte titel van het onderzoek/acroniem C2a.

In het Engels:

Infinity TAS impingement

C2b. *In het Nederlands: (Let op: deze korte titel wordt vermeld binnen ToetsingOnline)*

Infinity enkelprothese inklemming

C3. Trefwoorden (maximaal 4, plaats elk trefwoord op een aparte regel) C3a.

In het Engels:

- Impingement
- Total ankle arthroplasty

C3b. *In het Nederlands*

C4. Beschrijf het belang van het onderzoek en de beoogde toepassing van de resultaten
(verwijs eventueel naar de relevante pagina's in het protocol).

C5. [Vraag verwijderd.]

C6. *Betreft het onderzoek een multicenter-onderzoek?*

- nee (ga naar vraag C8)
 ja, alleen in Nederland
 ja, internationaal binnen de Europese Unie
 ja, internationaal, ook buiten de Europese Unie

C6a *In welk(e) land(en) zal het onderzoek worden uitgevoerd? Landen:*

C7. Is er bij multicenter-onderzoek sprake van een coördinerend onderzoeker?

- ja, namelijk
 nee

C8. Wie is/zijn medisch verantwoordelijk voor de proefpersonen die deelnemen aan het onderzoek

Het MUMC+

C9. In welk centrum/welke centra (incl. huisartsenpraktijken) in Nederland wordt het onderzoek uitgevoerd? Geef per centrum op: aantal proefpersonen, naam hoofdonderzoeker, naam onafhankelijke deskundige. **PD Type Centrum ->**

- PD Universitair Medische Centra**
PD Universiteiten
PD Ziekenhuizen en Instellingen
PD GGZ instellingen / Psychiatrische ziekenhuizen
PD Clinical Research Organisations (CRO's) PD
Huisartsenpraktijk
PD Overige, namelijk

C10. *Betreft het onderzoek met:*

- mensen

- geslachtscellen
- (rest-)embryo's
- foetussen in utero

Indien mensen aangevinkt, meerdere antwoorden mogelijk (C10a verplicht)

C10a

- preterme pasgeborenen (< 37 weken zwangerschap)
- pasgeborenen (0-27 dagen)
- babies en peuters (28 dagen – 23 maanden)
- kinderen (2-11 jaar)
- jongeren (12-15 jaar)
- adolescenten (16-17 jaar)
- volwassenen (18-64 jaar)
- ouderen (65 jaar en ouder)
- zwangere vrouwen
- vrouwen die borstvoeding geven

C11. Beoogd totaal aantal proefpersonen/(rest-)embryo's/foetussen in utero: C11a.

In Nederland **20**

Bij internationaal onderzoek:

C11b. Totaal in de Europese Unie <in-european-community> C11c.
In het hele onderzoek <in-whole-trial>

C12. [Vraag verwijderd.]

C13. Onderzoeksgebied:

- etiologie
- organisatorisch/zorgonderzoek
- diagnostiek <diagnosis>
- preventie <prophylaxis>
- therapie <therapy>
- veiligheid <safety>
- werkzaamheid <efficacy>
- farmacokinetiek <pharmacokinetic>
- farmacodynamiek <pharmacodynamic>
- bio-equivalentie <bioequivalence>
- dosis-respons <dose-response>
- farmacogenomics <pharmacogenomics>
- farmaco-economie <pharmacoconomics>
- anders, <other> namelijk <other details>

C14. Type onderzoek:

- observationeel onderzoek zonder invasieve metingen
- observationeel onderzoek met invasieve metingen
- interventie-onderzoek

C15. In welke fase kan het onderzoek worden ingedeeld?

- fase I
- fase II

- fase III
- fase IV
- overige onderzoeken waarbij geneesmiddelen worden toegepast
- niet van toepassing

C16. Voor onderzoek met geneesmiddelen zoals bedoeld in de Wet medischwetenschappelijk onderzoek met mensen (WMO), welk(e) onderzoeksproduct(en) word(t)en) onderzocht of als referentie gebruikt of gebruikt om nadere informatie over een toegelaten toepassing te verkrijgen? (alleen verplicht voor onderzoek met geneesmiddelen in de zin van de WMO – vraag B1 = ja)

C17. Is er sprake van een ander(e) onderzoeksproduct en/of interventie dan vermeld bij vraag C16 (zie toelichting)? [kan zowel voor observationeel als interventieonderzoek worden ingevuld als het product (verder) onderzocht wordt]

- Ja
- Nee (ga naar vraag C19)

C17a.

C17a1

Medisch hulpmiddel (medisch hulpmiddel, actief implantaat of in-vitro diagnosticum), namelijk

In het Engels: 3D stress test footplate

In het Nederlands: 3D voetplaat

wie is de fabrikant? UTwente faculty of Biomechanical Engineering
heeft het hulpmiddel een CE-markering?

Ja, en het hulpmiddel wordt in dit onderzoek gebruikt volgens de beoogde toepassing (*within intended purpose*)

ja, maar het betreft een nieuwetoepassing (*outside intended purpose*)

nee

C17a2 Betreft het een

- medisch hulpmiddel
- actief implantaat
- in-vitro-diagnosticum

C17a3 classificatie medisch hulpmiddel (~~in geval van medisch hulpmiddel/actief implantaat~~):

- Klasse I
- Klasse IIa-
- Klasse IIb-
- Klasse III
- nvt

C17a4 Is het medisch hulpmiddel invasief of niet invasief?

- invasief
- niet invasief

C17a5. Wat voor categorie klinisch onderzoek betreft het op grond van Medical Device Regulation (MDR 2017/745)

- klinisch onderzoek waarvan de klinische data gebruikt kunnen gaan worden in het klinisch evaluatie rapport voor het verkrijgen/uitbreiden CE markering (MDR, artikel 62 of 74.2)
- klinisch onderzoek in het kader van post-marketing follow up (PMCF investigation) waarbij de deelnemers worden onderworpen aan extra invasieve en/of belastende procedures (MDR, artikel 74.1)
- ander klinisch onderzoek naar de prestaties, effectiviteit en/of veiligheid van een medische hulpmiddel (MDR, artikel 82)
- nvt

C17a6. classificatie in-vitro-diagnosticum (in geval van in-vitro diagnosticum)

- klasse A
- klasse B
- klasse C
- klasse D
- nvt

C17b. Operatie, namelijk:

In het Engels:

In het Nederlands:

C17c. Psychosocialetherapie,namelijk:

In het Engels:

In het Nederlands:

C17d. Voeding(stoffen), namelijk:

In het Engels:

In het Nederlands:

C17e. Bewegingstherapie, namelijk:

In het Engels:

In het Nederlands:

C17f. radioactieve straling, namelijk:

In het Engels: CT scans of both feet in 5 different positions

In het Nederlands: CT-scans van beide voeten in 5 verschillende standen

C17g. Blootstellingsonderzoek (bijv pesticidenonderzoek), namelijk:

In het Engels:

In het Nederlands:

C17h. Celtherapie (niet behorende tot geavanceerde therapie/ATMP) Oorsprong van de cellen:

- autoloog
- allogeen

specialiténaam (in het Engels): specialiténaam
 (in het Nederlands):.....

C17i. anderonderzoeksproduct/interventie, namelijk

In het Engels:.....
 In het Nederlands:

C18. Worden de onderzoeksproducten voor deze studie door de verrichter gratis verstrekt?

- ja
- nee
- gedeeltelijk, namelijk.....
- niet van toepassing.

C19. Is/zijn er (een) controlegroep(en)?

- ja <controlled>Y</controlled>

- ja, geneesmiddel < comparator-medical-product>
- ja, placebo <comparator-placebo>
- ja, geen interventie
- ja, anders

namelijk een voet mét Infinity TAS en een voet zonder Infinity TAS

- nee <controlled>N</controlled>

C20. Betreft het een gerandomiseerd onderzoek?

- ja <randomised>Y</randomised>

- open <open>
- enkelblind <single blind>
- dubbelblind <double-blind>
- parallel <parallel-group>
- anders namelijk <other-type-details>
- cross-over <cross-

- nee

C21. Op welke klasse(n) van aandoeningen heeft het onderzoek betrekking (maximaal 3):

- hartaandoeningen PD hartaandoeningen
- congenitale, familiaire en genetische aandoeningen
- Bloed- en lymfestelsel aandoeningen
- zenuwstelsel aandoeningen PD zenuwstelsel aandoeningen
- oogaandoeningen PD oogaandoeningen
- evenwichtsorgaan- en ooraandoeningen PD evenwichtsorgaan- en
- ademhalingsstelsel-, thorax- en mediastinumaandoeningen

- maagdarmstelselaandoeningen
PD maagdarmstelselaandoeningen
- nier- en urinewegaandoeningen
PD nier- en urinewegaandoeningen
- huid- en onderhuidaandoeningen
PD huid- en onderhuidaandoeningen
- skeletspierstelsel- en bindweefselaandoeningen
PD skeletspierstelsel- en bindweefselaandoeningen
- endocriene aandoeningen PD endocriene aandoeningen
- voedingsstoornissen en metabole ziekten
PD voedingsstoornissen en metabole ziekten
- infecties en parasitaire aandoeningen
PD infecties en parasitaire aandoeningen
- letsls, intoxicaties en verrichtingscomplicaties
PD letsls, intoxicaties en verrichtingscomplicaties
- neoplasmata, benigne, maligne en niet-gespecificeerd (incl cysten en poliepen) PD neoplasmata, benigne, maligne en niet-gespecificeerd (incl cysten en poliepen)
- chirurgische en medische verrichtingen
PD chirurgische en medische verrichtingen
- bloedvataandoeningen PD bloedvataandoeningen
- algemene aandoeningen en aandoeningen op de plek van toediening
PD algemene aandoeningen en aandoeningen op de plek van toediening
- zwangerschap, perinatale periode en puerperium
PD zwangerschap, perinatale periode en puerperium
- sociale omstandigheden PD sociale omstandigheden
- immuunsysteemaandoeningen
PD immuunsysteemaandoeningen
- lever- en galaandoeningen
PD lever- en galaandoeningen
- voortplantingsstelsel- en borstaandoeningen
PD voortplantingsstelsel- en borstaandoeningen
- psychische stoornissen
PD psychische stoornissen
- Overig, namelijk

C22. Geef twee synoniemen voor de aandoening die bestudeerd wordt, waarvan ten minste één lekenterm.

In het Engels: Ankle implant impingement range of motion; Ankle implant movement due to placement complications

In het Nederlands: Enkel implantaat inklemming bewegingsvrijheid; Enkle implantaat beweging als gevolg van plaatsingsproblemen

C23. Beoogde start- en einddatum van het onderzoek:

C23a. Start Datum (dd-mm-jjjj): 1-3-2025

C23b. Eind Datum (dd-mm-jjjj): 1-3-2026

D. Sectie - Proefpersonen

D1. Is er een proefpersonenverzekering conform de WMO-eisen afgesloten of wordt aan de oordelende toetsingscommissie ontheffing gevraagd?

- proefpersonenverzekering is afgesloten bij verzekерingsmaatschappij PD verzekерingsmaatschappijen
- ontheffing van de verzekering wordt gevraagd
- niet van toepassing, het onderzoek valt onder de Embryowet en er is geen sprake van proefpersonen

D2. Gezonode proefpersonen en/of patiënten in de studie

gezonode proefpersonen (a) <healthy-volunteers>

Aantal:

patiënten (b) <patients>

Aantal: 20

D3. [Vraag verwijderd]

D4. Voornaamste inclusiecriteria

D4a. In het Engels: Infinity TAS implanted; at least 1-year post-surgery; 10 subjects should present evidence of impingement; 10 subjects should present no evidence of impingement

D4b. In het Nederlands: Infinity enkelprothese geïmplanteerd; ten minste 1 jaar post-op; 10 proefpersonen moeten inklemming hebben; 10 proefpersonen moeten geen inklemming hebben.

D5. Voornaamste exclusiecriteria:

D5a. In het Engels: residence outside province of Limburg; inability to travel to MUMC+; have underwent prosthesis revision surgery

D5b. In het Nederlands: woont buiten provincie Limburg; geen mogelijkheid om naar MUMC+ te reizen; prothese revisie operatie ondergaan

D6. Bij welke categorie proefpersonen wordt het onderzoek uitgevoerd (meerdere antwoorden mogelijk)

16 jaar of ouder en wilsbekwaam (ga naar vraag D10)

16 jaar of ouder en wilsonbekwaam (ga naar vraag D7)

12 t/m 15 jaar en in staat tot het geven van geïnformeerde toestemming (ga naar vraag D8)

12 t/m 15 jaar en niet in staat tot het geven van geïnformeerde toestemming (wilsonbekwaam) (ga naar vraag D7) jonger dan 12 jaar (ga naar vraag D8)

D7. Indien (sommige)proefpersonen wilsonbekwaam zijn, tot welke categorie behoren zij?

mensen met een verstandelijke handicap

mensen met een psychiatrische aandoening

mensen met een dementieel syndroom

mensen met een verminderd bewustzijn

anders, namelijk

D8. Waarom wordt het onderzoek niet met meerderjarige/wilsbekwame proefpersonen uitgevoerd?

.....

D9. [Vraag verwijderd.]

D10. Verkeren (sommige) proefpersonen in een afhankelijkheidssituatie ten opzichte van de onderzoeker of degene die de deelnemers werft? (lees de toelichting voor voorbeelden wanneer er sprake kan zijn van een afhankelijkheidssituatie)

- ja
 nee

10a. Zo ja, waardoor?

.....
10b. Waarom wordt het onderzoek juist met deze proefpersonen uitgevoerd en hoe worden de belangen van de proefpersonen gewaarborgd?

Deze proefpersonen hebben in één enkel de Infinity prothese gekregen en leeft het dagelijks leven er mee.

D11. Waaruit bestaat de vergoeding voor de proefpersonen?

- geen vergoeding
 reiskosten
 financiële vergoeding (in Euro's).....
 andere vergoeding, namelijk.....

D12. Is deze vergoeding afhankelijk van bepaalde voorwaarden, bijvoorbeeld het voltooien van (een deel van) het onderzoek?

- Ja (motiveer), namelijk
 nee
 niet van toepassing

E. Sectie - Voor- en nadelen

E1. Wordt er bij dit onderzoek een rechtstreeks therapeutisch effect beoogd bij de proefpersonen / patiënten?

- ja (therapeutisch onderzoek)
- nee (niet-therapeutisch onderzoek)

E1a. Zo ja, geef kort aan waaruit dit therapeutisch effect bestaat.

.....

E1b. Zo nee, kan deelname op een andere manier ten goede komen aan de proefpersoon?

- Ja (motiveer), namelijk
- nee

E2. Waaruit bestaat de belasting van het onderzoek (en een eventueel daaraan voorafgaande keuring) voor de proefpersonen?

Tijdsbeslag: per bezoek 40 minuten

totaal 40 minuten

totale duur van de studie voor de individuele proefpersoon: 1 bezoek

E3. Worden de proefpersonen in verband met het onderzoek in het ziekenhuis opgenomen of wordt een opname verlengd?

- ja, het verblijf in het ziekenhuis/instituut wordt in verband met het onderzoek verlengd

- ja, ze worden voor het onderzoek in het ziekenhuis/instituut opgenomen

- nee

E3a. Zo ja, hoe lang? dag(en) (extra)

hoe vaak? maal

E4. Beschrijf in hoeverre proefpersonen worden onderworpen aan handelingen dan wel een gedragswijze krijgen opgelegd, zoals vragenlijst, interviews, lichamelijk/psychologisch onderzoek, ontzegging, dieet (voor invasieve ingrepen: zie vraag E6)

De proefpersonen krijgen vragenlijsten om de kwaliteit van leven en pijn met de prothese te kwantificeren. Daarna worden beide voeten van de proefpersoon bevestigd aan voetplaten waarmee de voeten in 5 extreme standen worden gebracht. In elke stand wordt een photon-counting CT-scan gemaakt.

E5. Worden de proefpersonen getest op bepaalde aandoeningen/condities?

- ja (motiveer), namelijk

- nee

E6. Welke extra (invasieve) ingrepen (anders dan bij de standaard behandeling) moeten de proefpersonen in het kader van het onderzoek ondergaan:

- | | | |
|--|------------|---------------|
| <input type="checkbox"/> niet van toepassing | maal | ml/keer |
| <input type="checkbox"/> venapunctie | maal | ml/keer |
| <input type="checkbox"/> arteriepunctie | maal | ml/keer |
| <input type="checkbox"/> intraveneuze injectie | maal | ml/keer |

- | | | |
|---|------------------------|---------------|
| <input type="checkbox"/> intra-arteriële injectie | maal |ml/keer |
| <input type="checkbox"/> subcutane injectie | maal | ml/keer |
| <input type="checkbox"/> intramusculaire injectie | maal | ml/keer |
| <input type="checkbox"/> intra- of periarticulaire injectie | maal | ml/keer |
| <input type="checkbox"/> liquorafname |maal | ml/keer |
| <input type="checkbox"/> scopie, aard scopie:
..... |maal | |
| <input type="checkbox"/> biopsie, aard biopsie:
..... |maal | |
| <input type="checkbox"/> catheterisatie, aard catheterisatie:
..... |maal | |
| <input type="checkbox"/> onderzoek met stralenbelasting, aard onderzoek: | | |
| photon-counting CT-scan
..... | 1 maal 0,55 mSv/keer | |
| |maal.....mSv/keer | |
| |maal.....mSv/keer | |
| <input type="checkbox"/> vaginaal/rectaal |maal | |
| <input type="checkbox"/> andere ingrepen, namelijk (beschrijf naar ernst en frequentie):
..... | | |

E7. [Vraag verwijderd]

E8. [Vraag verwijderd]

E9. Geef aan welke risico's er voor proefpersonen zijn verbonden aan deelname aan het onderzoek.

Blootstelling aan radioactieve straling (lage dosis). Oncomfortabelheid tijdens het veranderen van de voetstand in de voetplaten.

E9a. Geef op grond van uw eigen afweging aan waarom het uitvoeren van het onderzoek, in het licht van de belasting en/of risico's die voor proefpersonen aan deelname verbonden zijn, gerechtvaardigd is?

De belasting voor de proefpersonen is erg laag met maar één bezoek aan het ziekenhuis met een CT-scan. Omdat de photon-counting CT scanner gebruikt wordt is de stralingsdosis laag bij een hoge spatiële resolutie. De resultaten uit dit onderzoek kunnen gebruikt worden om te bepalen in hoeverre de beweging van de enkel met prothese wordt beïnvloed door de plaatsing van de prothese. De scans die worden gemaakt kunnen verder gebruikt worden voor onderzoek naar de botkwaliteit, gewrichtskwaliteit en zacht weefsel van de enkel met prothese.

E10. Indien het onderzoek bij minderjarige en/of wilsonbekwame proefpersonen wordt uitgevoerd en geen direct therapeutisch effect wordt beoogd: waarom kunnen belasting en risico's als minimaal worden beschouwd in vergelijking met de standaardbehandeling (verwijs eventueel naar de relevante pagina's in het protocol)?

.....
 niet van toepassing

E11. Kan de eventuele therapie na beëindiging van het onderzoek worden voortgezet?

O Ja (motiveer), in welk kader en voor hoelang?

- Nee (motiveer), omdat
 niet van toepassing

E12. Heeft deelname aan het onderzoek voor de proefpersoon tot gevolg dat van de standaardbehandeling of -diagnostiek kan worden afgeweken of deze kan worden uitgesteld?

- ja
 nee
 niet van toepassing

E12a. Zo ja, waaruit bestaat de afwijking of het uitstel en waarom is afwijking/uitstel verantwoord?

.....

F. Sectie - Informatie en privacy

F1. Hoe worden de proefpersonen geworven en door wie (onderzoeker, behandelend arts, andere persoon) wordt de proefpersoon/wettelijke vertegenwoordiger geïnformeerd en om toestemming gevraagd?

.....

F2. Hoeveel bedenkijd krijgen de proefpersonen/wettelijke vertegenwoordigers om te beslissen over deelname?

.....

F3. Wordt de huisarts, behandelend specialist en/of apotheker van de proefpersoon geïnformeerd over diens deelname aan het onderzoek? ja (de proefpersoon dient hiervoor toestemming te geven)

nee, omdat.....

F4. Worden persoonsgegevens gecodeerd?

- ja
 nee, omdat

F4a. Zo ja, hoe is deze codering opgebouwd?

.....

F4b. Wie heeft toegang tot de sleutel van deze code?

.....

F4c. Wie hebben toegang tot de brondocumenten en eventuele andere tot de persoon herleidbare gegevens?

.....

F5 Hoe wordt het lichaamsmateriaal gedurende het onderzoek bewaard?

- in tot de proefpersoon herleidbare vorm (gecodeerd)
 in niet tot de proefpersoon herleidbare vorm (volledig geanonimiseerd)
 niet van toepassing

F5a Hoe wordt het afgenumen lichaamsmateriaal gecodeerd?

.....

F5b. Wie heeft toegang tot de sleutel van de code?

.....

F5c. Wie heeft/hebben toegang tot het materiaal gedurende het onderzoek?

.....

F6. Wordt afgenumen lichaamsmateriaal na afloop van het onderzoek vernietigd?

- ja
- nee (motiveer), omdat.....
- niet van toepassing

F6a. Hoe wordt het materiaal **na afloop** van het onderzoek bewaard:

- in tot de proefpersoon herleidbare vorm (gecodeerd)
- in niet tot de proefpersoon herleidbare vorm (volledig geanonimiseerd)

F6b. Hoe lang wordt het materiaal bewaard?

.....

F6c. Wie heeft/hebben toegang tot het materiaal?

.....

F6d. Wordt aan de proefpersoon toestemming gevraagd voor het bewaren en analyseren van het materiaal?

- ja
- nee

F6e. Wordt aan de proefpersoon opnieuw toestemming gevraagd als in de toekomst nieuwe analyses gedaan worden?

- ja
- nee

F7. Kunnen proefpersonen na afloop van het onderzoek opnieuw benaderd worden (bijvoorbeeld voor nader onderzoek of follow-up)?

- ja
- nee

F7a. Wordt aan de proefpersoon hiervoor in het voorliggende onderzoek toestemming gevraagd?

- ja
- nee

G. Sectie - Financieel

G1. *Door welke geldstroom wordt het onderzoek gefinancierd?*

- eerste geldstroom (Geld van Ministerie van OC&W aan universiteiten)

- tweede geldstroom (NWO of KNAW), namelijk
- derde geldstroom (anders dan 1^e of 2^e geldstroom, zoals collectebusfondsen, Europese Unie, vakministeries of bedrijven), namelijk EFAS grant

G2. *Wordt het onderzoek (mede) gefinancierd door de industrie/bedrijven?*

- ja, door de industrie/bedrijf zoals is opgegeven bij vraag B6/B7
(opdrachtgever van het onderzoek)
- ja, (ook) door andere industrie/bedrijven dan de opdrachtgever
- nee

G2a. *Geef de namen van industrie/bedrijven indien anders dan de opdrachtgever/verrichter (max 5).*

- PD Universitair Medisch Centrum
- PD GGZ instellingen / Psychiatrische Ziekenhuizen
- PD Overige Ziekenhuizen
- PD Farmaceutische industrie
- PD Biotechnologische industrie
- PD Voedingsmiddelen industrie
- PD Medische Hulpmiddelen industrie
- PD Overige industrie
- PD Clinical Research Organisations (CRO's)
- PD Universiteiten
- PD Overige Centra

G3. Wat is de hoogte van de vergoeding die de arts/onderzoeker cq onderzoeksafdeling/maatschap ontvangt voor de uitvoering van het onderzoek?

- Per patiënt of proefpersoon (bedrag in euro's): 220
- Per deelnemend centrum (bedrag in euro's): 4400

G3a. Hoe is de vergoeding opgebouwd?

€180 voor de CT-scans, tot €40 reiskostenvergoeding. Dit voor 20 proefpersonen

G4 Heeft/hebben de onderzoeker(s) gedurende de afgelopen vijf jaar op een of andere wijze een persoonlijke financiële relatie (gehad) met de verrichter/sponsor van het huidige onderzoek?

- Ja (licht toe)
- nee

G4a Zo ja, geef aan welke relatie dit is of is geweest

.....

H. [Sectie verwijderd]

I. Sectie - Indiening en beoordeling

- I1. *Sla het formulier eerst op en selecteer vervolgens een METC of de CCMO*
- METC Academisch Ziekenhuis Maastricht / Universiteit Maastricht

J. Sectie - Aanvullende opmerkingen

Aanvullende opmerkingen

Voorbeeld

K. Sectie - SAMENVATTING

K1. Nederlandse samenvatting:

Achtergrond van het onderzoek: Het Infinity Total Ankle System wordt gebruikt om patiënten met eindstadium enkelartrose te behandelen, met als doel de mobiliteit van de achtervoet te herstellen. Een mogelijke complicatie van een totale enkelprothese (TAA) is weefselbeknelling, wat de mobiliteit belemmt en pijn veroorzaakt. Hoewel de bewegingsvrijheid van de achtervoet kwantitatief is bestudeerd, is er nog geen onderzoek gedaan naar de bewegingsvrijheid van de achtervoet met een geïmplanteerde enkelprothese, met of zonder beknelling.

Doel van het onderzoek: Het Infinity Total Ankle System wordt gebruikt om patiënten met eindstadium enkelartrose te behandelen, met als doel de mobiliteit van de achtervoet te herstellen. Een mogelijke complicatie van een totale enkelprothese (TAA) is weefselbeknelling, wat de mobiliteit belemmt en pijn veroorzaakt. Hoewel de bewegingsvrijheid van de achtervoet kwantitatief is bestudeerd, is er nog geen onderzoek gedaan naar de bewegingsvrijheid van de achtervoet met een geïmplanteerde enkelprothese, met of zonder beknelling.

Onderzoeksopzet: Dit is een experimentele studie met patiënten die het Infinity TAS-implantaat hebben ontvangen. Deelnemers ondergaan 5 CT-scans van beide voeten als volgt: 1. Neutrale scan met een dosis van 0,11 mSv, 2. Met behulp van de 3D CT-stresstest wordt elke voet geplaatst in een 3D-voetplaat die de voeten in een extreme positie ten opzichte van het onderbeen kan plaatsen, d.w.z. dorsaalflexie, plantairflexie, inversie en eversie. Na het instellen van elke positie wordt een CT-scan gemaakt. De achtervoetbeenderen worden in elke positie gesegmenteerd en hun relatieve verplaatsingen en rotaties worden vergeleken met de neutrale positie, waarbij de talus is gefixeerd, wat de kwantitatieve bewegingsvrijheid oplevert.

Onderzoekspopulatie: De studiepopulatie bestaat uit 20 vrijwilligers die het Infinity TAS in één enkel hebben en een gezonde contralaterale enkel. De helft van de proefpersonen heeft beknelling in de ruimte van het Infinity TAS, de andere helft niet.

Onderzoeksvariabelen/uitkomstmaten: De belangrijkste studieparameter is de bewegingsvrijheid van het talocrurale, subtalare en naviculaire gewricht, uitgedrukt als een rotatieas met bijbehorende graden van rotatie en millimeters van translatie, zowel voor de geïmplanteerde als voor de contralaterale enkel.

Omschrijving en inschatting van belasting en risico: De proefpersonen wordt gevraagd één keer naar het MUMC+ te komen voor het maken van 5 CT-scans van hun enkels in 5 verschillende posities. De totale effectieve stralingsdosis bedraagt ongeveer 0,55 mSv. De proefpersonen kunnen enige ongemakken ervaren wanneer hun voeten worden gepositioneerd met behulp van de voetplaten, maar de maximale posities worden ingesteld op basis van hun pijntolerantie, wat overeenkomt met conventionele klinische stresstests. Dit ongemak wordt zoveel mogelijk geminimaliseerd door de arts die de voetplaat gebruikt.

K2. Engelse samenvatting:

Research background: The Infinity Total Ankle System is used to treat patients with end-stage ankle arthritis, with the aim to restore mobility of the hindfoot. A possible complication of TAA is tissue impingement which hinders mobility and causes pain. Although the range of motion of the hindfoot has been studied quantitatively, none has investigated the range of motion of the hindfoot with an implanted ankle prosthesis, with or without impingement.

Objective: The objective of the study is to determine quantitatively, via a 3D CT-stress test how impingement of the Infinity Total Ankle System (TAS) influences the range of motion of the hindfoot. The secondary objectives are to determine the range of motion of Infinity TAS ankles compared to their contralateral healthy ankles; and to determine whether the 3D CT-stress test might be suitable to assess loosening the Infinity TAS components.

Study design: This is an experimental study with patients who have received the Infinity TAS implant. Participants received 5 CT scans of both feet as follows: 1. Neutral scan at 0,11 mSv dose, 2. Using the 3D CT-stress test each foot will be placed in a 3D foot plate that allows the feet to be positioned in an extreme position relative to the lower leg i.e. dorsiflexion, plantarflexion, inversion and eversion. After each position is set, a CT scan is made. The hindfoot bones in each position are segmented and their relative displacements and rotations are assessed compared to the neutral position with the talus being fixed, which gives the quantitative range of motion.

Study population: The study population consists of 20 volunteers who have received the Infinity TAS in one ankle and have a healthy contralateral ankle. Half of the subjects have gutter impingement of the Infinity TAS and half do not.

Main study parameters/endpoints: The main study parameter is the range of motion of the talocrucal, subtalar and navicular joint expressed as a rotation axis with accompanying degrees of rotation and millimeters of translation both for the implanted as for the contralateral ankle.

Nature and extent of the burden and risks associated with participation, benefit and group relatedness: The subjects are asked to come to the MUMC+ once to make 5 CT scans of their ankles in 5 different positions. The total effective radiation dose will come to around 0,55 mSv. The subjects can experience some discomfort whilst their feet are positioned using the foot plates, but maximum positions are set based on their pain tolerance with that mimicking the conventional clinical stress tests. This discomfort is minimized by the physician using the foot plate as much as possible.

ONDERTEKENING

De verrichter en indiener verklaren hierbij:

- a. het formulier (en samenvatting) volledig en naar waarheid te hebben ingevuld;
- b. de antwoorden op de vragen uit het ABR formulier niet in strijd zijn met het bijbehorende onderzoeks dossier en onderzoekscontract

Naar waarheid getekend, door de verrichter
(=opdrachtgever)
datum

door de indiener
datum

Handtekening
naam ..
functie.....

Handtekening
naam ..
functie.....

C1: Research Protocol

PROTOCOL TITLE

“Influence of impingement of Infinity total ankle system on hindfoot range of motion”

Protocol ID	<i><include protocol ID given by sponsor or investigator></i>
Short title	Infinity TAS impingement
EudraCT number	<i><only applicable for studies with an investigational medicinal product></i>
Version	1
Date	17-12-2024
Coordinating investigator/project leader	Drs. J.P. Hermus <i>Academic Medical Center Department of Orthopedic surgery P. Debyelaan 25, 6229 HX Maastricht +31 43 3875433 Email: j.hermus@mumc.nl</i>
Principal investigator	Drs. J.P. Hermus <i>Academic Medical Center Department of Orthopedic surgery P. Debyelaan 25, 6229 HX Maastricht +31 43 3875433 Email: j.hermus@mumc.nl</i>
Executing investigators	Prof. dr. ir. G.J.M. Tuijthof <i>University of Twente Department of Biomechanical Engineering De Horst 2, 7522 LW Enschede +31 53 4892500 Email: g.j.m.tuijthof@utwente.nl</i> Prof. dr. M. Poeze <i>Academic Medical Center Department of Trauma Surgery P. Debyelaan 25, 6229 HX Maastricht +31 43 3874900 Email: m.poeze@mumc.nl</i>
Independent expert (s)	Prof. dr. J.J.C. Arts <i>Academic Medical Center Department of Orthopedic surgery P. Debyelaan 25, 6229 HX Maastricht +31 43 3875433 Email: j.arts@mumc.nl</i>

PROTOCOL SIGNATURE SHEET

Name	Signature	Date
Head of Department: <i><include name and function></i>		
[Coordinating Investigator/Project leader/Principal Investigator]: <i><please include name and function></i>		

TABLE OF CONTENTS

1.	INTRODUCTION AND RATIONALE.....	8
2.	OBJECTIVES.....	8
3.	STUDY DESIGN.....	9
4.	STUDY POPULATION	9
4.1	Population (base)	9
4.2	Inclusion criteria	10
4.3	Exclusion criteria.....	10
4.4	Sample size calculation	10
5.	INVESTIGATIONAL PRODUCT	11
5.1	Name and description of investigational product(s)	11
5.2	Summary of findings from non-clinical studies.....	11
5.3	Summary of findings from clinical studies	11
5.4	Summary of known and potential risks and benefits	11
6.	NON-INVESTIGATIONAL PRODUCT	12
6.1	Name and description of non-investigational product(s)	12
6.2	Summary of findings from non-clinical studies.....	12
6.3	Summary of findings from clinical studies	12
6.4	Summary of known and potential risks and benefits	12
7.	METHODS	12
7.1	Study parameters/endpoints	12
7.1.1	Main study parameter	12
7.1.2	Secondary study parameters/endpoints	13
7.2	Study procedures	13
7.3	Withdrawal of individual subjects	14
7.4	Replacement of individual subjects after withdrawal	14
8.	SAFETY REPORTING.....	14
8.1	Temporary halt for reasons of subject safety.....	14
8.2	AEs, SAEs and SUSARs.....	14
8.2.1	Adverse events (AEs).....	14
8.2.2	Serious adverse events (SAEs)	14
8.3	Follow-up of adverse events.....	15
9.	STATISTICAL ANALYSIS	15
9.1	Primary study parameter(s)	15
9.2	Secondary study parameter(s)	16
10.	ETHICAL CONSIDERATIONS	17
10.1	Regulation statement	17
10.2	Recruitment and consent	17
10.3	Benefits and risks assessment, group relatedness	17
10.4	Compensation for injury.....	17
11.	ADMINISTRATIVE ASPECTS, MONITORING AND PUBLICATION.....	18
11.1	Handling and storage of data and documents	18

11.2	Amendments	18
11.3	Annual progress report	18
11.4	Temporary halt and (prematurely) end of study report.....	18
12.	STRUCTURED RISK ANALYSIS	19
12.1	Potential issues of concern	19
12.2	Synthesis	19
13.	REFERENCES	20

LIST OF ABBREVIATIONS AND RELEVANT DEFINITIONS

ABR	General Assessment and Registration form (ABR form), the application form that is required for submission to the accredited Ethics Committee; in Dutch: Algemeen Beoordelings- en Registratieformulier (ABR-formulier)
AE	Adverse Event
AR	Adverse Reaction
CA	Competent Authority
CCMO	Central Committee on Research Involving Human Subjects; in Dutch: Centrale Commissie Mensgebonden Onderzoek
CV	Curriculum Vitae
DSMB	Data Safety Monitoring Board
EU	European Union
EudraCT	European drug regulatory affairs Clinical Trials
GCP	Good Clinical Practice
GDPR	General Data Protection Regulation; in Dutch: Algemene Verordening Gegevensbescherming (AVG)
IB	Investigator's Brochure
IC	Informed Consent
IMP	Investigational Medicinal Product
IMPD	Investigational Medicinal Product Dossier
METC	Medical research ethics committee (MREC); in Dutch: medisch-ethische toetsingscommissie (METC)
(S)AE	(Serious) Adverse Event
SPC	Summary of Product Characteristics; in Dutch: officiële productinformatie IB1-tekst
Sponsor	The sponsor is the party that commissions the organisation or performance of the research, for example a pharmaceutical company, academic hospital, scientific organisation or investigator. A party that provides funding for a study but does not commission it is not regarded as the sponsor, but referred to as a subsidising party.
SUSAR	Suspected Unexpected Serious Adverse Reaction
UAVG	Dutch Act on Implementation of the General Data Protection Regulation; in Dutch: Uitvoeringswet AVG
WMO	Medical Research Involving Human Subjects Act; in Dutch: Wet Medisch-wetenschappelijk Onderzoek met Mensen

SUMMARY

Rationale: The Infinity Total Ankle System is used to treat patients with end-stage ankle arthritis, with the aim to restore mobility of the hindfoot. A possible complication of TAA is tissue impingement which hinders mobility and causes pain. Although the range of motion of the hindfoot has been studied quantitatively, none has investigated the range of motion of the hindfoot with an implanted ankle prosthesis, with or without impingement.

Objective: The objective of the study is to determine quantitatively, via a 3D CT-stress test how impingement of the Infinity Total Ankle System (TAS) influences the range of motion of the hindfoot. The secondary objectives are to determine the range of motion of Infinity TAS ankles compared to their contralateral healthy ankles; and to determine whether the 3D CT-stress test might be suitable to assess loosening the Infinity TAS components.

Study design: This is an experimental study with patients who have received the Infinity TAS implant. Participants received 5 CT scans of both feet as follows: 1. Neutral scan at 0,11 mSv dose, 2. Using the 3D CT-stress test each foot will be placed in a 3D foot plate that allows the feet to be positioned in an extreme position relative to the lower leg i.e. dorsiflexion, plantarflexion, inversion and eversion. After each position is set, a CT scan is made. The hindfoot bones in each position are segmented and their relative displacements and rotations are assessed compared to the neutral position with the talus being fixed, which gives the quantitative range of motion.

Study population: The study population consists of 20 volunteers who have received the Infinity TAS in one ankle and have a healthy contralateral ankle. Half of the subjects have gutter impingement of the Infinity TAS and half do not.

Main study parameters/endpoints: The main study parameter is the range of motion of the talocrucal, subtalar and navicular joint expressed as a rotation axis with accompanying degrees of rotation and millimeters of translation both for the implanted as for the contralateral ankle.

Nature and extent of the burden and risks associated with participation, benefit and group relatedness: The subjects are asked to come to the MUMC+ once to make 5 CT scans of their ankles in 5 different positions. The total effective radiation dose will come to around 0,55 mSv. The subjects can experience some discomfort whilst their feet are positioned using the foot plates, but maximum positions are set based on their pain tolerance with that mimicking the conventional clinical stress tests. This discomfort is minimized by the physician using the foot plate as much as possible.

1. INTRODUCTION AND RATIONALE

People who suffer from end-stage ankle arthritis can experience significant pain and disability, similar to the pain and decrease in quality of life experienced by people with end-stage hip arthritis [1]. Unlike hip arthritis, primary osteoarthritis is not the most common cause of ankle arthritis, as this is most often caused by prior ankle trauma or ankle instability due to ligamentous injury accounting for approximately 70% of cases, with inflammatory arthropathy the second cause (12%) [2]. Total ankle arthroplasty, or TAA, has only recently been adopted as the standard operative treatment for ankle arthritis over arthrodesis [3]. Although arthrodesis is effective in pain relief and overall improvement in quality of life in the short term, long-term studies show that fusion causes increased stresses on adjacent joints, requiring additional arthrodesis surgery [4].

At the Maastricht University Medical Center+ (MUMC+), the most used prosthesis for ankle arthroplasty is the Infinity Total Ankle System (TAS) (Wright Medical Technology Inc., Memphis, TN) to reduce pain in the ankle whilst restoring the mobility of the joint as much as possible. The infinity TAS is a fourth-generation, fixed-bearing, total ankle replacement consisting of a talar dome, a tibial tray, and an ultrahigh molecular weight polyethylene (UHMWPE) component.

Follow-up studies of TAA have shown improved quality of life, movement, and reduced pain [3], [5], [6]. However, the most common cause for subsequent surgery is gutter impingement by the implant, which can cause pain in the ankle after TAA due to the talar implant impinging against either malleolus. Impingement is caused by multiple factors including implant placement and presents itself during ankle movement [7].

Early research on hindfoot range of motion is promising but is not performed on hindfeet with implants. With the upcoming technology of segmentation-based assessment, accurate quantitative data regarding hindfoot range of motion of the Infinity TAS can aid in improving surgical outcomes.

2. OBJECTIVES

The objective of the study is to determine quantitatively, via a 3D CT-stress test how impingement of the Infinity Total Ankle System (TAS) influences the range of motion of the hindfoot.

Secondary objectives are as follows:

- Determine whether the range of motion of the hindfoot is influenced by a change in the surgical placement of the Infinity TAS to prevent gutter impingement,

- Determine the influence of the Infinity TAS on the range of motion of the hindfoot as compared to the healthy contralateral ankle,
- Determine whether there is loosening of the Infinity TAS components.

3. STUDY DESIGN

This is an experimental study involving human subjects with a history of ankle arthrosis and who have had arthroplasty with the Infinity TAS. To this end, patients with a single-sided implant and otherwise healthy contralateral ankle will be asked to participate in the study. We aim to include half of the patients who have impingement complaints and are scheduled for surgery and the other half of the patients who have no complaints at all. All participants will receive 5 CT scans of both feet made simultaneously, where the contralateral healthy ankle will act as a control.

The methodology employed is based on previously METC- approved and performed research [8], [9], [10], [11]. As indicated, the ranges of motion of the tibiotalar joints (with and without Infinity TAS), talocalcaneal, and talonavicular joint are determined from the CT scans. Based on the segmentation of the bones from CT-scans made in various extreme positions, the relative translation and rotation is determined which defines the range of motion at joint level in the hindfoot.

The study is performed at the Maastricht University Medical Center (MUMC+) (Maastricht, The Netherlands). Patients are asked to come once for CT scans of their ankles.

Time frame

Inclusion will take place until the total number of 20 subjects is achieved. The acquisition of the 5 CT scans per patient will take approximately 20 minutes. Including intake and signing the informed consent form, the research will last 30 minutes to an hour per test subject. See Appendix C for the scan protocol.

The exact planning of CT scan acquisition is made in collaboration with the Department of Radiology.

4. STUDY POPULATION

4.1 Population (base)

The study population is based on orthopaedic patients from the MUMC+ who have received an Infinity TAS.

- Half should have impingement of the Infinity TAS
- Half should not have impingement complications

4.2 Inclusion criteria

In order to be eligible to participate in this study, a subject must meet all of the following criteria:

- Implantation of the Infinity Total Ankle System (TAS): Subjects must have had the Infinity total ankle system implanted to ensure relevance to the study's focus on this specific prosthesis.
- Time since surgery: Subjects must be at least 1-year post-surgery to allow for acquaintance with the prosthesis, sufficient healing, and to observe the development or absence of impingement.
- Presence or absence of gutter impingement:
 - For one group, subjects must present with confirmed clinical and/or radiographic evidence of gutter impingement.
 - For the other group, subjects must have no clinical or radiographic signs of impingement.
- Informed consent: Subjects must provide informed consent and demonstrate understanding of the study procedures.

4.3 Exclusion criteria

A potential subject who meets any of the following criteria will be excluded from participation in this study:

- Residence outside the province of Limburg: Subjects who reside outside of Limburg will be excluded to ensure proximity. An exception can be made if a subject is willing to travel a longer distance.
- Inability to travel to MUMC+: Subjects for whom transport to the MUMC+ is not feasible will be excluded to ensure access to study procedures.
- Prosthesis revision surgery: Subjects who have undergone revision surgery of the implanted prosthesis will be excluded, as this may affect study outcomes and confound the incidence of impingement.

4.4 Sample size calculation

According to the meta-analysis by Hermus et al. [12], the incidence of impingement for implanted Infinity prostheses is approximately 6%. Based on this incidence rate, we initially calculated a sample size of 3, given that approximately 50 total ankle arthroplasties (TAAs) have been performed in MUMC+ since 2017.

However, a sample size of 3 may not provide sufficient precision or statistical power for meaningful conclusions, as small sample sizes are highly susceptible to variability. By increasing the sample size to 10, we aim to improve the robustness of the study and

ensure more reliable detection of impingement cases. This larger sample will provide a more representative picture of the population, reducing the margin of error and increasing the generalizability of the findings.

As the number of subjects in both study groups should be equal, the total number of subjects should be 20: 10 subjects with impingement and 10 subjects without impingement.

5. INVESTIGATIONAL PRODUCT

5.1 Name and description of investigational product(s)

Infinity Total Ankle System. Modern, fourth-generation, fixed-bearing, total ankle replacement consisting of a talar dome, a tibial tray, and an ultrahigh molecular weight polyethylene (UHMWPE) component. The UHMWPE component is fixed to the tibial tray and articulates with the talar dome to emulate the movement of the talocrural joint.

5.2 Summary of findings from non-clinical studies

See the information provided by Wright Medical Group in the brochure of the Infinity Total Ankle System. Document 010393b_infinity-total-ankle-system-brochure.pdf

5.3 Summary of findings from clinical studies

Townshend et al. performed a clinical follow-up study of two to five years with 503 Infinity TAA patients [13]. The average follow-up of patients was 44.9 months and it was found that the 2-year survival rate was 98.8% and the revision reoperation rate was 1.6%. There were no cases of hardware removal, debridement of osteolytic cysts, or deep infections requiring debridement.

They conclude that early clinical results and the small rate of adverse events support the use of the Infinity TAS for end-stage ankle arthritis treatment.

5.4 Summary of known and potential risks and benefits

Some intraoperative and postoperative risks of implanting the Infinity TAS are:

- Pain;
- Damage to blood vessels;
- Delayed wound healing;
- Deep wound infection which may lead to removal of the prosthesis;
- Bone fracture by trauma or excessive loading; and
- Inadequate range of motion due to improper selection or positioning of components.

Benefits of implanting the Infinity TAS are:

- Pain relief
- Improved range of motion
- Improved quality of life

For the complete risks and benefits, see the information provided by Wright Medical

Group in the brochure of the Infinity Total Ankle System.

Infinity_TAS_surgeon_information.pdf

6. NON-INVESTIGATIONAL PRODUCT

6.1 Name and description of non-investigational product(s)

3D foot plate. The intended use of the 3D foot plate is to move and fixate the foot in a certain extreme position relative to the lower leg for a short period of time. The device is to be operated by a medical professional who has been trained in performing clinical stress tests of the ankle and hindfoot.

6.2 Summary of findings from non-clinical studies

See dossier D2, the IMDD for information on the foot plate.

6.3 Summary of findings from clinical studies

There are no clinical studies for this 3D footplate. There was a pre-clinical study of an earlier version of this 3D foot plate where usability was tested by medical professionals who have been trained in performing clinical stress tests of the ankle and hindfoot. It was found that the 3D foot plate was easy to use and understand, and fitted with the dimensions of the CT-scanner [14].

6.4 Summary of known and potential risks and benefits

See dossier D2, the IMDD for a complete risk analysis of the foot plate.

7. METHODS

7.1 Study parameters/endpoints

7.1.1 Main study parameter

The main study parameters are the degrees of rotation and millimetres of translation of the tibia, tibial prosthesis component, talar prosthesis component, talus, calcaneus, and navicular bone when moving the foot from extreme dorsal flexion to extreme plantarflexion position and extreme eversion to extreme inversion (Appendix A). These rotations and translations result in the range of motion of the tibiotalar joint as replaced by the Infinity TAS, talocalcaneal joint, and talonavicular joint as a result of impingement of the implant after implanting the Infinity TAS.

7.1.2 Secondary study parameters/endpoints

The secondary parameters are the degrees of rotation and millimetres of translation of the tibia, tibial prosthesis component, talar prosthesis component, talus, calcaneus, and navicular bone when moving the foot from extreme dorsal flexion to extreme plantarflexion position and extreme eversion to extreme inversion (Appendix A). These rotations and translations result in the range of motion of the tibiotalar joint as replaced by the Infinity TAS, talocalcaneal joint, and talonavicular joint as a result of implanting the Infinity TAS. The final parameter is the movement of Infinity TAS components with respect to their adjoined bones, the tibia and the talus. This is expressed as the difference in degrees of rotation and millimetres of translation between the distal tibia and the tibial plate, and between the talus and the talar dome.

7.2 Study procedures

The subjects will be imaged at the Radiology Department. The routine settings of the photon-counting CT-scanner for imaging of the ankle are presented in Appendix A.

Data acquisition

The CT scans are made according to the protocol in Appendix A. This yields five CT scans per patient.

Data processing

The CT scans are processed and separate segmentations are created of the tibia, tibial plate, talar dome, talus, calcaneus, and navicular. These segmentations are converted to point cloud data to be used in the next steps. Bayesian Coherent

Point Drift is used to virtually move a segmented part from the neutral position CT scan toward the same part in the extreme position CT scan, yielding the rotation and translation parameters of an individual bone for an individual extreme foot position.

The rotation and translation parameters are used to describe the range of motion of the tibiotalar joint (talus movement with respect to the tibia), Infinity TAS (talar dome w.r.t. the tibial plate), talocalcaneal joint (calcaneus w.r.t. the talus), and talonavicular joint (navicular w.r.t. the talus).



Figure 1: 3D foot plate with both feet in neutral position

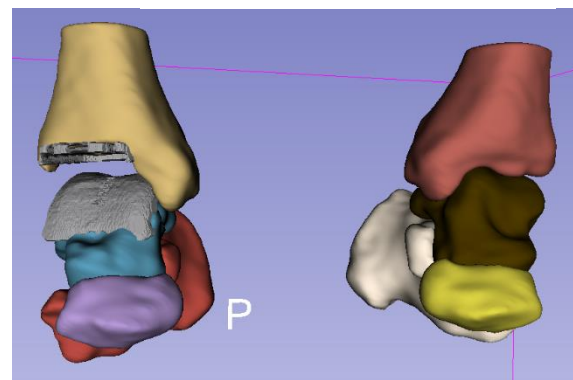


Figure 2: 3D segmentation of the hindfoot bones and Infinity TAS components in right ankle

7.3 Withdrawal of individual subjects

Subjects can leave the study at any time for any reason if they wish to do so without any consequences. The investigator can decide to withdraw a subject from the study for urgent medical reasons.

7.4 Replacement of individual subjects after withdrawal

The subjects that were initially included but for any reason are not able to complete the CT investigation will be compensated by the inclusion of additional subjects, until the desired sample size is achieved.

8. SAFETY REPORTING

8.1 Temporary halt for reasons of subject safety

In accordance to section 10, subsection 4, of the WMO, the sponsor will suspend the study if there is sufficient ground that continuation of the study will jeopardise subject health or safety. The sponsor will notify the accredited METC without undue delay of a temporary halt including the reason for such an action. The study will be suspended pending a further positive decision by the accredited METC. The investigator will take care that all subjects are kept informed.

8.2 AEs, SAEs and SUSARs

8.2.1 Adverse events (AEs)

Adverse events are defined as any undesirable experience occurring to a subject during the study, whether or not considered related to the investigational product or the research methodology. All adverse events reported spontaneously by the subject or observed by the investigator or his staff will be recorded.

8.2.2 Serious adverse events (SAEs)

A serious adverse event is any untoward medical occurrence or effect that

- results in death;
- is life threatening (at the time of the event);
- requires hospitalisation or prolongation of existing inpatients' hospitalisation;
- results in persistent or significant disability or incapacity;
- is a congenital anomaly or birth defect; or
- any other important medical event that did not result in any of the outcomes listed above due to medical or surgical intervention but could have been based upon appropriate judgement by the investigator.

An elective hospital admission will not be considered as a serious adverse event.

The investigator will report all SAEs to the sponsor without undue delay after obtaining knowledge of the events.

The sponsor will report the SAEs through the web portal *ToetsingOnline* to the accredited METC that approved the protocol, within 7 days of first knowledge for SAEs that result in death or are life threatening followed by a period of maximum of 8 days to complete the initial preliminary report. All other SAEs will be reported within a period of maximum 15 days after the sponsor has first knowledge of the serious adverse events.

8.3 Follow-up of adverse events

All AEs will be followed until they have abated, or until a stable situation has been reached. Depending on the event, follow up may require additional tests or medical procedures as indicated, and/or referral to the general physician or a medical specialist. SAEs need to be reported till end of study within the Netherlands, as defined in the protocol

9. STATISTICAL ANALYSIS

Descriptive statistics of numerical data

The range of motion parameters (see Table 1) as computed in Chapter 7.2 are presented as the mean and standard deviation degrees of rotation and millimeters of translation of the prosthesis and the joints. The kinematic parameters are presented separately for subjects with impingement, without impingement, and the contralateral ankle without Infinity prosthesis. As the latter does not include prosthesis parts (tibial plate and talar dome), their movement relative to each other will not be included and the range of motion of the talotibial joint is used to evaluate the range of motion of the Inifinity prosthesis.

9.1 Primary study parameter(s)

To determine whether there is a difference in range of motion between impinged prosthesis and non-impinged prosthesis, paired t-tests will be performed in case of normally distributed data (or else Wilcoxon signed rank tests) of the following conditions:

Table 1: Impingement relationships of ankle joint range of motion

Rotation (degrees)	Translation (mm)	Comparison
Tibiotalar joint (plantar flexion – dorsal flexion)	Tibiotalar joint (plantar flexion – dorsal flexion)	With impingement vs without impingement

Tibiotalar joint (inversion - eversion)	Tibiotalar joint (inversion - eversion)	With impingement vs without impingement
Talocalcaneal joint (plantar flexion – dorsal flexion)	Talocalcaneal joint (plantar flexion – dorsal flexion)	With impingement vs without impingement
Talocalcaneal joint (inversion – eversion)	Talocalcaneal joint (inversion - eversion)	With impingement vs without impingement
Talonavicular joint (plantar flexion – dorsal flexion)	Talonavicular joint (plantar flexion – dorsal flexion)	With impingement vs without impingement
Talonavicular joint (inversion – eversion)	Talonavicular joint (inversion – eversion)	With impingement vs without impingement

9.2 Secondary study parameter(s)

To determine whether there is a difference in range of motion between prosthesis and no prosthesis, paired t-tests will be performed in case of normally distributed data (or else Wilcoxon signed rank tests) of the following conditions:

Table 2: Infinity TAS relationships of ankle joint range of motion

Rotation (degrees)	Translation (mm)	Comparison
Tibiotalar joint (plantar flexion – dorsal flexion)	Tibiotalar joint (plantar flexion – dorsal flexion)	With Infinity TAS vs. without Infinity TAS
Tibiotalar joint (inversion - eversion)	Tibiotalar joint (inversion - eversion)	With Infinity TAS vs. without Infinity TAS
Talocalcaneal joint (plantar flexion – dorsal flexion)	Talocalcaneal joint (plantar flexion – dorsal flexion)	With Infinity TAS vs. without Infinity TAS
Talocalcaneal joint (inversion – eversion)	Talocalcaneal joint (inversion - eversion)	With Infinity TAS vs. without Infinity TAS
Talonavicular joint (plantar flexion – dorsal flexion)	Talonavicular joint (plantar flexion – dorsal flexion)	With Infinity TAS vs. without Infinity TAS
Talonavicular joint (inversion – eversion)	Talonavicular joint (inversion – eversion)	With Infinity TAS vs. without Infinity TAS

To determine whether there is movement between the prosthesis parts and their respective bones, the rotation and translation of the tibiotalar joint will be compared to the Infinity TAS using a student's t-test. If it is found that there is a significant difference between the two groups, there is movement of the prosthesis relative to the bones.

Table 3: Infinity TAS loosening computation relationships

Rotation (degrees)	Translation (mm)	Comparison
Plantar flexion – dorsal flexion	Plantar flexion – dorsal flexion	Tibial plate vs. distal tibia
Plantar flexion – dorsal flexion	Plantar flexion – dorsal flexion	Talar dome vs. talus
Inversion – eversion	Inversion – eversion	Tibial plate vs. distal tibia

Inversion – eversion	Inversion – eversion	Talar dome vs. talus
----------------------	----------------------	----------------------

10. ETHICAL CONSIDERATIONS

10.1 Regulation statement

This study will be conducted according to the Declaration of Helsinki and the WMO.

10.2 Recruitment and consent

<Please give a description of the recruitment and informed consent procedures. How and by whom (investigator, supervising doctor, other person) will subjects be informed about the study and asked for their consent? How much time will they be given to consider their decision? The patient information letter and informed consent form should be attached as a separate document.>

10.3 Benefits and risks assessment, group relatedness

This is an experimental study that involves a low burden to the subjects. The risk of the radiation from the CT scan is low, 0.55 mSv, see document K6. The study includes one visit to the hospital for the experiment. Each subject has to fill out the informed consent form and a questionnaire. The risk of using the 3D foot plate is that the patient can be harmed if the 3D foot plate is not used properly and too much stress is put on the patient's foot. There is no direct benefit for the study subjects. Prospective users of the Infinity TAS device may benefit from the outcome of the study as the results of the study may improve indications for applying the Infinity TAS and improvement of surgical placement of the prosthesis.

10.4 Compensation for injury

The sponsor/investigator has a liability insurance which is in accordance with article 7 of the WMO.

The sponsor (also) has an insurance which is in accordance with the legal requirements in the Netherlands (Article 7 WMO). This insurance provides cover for damage to research subjects through injury or death caused by the study.

The insurance applies to the damage that becomes apparent during the study or within 4 years after the end of the study.

11. ADMINISTRATIVE ASPECTS, MONITORING AND PUBLICATION

11.1 Handling and storage of data and documents

< Please describe the procedures for handling data, how data are coded, who has access to the source data, by whom the key to the code is safeguarded, how long data and/or human material will be kept, which steps are taken to ensure data security and how the subject's privacy is protected.>

11.2 Amendments

A 'substantial amendment' is defined as an amendment to the terms of the METC application, or to the protocol or any other supporting documentation, that is likely to affect to a significant degree:

- the safety or physical or mental integrity of the subjects of the trial;
- the scientific value of the trial;
- the conduct or management of the trial; or
- the quality or safety of any intervention used in the trial.

All substantial amendments will be notified to the METC and to the competent authority.

Non-substantial amendments will not be notified to the accredited METC and the competent authority, but will be recorded and filed by the sponsor.

11.3 Annual progress report

The sponsor/investigator will submit a summary of the progress of the trial to the accredited METC once a year. Information will be provided on the date of inclusion of the first subject, numbers of subjects included and numbers of subjects that have completed the trial, serious adverse events/ serious adverse reactions, other problems, and amendments.

11.4 Temporary halt and (prematurely) end of study report

The sponsor will notify the accredited METC and the competent authority of the end of the study within a period of 90 days. The end of the study is defined as the last patient's last visit.

The sponsor will notify the METC immediately of a temporary halt of the study, including the reason of such an action.

In case the study is ended prematurely, the sponsor will notify the accredited METC and the competent authority within 15 days, including the reasons for the premature termination.

Within one year after the end of the study, the investigator/sponsor will submit a final study report with the results of the study, including any publications/abstracts of the study, to the accredited METC and the Competent Authority.

12. STRUCTURED RISK ANALYSIS

12.1 Potential issues of concern

12.2 Synthesis

Chapter 12.1 is skipped as the Infinity TAS has been studied before. Early models of the 3D foot plate have also been studied before, see Chapter 6. The biggest risks of the study are exposure to radiation, which has been reduced to as low as reasonably practicable, and discomfort with using the 3D foot plate. A structured risk analysis of using the 3D foot plate is included in dossier D2 IMDD file “5.01.3D Foot Plate - Hazard Traceability Matrix v1.0.xlsx”. The risks are not critical and easy to control, as long as the instructions are followed carefully.

13. REFERENCES

- [1] M. Glazebrook *et al.*, "Comparison of health-related quality of life between patients with end-stage ankle and hip arthroscopy," *J Bone Joint Surg Am*, vol. 90, no. 3, pp. 499–505, 2008, doi: 10.2106/JBJS.F.01299.
- [2] C. A. Demetracopoulos, J. P. Halloran, P. Maloof, S. B. Adams, and S. G. Parekh, "Total ankle arthroplasty in end-stage ankle arthritis," *Curr Rev Musculoskelet Med*, vol. 6, no. 4, pp. 279–284, Jul. 2013, doi: 10.1007/S12178-013-9179-6/FIGURES/4.
- [3] H. G. Jung, S. H. Lee, M. H. Shin, D. O. Lee, J. S. Eom, and J. S. Lee, "Anterior Heterotopic Ossification at the Talar Neck after Total Ankle Arthroplasty," *Foot Ankle Int*, vol. 37, no. 7, pp. 703–708, Jul. 2016, doi: 10.1177/1071100716642757.
- [4] S. Fuchs, C. Sandmann, A. Skwara, and C. Chylarecki, "Quality of life 20 years after arthrodesis of the ankle. A study of adjacent joints," *J Bone Joint Surg Br*, vol. 85, no. 7, pp. 994–998, Sep. 2003, doi: 10.1302/0301-620X.85B7.13984.
- [5] G. H. Saito, A. E. Sanders, C. de Cesar Netto, M. J. O'Malley, S. J. Ellis, and C. A. Demetracopoulos, "Short-Term Complications, Reoperations, and Radiographic Outcomes of a New Fixed-Bearing Total Ankle Arthroplasty," *Foot Ankle Int*, vol. 39, no. 7, pp. 787–794, Jul. 2018, doi: 10.1177/1071100718764107.
- [6] R. M. Queen, J. C. De Biassio, R. J. Butler, J. K. DeOrio, M. E. Easley, and J. A. Nunley, "Changes in pain, function, and gait mechanics two years following total ankle arthroplasty performed with two modern fixed-bearing prostheses," *Foot Ankle Int*, vol. 33, no. 7, pp. 535–542, Jul. 2012, doi: 10.3113/FAI.2012.0535.
- [7] J. Kim and C. Demetracopoulos, "Outcomes of Total Ankle Arthroplasty After Reoperation due to Gutter Impingement," *Foot Ankle Clin*, vol. 29, no. 1, pp. 111–122, Mar. 2024, doi: 10.1016/J.FCL.2023.08.005.
- [8] L. Beimers, G. J. Maria Tuijthof, L. Blankevoort, R. Jonges, M. Maas, and C. N. van Dijk, "In-vivo range of motion of the subtalar joint using computed tomography," *J Biomech*, vol. 41, no. 7, pp. 1390–1397, 2008, doi: 10.1016/J.JBIOMECH.2008.02.020.
- [9] L. Beimers, J. W. K. Louwerens, G. J. M. Tuijthof, R. Jonges, C. N. N. Van Dijk, and L. Blankevoort, "CT measurement of range of motion of ankle and subtalar joints following two lateral column lengthening procedures," *Foot Ankle Int*, vol. 33, no. 5, pp. 386–393, May 2012, doi: 10.3113/FAI.2012.0386.
- [10] G. J. M. Tuijthof *et al.*, "Determination of consistent patterns of range of motion in the ankle joint with a computed tomography stress-test," *Clin Biomech (Bristol, Avon)*, vol. 24, no. 6, pp. 517–523, Jul. 2009, doi: 10.1016/J.CLINBIOMECH.2009.03.004.
- [11] R. P. Kleipool *et al.*, "The Mechanical Functionality of the EXO-L Ankle Brace," *American Journal of Sports Medicine*, vol. 44, no. 1, pp. 171–176, Jan. 2016, doi: 10.1177/0363546515611878.
- [12] J. P. Hermus, J. A. Voesenek, E. H. E. van Gansewinkel, M. A. Witlox, M. Poeze, and J. J. Arts, "Complications following total ankle arthroplasty: A systematic literature review and meta-analysis," *Foot and Ankle Surgery*, vol. 28, no. 8, pp. 1183–1193, Dec. 2022, doi: 10.1016/J.FAS.2022.07.004.
- [13] D. Townshend *et al.*, "Two to Five-Year Outcomes of Total Ankle Arthroplasty with the Infinity Fixed-Bearing Implant: A Concise Follow-up of a Previous Report& midast; A," *Journal of Bone and Joint Surgery*, vol. 105, no. 23, pp. 1846–1856, Dec. 2023, doi: 10.2106/JBJS.22.01294.
- [14] G. J. M. Tuijthof *et al.*, "A novel foot plate to assess 3D range of motion of the hindfoot," *Int J Ind Ergon*, vol. 42, no. 1, pp. 41–48, Jan. 2012, doi: 10.1016/J.ERGON.2011.10.006.

APPENDIX A: Computer Tomography Protocol

A – The patient is positioned supine on the CT-scan board in the most comfortable way possible. Both feet are placed on either 3D foot plate (Figure 1) and firmly fixated to the foot plate by two Velcro straps, one over the ankle and one over the forefoot. The lower legs are wrapped in towels and fixated to the leg support.

B – Both feet are placed in a neutral position using the foot plate. The neutral position is defined as 90° to the anatomical axis.

C – The initial CT-scan is performed with the feet in neutral position. The Siemens PCT Alpha is used with these settings:

- Tube voltage: 140 kV
- IQ level 50
- CDTI_{vol}: 4,55 mGy
- Collimator: 120*0,2
- Pitch: 0,8
- Rotation time: 0,5s
- Preset: RoutineSpiralAdultExtremitiesHighresultraQuantumplus

D – Four more scans are obtained with the feet in extreme positions: plantar flexion, dorsal flexion, eversion, and inversion. For each of these positions, the foot plates are adjusted as far as possible to place the feet in the extreme position whilst being as comfortable as possible. The same CT scan settings are used for the four extreme positions.

The average dose length product (DLP) of the ankle is 50 mGy cm. Five CT scans are made for both ankles which makes the DPL = 2*50*5 = 500 mGy cm.

Effective dose = 500*0,0011 = 0,55 mSv (with 0,0011 the conversion factor of the ankle)

Timeline

Stage	Time	Total time
Test subject positioning on the CT table	2 min	2 min
Feet attachment to 3D foot plates and neutral positioning	3 min	5 min
CT scanning and placing feet in extreme positions	15 min	20 min

E1E2: Patient information (Dutch)

Proefpersoneninformatie voor deelname aan medisch-wetenschappelijk onderzoek

Infinity enkelprothese inklemming

Officiële titel: *Invloed van inklemming van de Infinity enkelprothese op achtervoet bewegingsvrijheid.*

Inleiding

Geachte heer/mevrouw,

Met deze informatiebrief willen we u vragen of u wilt meedoen aan medisch-wetenschappelijk onderzoek. Meedoen is vrijwillig. U krijgt deze brief omdat u een enkelprothese heeft.

U leest hier om wat voor onderzoek het gaat, wat het voor u betekent, en wat de voordelen en nadelen zijn. Het is veel informatie. Wilt u de informatie doorlezen en beslissen of u wilt meedoen? Als u wilt meedoen, kunt u het formulier invullen dat u vindt in bijlage [D].

Stel uw vragen

U kunt uw beslissing nemen met de informatie die u in deze informatiebrief vindt. Daarnaast raden we u aan om dit te doen:

- Stel vragen aan de onderzoeker die u deze informatie geeft.
- Praat met uw partner, familie of vrienden over dit onderzoek.
- Lees de informatie op www.rijksoverheid.nl/mensenonderzoek.

1. Algemene informatie

Technische Universiteit Eindhoven (TU/e) heeft dit onderzoek opgezet in samenwerking met het Maastrichts Universitair Medisch Centrum (MUMC+). Hieronder noemen we TU/e en MUMC+ steeds de ‘opdrachtgever’. Onderzoekers, dit kunnen ook artsen zijn, voeren het onderzoek uit het MUMC+.

Deelnemers aan een medisch-wetenschappelijk onderzoek worden vaak proefpersonen genoemd. Zowel patiënten als mensen die gezond zijn, kunnen proefpersoon zijn.

De medisch-ethische toetsingscommissie Academisch Ziekenhuis Maastricht / Universiteit Maastricht heeft dit onderzoek goedgekeurd.

2. Wat is het doel van het onderzoek?

In dit onderzoek bekijken we hoe beweeglijk de enkel is bij eventuele weefsel inklemming met de Infinity enkelprothese na implantatie. Verder onderzoeken we hoe implantatie van de Infinity enkelprothese de beweeglijkheid van de enkel beïnvloedt.

3. Wat is de achtergrond van het onderzoek?

Patiënten met enkelartrose krijgen tegenwoordig een enkelprothese om pijn te verminderen en beweging te verbeteren. Echter komt het in sommige gevallen voor dat er botsing optreed tussen de prothese en de botten tijdens beweging van de enkel. Dit kan pijn doen en de beweeglijkheid van de enkel beperken. Het is nog niet duidelijk wat precies de invloed is. In eerdere onderzoeken is de beweeglijkheid van de enkel zonder prothese precies bepaald met gebruik van

4. Hoe verloopt het onderzoek?

Hoelang duurt het onderzoek?

Doet u mee met het onderzoek? Dan duurt dat in totaal 1 uur.

Stap 1: bent u geschikt om mee te doen?

We willen eerst weten of u geschikt bent om mee te doen. Daarom doet de onderzoeker een onderzoek naar uw medische geschiedenis.

Let op: het kan voorkomen dat u gezond bent, maar dat u toch niet geschikt bent om mee te doen. De onderzoeker zal u daar meer over vertellen.

Stap 2: onderzoeken en metingen

Voor het onderzoek is het nodig dat u 1 keer naar het MUMC+ komt. Een bezoek duurt 30 minuten.

We doen het volgende onderzoek: er wordt 5 keer een CT-scan gemaakt van de voeten, dit gaat als volgt. U neemt plaats op de CT bank en u plaatst uw voeten op beide voetplaten. Met de voetplaat kunnen we uw voeten in een bepaalde stand zetten en scannen om uiteindelijk de beweeglijkheid van de enkel te bepalen. Uw voeten worden 5 keer in een stand gezet en elke keer wordt er een CT-scan gemaakt van beide voeten gemaakt.

5. Welke afspraken maken we met u?

We willen graag dat het onderzoek goed verloopt. Daarom maken we de volgende afspraken met u:

- U doet tijdens dit onderzoek niet mee aan een ander medisch-wetenschappelijk onderzoek.
- U komt naar de afspraak.
- U neemt contact op met de onderzoeker in deze situaties:
 - U wordt in een ziekenhuis opgenomen of behandeld.
 - U krijgt plotseling problemen met uw gezondheid.

- U wilt niet meer meedoen met het onderzoek.
- Uw telefoonnummer, adres of e-mailadres verandert.

6. Van welke bijwerkingen, nadelige effecten of ongemakken kunt u last krijgen?

Wat zijn de nadelen van onderzoeken die gebruik maken van straling?

Bij CT-scan gebruiken we röntgenstraling. In dit onderzoek krijgt u in totaal ongeveer 0,55 mSv aan röntgenstraling. Ter vergelijking: de 'gewone' straling die iedereen in Nederland krijgt, is ongeveer ~2,9 mSv per jaar. Het kan geen kwaad als u voor een medische reden een onderzoek of behandeling met straling moet ondergaan.

- Krijgt u vaker een onderzoek met straling? Bespreek dan met de onderzoeker of het verstandig is dat u meedoet.
- De straling die we tijdens het onderzoek gebruiken kan leiden tot schade aan uw gezondheid. Maar dit is een klein risico. Wel adviseren we u de komende tijd niet nog een keer mee te doen aan een wetenschappelijk onderzoek met straling.

Wat zijn de mogelijke ongemakken van metingen tijdens het onderzoek?

- Het plaatsen van de voet in een bepaalde stand kan vervelend voelen zijn doordat er spanning komt op de enkelbanden. Geef aan de arts aan als u daar teveel last van heeft.

7. Wat zijn de voordelen en de nadelen als u meedoet aan het onderzoek?

Meedozen aan het onderzoek kan voordelen en nadelen hebben. Hieronder zetten we ze op een rij. Denk hier goed over na, en praat erover met anderen.

Als u meedoet aan dit onderzoek betekent het niet dat u minder last krijgt van uw eventuele bestaande problemen met de enkelprothese. Maar met uw deelname helpt u mee het plaatsen en gebruik van enkelprotheses nog meer te verbeteren, en de oorzaken van u eventuele bestaande problemen preciezer te achterhalen.

Meedozen aan het onderzoek kan deze nadelen of gevolgen hebben:

- Meedozen aan het onderzoek kost u extra tijd.
- U moet zich houden aan de afspraken die horen bij het onderzoek.

Wilt u niet meedozen?

U beslist zelf of u meedoet aan het onderzoek.

8. Wanneer stopt het onderzoek?

De onderzoeker laat het u weten als er nieuwe informatie over het onderzoek komt die belangrijk voor u is. De onderzoeker vraagt u daarna of u blijft meedoen.

In deze situaties stopt voor u het onderzoek:

- Alle onderzoeken volgens het schema zijn voorbij.
- Een van de volgende instanties besluit dat het onderzoek moet stoppen:
 - MUMC+
 - de overheid, of
 - de medisch-ethische commissie die het onderzoek beoordeelt.

Wat gebeurt er als u stopt met het onderzoek?

De onderzoekers gebruiken de gegevens die tot het moment van stoppen zijn verzameld. Het hele onderzoek is afgelopen als alle deelnemers klaar zijn.

9. Wat gebeurt er na het onderzoek?

Krijgt u de resultaten van het onderzoek?

Ongeveer 3 maanden nadat het onderzoek is afgerond laat de onderzoeker u weten wat de belangrijkste uitkomsten zijn van het onderzoek.

10. Wat doen we met uw gegevens?

Doet u mee met het onderzoek? Dan geeft u ook toestemming om uw gegevens te verzamelen, gebruiken en bewaren.

Welke gegevens bewaren we?

We bewaren deze gegevens:

- uw geslacht
- uw geboortedatum
- (medische) gegevens die we tijdens het onderzoek verzamelen

Waarom verzamelen, gebruiken en bewaren we uw gegevens?

We verzamelen, gebruiken en bewaren uw gegevens om de vragen van dit onderzoek te kunnen beantwoorden. En om de resultaten te kunnen publiceren. Gegevens kunnen worden gebruikt door de opdrachtgever en bedrijven die de opdrachtgever helpen bij het analyseren van de onderzoeksgegevens.

Hoe beschermen we uw privacy?

Om uw privacy te beschermen geven wij uw gegevens een code. Op al uw gegevens zetten we alleen deze code. De sleutel van de code bewaren we op een beveiligde plek in het ziekenhuis. Als we uw gegevens en lichaamsmateriaal verwerken, gebruiken we steeds alleen die code. Ook in rapporten en publicaties over het onderzoek kan niemand terughalen dat het over u ging.

Wie kunnen uw gegevens zien?

Sommige personen kunnen wel uw naam en andere persoonlijke gegevens zonder code inzien. Dit kunnen gegevens zijn die speciaal voor dit onderzoek zijn verzameld, maar ook gegevens uit uw medisch dossier.

Dit zijn mensen die controleren of de onderzoekers het onderzoek goed en betrouwbaar uitvoeren. Deze personen kunnen bij uw gegevens komen:

- Leden van de commissie die de veiligheid van het onderzoek in de gaten houdt.
- Een controleur die voor de onderzoeker werkt.

Deze personen houden uw gegevens geheim. Voor inzage door deze personen vragen wij u toestemming te geven. De Inspectie Gezondheidszorg en Jeugd kan zonder uw toestemming uw gegevens inzien.

Hoelang bewaren we uw gegevens en lichaamsmateriaal?

We bewaren uw gegevens [...] jaar [in het ziekenhuis/ huisartsenpraktijk/
onderzoekscentrum]. <indien van toepassing> En [...] jaar bij de opdrachtgever.

Mogen we uw gegevens gebruiken voor ander onderzoek?

Uw verzamelde gegevens kunnen ook van belang zijn voor ander wetenschappelijk onderzoek op het gebied van enkelartrosebehandeling met prothese. Daarvoor zullen uw gegevens [...] jaar worden bewaard [in het ziekenhuis/ onderzoekscentrum/ ...]. In het toestemmingformulier geeft u aan of u dit goed vindt. Geeft u geen toestemming? Dan kunt u nog steeds meedoen met dit onderzoek. U krijgt dezelfde zorg.

Kunt u uw toestemming voor het gebruik van uw gegevens weer intrekken?

U kunt uw toestemming voor het gebruik van uw gegevens op ieder moment intrekken. Zeg dat dan tegen de onderzoeker. Maar let op: trekt u uw toestemming in, en hebben onderzoekers dan al gegevens verzameld voor een onderzoek? Dan mogen zij deze gegevens nog wel gebruiken.

Wilt u meer weten over uw privacy?

- Wilt u meer weten over uw rechten bij de verwerking van persoonsgegevens? Kijk dan op www.autoriteitpersoonsgegevens.nl.
- Heeft u vragen over uw rechten? Of heeft u een klacht over de verwerking van uw persoonsgegevens? Neem dan contact op met degene die verantwoordelijk is voor de verwerking van uw persoonsgegevens. Voor uw onderzoek is dat:
 - MUMC+. Zie bijlage A voor contactgegevens, en website.
- Als u klachten heeft over de verwerking van uw persoonsgegevens, raden we u aan om deze eerst te bespreken met het onderzoeksteam. U kunt ook naar de Functionaris Gegevensbescherming van MUMC+ gaan. Of u dient een klacht in bij de Autoriteit Persoonsgegevens.

Waar vindt u meer informatie over het onderzoek?

Op de volgende website(s) vindt u meer informatie over het onderzoek. VOORBEELD
www.ClinicalTrials.gov en/of www.clinicaltrialsregister.eu en/of <https://euclinicaltrials.eu>. Na

het onderzoek kan de website een samenvatting van de resultaten van dit onderzoek tonen.
U vindt het onderzoek door te zoeken op ‘.....’ (**nummer: XXX**)

11. Krijgt u een vergoeding als u meedoet aan het onderzoek?

U krijgt een vergoeding van de reiskosten. De vergoeding voor meedoen aan dit onderzoek moet u mogelijk opgeven aan de Belastingdienst als ‘inkomen uit overig werk’. Vraag dit zo nodig na bij de Belastingdienst.

12. Bent u verzekerd tijdens het onderzoek?

U bent niet extra verzekerd voor dit onderzoek. Want meedoen aan het onderzoek heeft geen extra risico’s. Daarom hoeft de onderzoeker van de METC Academisch Ziekenhuis Maastricht / Universiteit Maastricht geen extra verzekering af te sluiten.

13. We informeren uw behandelend specialist

De onderzoeker stuurt uw behandelend specialist een e-mail om te laten weten dat u meedoet aan het onderzoek.

14. Heeft u vragen?

Vragen over het onderzoek kunt u stellen aan de onderzoeker.

Heeft u een klacht? Bespreek dit dan met de onderzoeker of de arts die u behandelt. Wilt u dit liever niet? Ga dan naar **[klachtenfunctionaris/klachtencommissie van uw ziekenhuis/instituut/Autoriteit Persoonsgegevens/ anders]**. In bijlage A staat waar u die kunt vinden.

15. Hoe geeft u toestemming voor het onderzoek?

U kunt eerst rustig nadenken over dit onderzoek. Daarna vertelt u de onderzoeker of u de informatie begrijpt en of u wel of niet wilt meedoen. Wilt u meedoen? Dan vult u het toestemmingsformulier in dat u bij deze informatiebrief vindt. U en de onderzoeker krijgen allebei een getekende versie van deze toestemmingsverklaring.

Dank voor uw tijd.

16. Bijlagen bij deze informatie

- A. Contactgegevens
- B. Informatie over de verzekering
- C. Schema onderzoekshandelingen / omschrijving onderzoekshandelingen of overzicht metingen
- D. Toestemmingsformulier(en)

Bijlage A: contactgegevens voor MUMC+

Onderzoeker:

Drs. J.P. Hermus.

E-mail: j.hermus@mumc.nl

+31 43 3875433

Onafhankelijk deskundige:

Prof. dr. J.J.C. Arts

Hoofddocent Translationeel Biomaterialen Onderzoek bij de afdeling Orthopaedische

Chirurgie bij MUMC+

j.arts@mumc.nl

+31 43 3881272

Klachten: [dienst of persoon met contactgegevens en bereikbaarheid]

Bijlage B: informatie over de verzekering

MUMC+ heeft een verzekering afgesloten voor iedereen die meedoet aan het onderzoek. De verzekering betaalt de schade die u heeft doordat u aan het onderzoek meedeed. Het gaat om schade die u krijgt tijdens het onderzoek, of binnen 4 jaar na het einde van uw deelname aan het onderzoek. U moet schade binnen 4 jaar melden bij de verzekeraar.

Heeft u schade door het onderzoek? Meld dit dan bij deze verzekeraar:

De verzekeraar van het onderzoek is:

Naam verzekeraar: Lloyd's Insurance Company S.A.
Adres: Bastion Tower, Marsveldplein 5, 1050 Brussel, België
Polisnummer: MCIEEA23134

De schaderegelaar van het onderzoek is:

Naam: Sedgwick
Adres: Westerstraat 21, 3016 DG Rotterdam Nederland
Contactpersoon: Vicky van Holten
E-mail: mciclaims@uk.sedgwick.com
Telefoonnummer: +31 62 0492876

De verzekering betaalt maximaal € 650.000 per persoon en € 5.000.000 voor het hele onderzoek.

Let op: de verzekering dekt de volgende schade **niet**:

- Schade door een risico waarover we u informatie hebben gegeven in deze brief. Maar dit geldt niet als het risico groter bleek te zijn dan we van tevoren dachten. Of als het risico heel onwaarschijnlijk was.
- Schade aan uw gezondheid die ook zou zijn ontstaan als u niet aan het onderzoek had meegedaan.
- Schade die ontstaat doordat u aanwijzingen of instructies niet of niet goed opvolgde.
- Schade door een behandelmethode die al bestaat. Of door onderzoek naar een behandelmethode die al bestaat.

Deze bepalingen staan in het 'Besluit verplichte verzekering bij medisch-wetenschappelijk onderzoek met mensen 2015'. Dit besluit staat in de Wettenbank van de overheid (<https://wetten.overheid.nl>).

Bijlage C: Schema onderzoekshandelingen

Hieronder vind u een schema van de onderzoekshandelingen. De tijd die er naast staat is een indicatie van hoe lang elke stap ongeveer duurt.

Handeling	Tijd	Totale tijd
Intake met laatste informatie over het onderzoek	10 min	10 min
Ondertekenen toestemmingsformulier	2 min	12 min
Plaatsnemen op de CT tafel	2 min	14 min
Voeten vastmaken aan de voetplaten en in neutrale stand zetten	3 min	17 min
CT-scan maken van voeten in neutrale stand	1 min	18 min
Stand van de voeten veranderen en CT-scan maken in elk van de 4 extreme standen	15 min	33 min
Voeten losmaken van de voetplaten. Einde onderzoek	2 min	35 min

Bijlage D: toestemmingsformulier proefpersoon

INFINITY ENKELPROTHESE INKLEMMING

- Ik heb de informatiebrief gelezen. Ook kan ik vragen stellen. Mijn vragen zijn goed genoeg beantwoord. Ik had genoeg tijd om te beslissen of ik meedoe.
- Ik weet dat meedoen vrijwillig is. Ook weet ik dat ik op ieder moment kan beslissen om toch niet mee te doen met het onderzoek. Of om ermee te stoppen. Ik hoef dan niet te zeggen waarom ik wil stoppen.
- Ik geef de onderzoeker toestemming om mijn specialist die mij behandelt te laten weten dat ik meedoe aan dit onderzoek.
- Ik geef de onderzoekers toestemming om mijn gegevens te verzamelen en gebruiken. De onderzoekers doen dit alleen om de onderzoeksvraag van dit onderzoek te beantwoorden.
- Ik weet dat voor de controle van het onderzoek sommige mensen al mijn gegevens kunnen inzien. Die mensen staan in deze informatiebrief. Ik geef deze mensen toestemming om mijn gegevens in te zien voor deze controle.
- Ik weet dat mijn gecodeerde gegevens naar landen buiten de EU worden gestuurd waar privacyregels van de EU niet gelden. Ik geef hiervoor toestemming.
- Wilt u in de tabel hieronder ja of nee aankruisen?

Ik geef toestemming om mijn gegevens te bewaren om dit te gebruiken voor ander onderzoek, zoals in de informatiebrief staat.	Ja <input type="checkbox"/>	Nee <input type="checkbox"/>
Ik geef toestemming om mij eventueel na dit onderzoek te vragen of ik wil meedoen met een vervolgonderzoek.	Ja <input type="checkbox"/>	Nee <input type="checkbox"/>

- Ik wil meedoen aan dit onderzoek.

Mijn naam is (proefpersoon):

Handtekening:

Datum : __ / __ / __

Ik verklaar dat ik deze proefpersoon volledig heb geïnformeerd over het genoemde onderzoek.

Wordt er tijdens het onderzoek informatie bekend die de toestemming van de proefpersoon kan beïnvloeden? Dan laat ik dit op tijd weten aan deze proefpersoon.

Naam onderzoeker (of diens vertegenwoordiger):.....

Handtekening:.....

Datum: __ / __ / __

Bijlage E: Toestemmingsformulier vertegenwoordiger

INFINITY ENKELPROTHESE INKLEMMING

Ik ben gevraagd om toestemming te geven voor deelname van deze persoon aan dit medisch-wetenschappelijke onderzoek:

Naam proefpersoon:

- Ik heb de informatiebrief voor de proefpersoon/vertegenwoordiger gelezen. Ook kon ik vragen stellen. Mijn vragen zijn goed genoeg beantwoord. Ik had genoeg tijd om te beslissen of ik wil dat deze persoon meedoet.
- Ik weet dat meedoen vrijwillig is. Ook weet ik dat ik op ieder moment kan beslissen dat deze persoon toch niet mee doet. Ik hoef dan niet te zeggen waarom ik dat wil.
- Ik geef de onderzoeker toestemming om de specialist die deze persoon behandelt te laten weten dat deze persoon meedoet aan dit onderzoek.
- Ik geef de onderzoekers toestemming om de gegevens van deze persoon te verzamelen en te gebruiken. De onderzoekers doen dit om alleen de onderzoeksvraag in dit onderzoek te beantwoorden.
- Ik weet dat voor de controle van het onderzoek sommige mensen toegang tot alle gegevens van deze persoon kunnen krijgen. Die mensen staan in deze informatiebrief. Ik geef deze mensen toestemming om de gegevens van deze persoon in te zien voor deze controle.
- Ik weet dat gecodeerde gegevens van deze persoon naar landen buiten de EU worden gestuurd waar privacyregels van de EU niet gelden. Ik geef hiervoor toestemming.
- Wilt u in de tabel hieronder ja of nee aankruisen?

Ik geef toestemming om de gegevens van deze persoon te bewaren om dit te gebruiken voor ander onderzoek, zoals in de informatiebrief staat.	Ja <input type="checkbox"/>	Nee <input type="checkbox"/>
Ik geef toestemming om deze persoon na dit onderzoek te vragen of hij/zij wil meedoen met een vervolgonderzoek.	Ja <input type="checkbox"/>	Nee <input type="checkbox"/>

- Ik ga ermee akkoord dat deze persoon meedoet aan dit onderzoek.

Naam wettelijk vertegenwoordiger:.....

Relatie tot de proefpersoon:

Handtekening:

Datum: __ / __ / __

Ik verklaar dat ik de persoon/personen hierboven volledig heb geïnformeerd over het genoemde onderzoek.

Wordt er tijdens het onderzoek informatie bekend die de toestemming van de vertegenwoordiger kan beïnvloeden? Dan laat ik dit op tijd aan hem/haar weten.

Naam onderzoeker (of diens vertegenwoordiger):.....

Handtekening:

Datum: __ / __ / __

Appendix D nnU-Net manual

Protocol methods training nnU-Net to segment foot bones

In this protocol, the protocol of training the machine learning network “nnU-Net” to automatically segment the bones in the foot and ankle is presented. Once trained, the model is able to load a CT scan of the foot and assign labels to the respected bones. This protocol only focuses on the foot and ankle and what settings of model training work best for this specific dataset, but nnU-Net can be used for a multitude of medical scans. The steps in this protocol can be followed for other scans as well, but some tweaking may be required.

1. Scan preprocessing

In the first chapter, the preprocessing of CT scans of the foot with pre-assigned segmentations in 3D Slicer 5.6.2 is discussed. To download 3D Slicer, use the following URL <https://download.slicer.org/>. Download the ‘Stable Release’ of your own system.

2. Setting up nnU-Net

In the second chapter, the nnU-Net environment is set up, and the preprocessed data is stored according to the architecture of nnU-Net.

3. nnU-Net training

In the third chapter, nnU-Net is trained on the data and model performance is evaluated.

4. Segmentation postprocessing

In the fourth chapter, test scans are segmented, post-processed and loaded into Slicer 5.6.2

Contents

1.	CT scan preprocessing protocol 3D Slicer 5.6.2	3
1.1	Download data	3
1.2	Import data.....	3
1.3	Transforming the CT scan.....	4
1.4	Cropping the CT scan and segmentation	5
1.5	Removing unwanted segments / altering segments	8
1.6	Create labelmap and export data	8
1.7	Repeat for all remaining scans	9
2.	Setting up nnU-Net in an online environment.....	10
2.1	Install nnU-Net.....	10
2.2	Setting up data folders	10
2.3	Setting up paths.....	12
2.4	Planning and preprocessing	13
3.	Training nnU-Net using Slurm	14
3.1	nnU-Net training	14
3.2	Investigating and adjusting training scripts.....	14
3.3	Slurm batch training.....	16
3.4	Evaluate model performance	17
3.5	Determine optimal model.....	18
4.	Scan segmentation and postprocessing	19

1. CT scan preprocessing protocol 3D Slicer 5.6.2

In this chapter, the preprocessing of segmented CT scans using 3D Slicer 5.6.2 is discussed. To download 3D Slicer, use the following URL <https://download.slicer.org/>. Download the ‘Stable Release’ of your own system.

1.1 Download data

First, the lower body CT scans and segmentations are downloaded from this database: <https://zenodo.org/records/8302449>. The database contains 30 zip-files, each containing a full lower-body CT scan with segmentations of all the bones in the scan (Fig. 1).

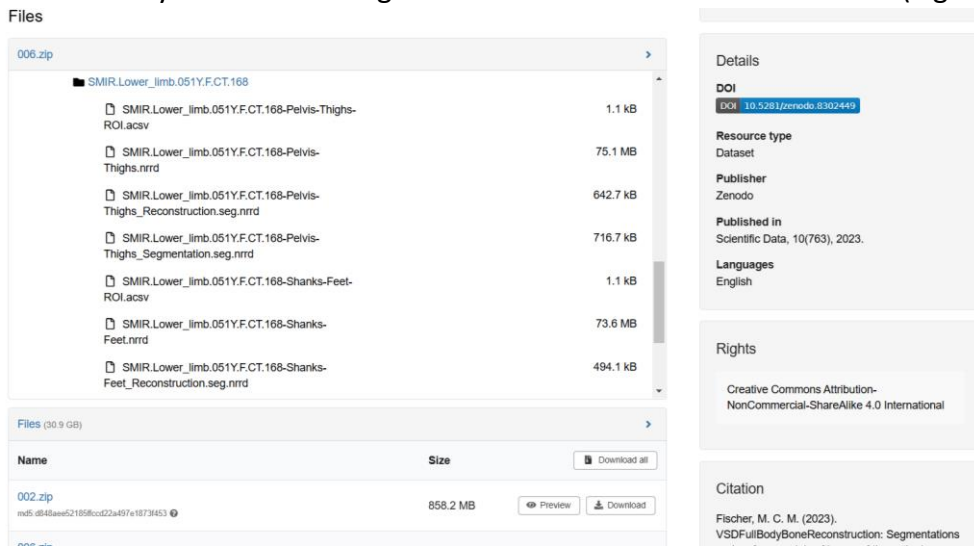


Figure 1: Lower body CT scan segmentation database

Download every zip-file, except from z057 as its CT scan is not useful, and unzip.

1.2 Import data

With the data downloaded, it’s time to load the first CT scan and its segmentations into Slicer.

1. Open Slicer and select ‘Add Data’ in the home screen (Fig. 2).

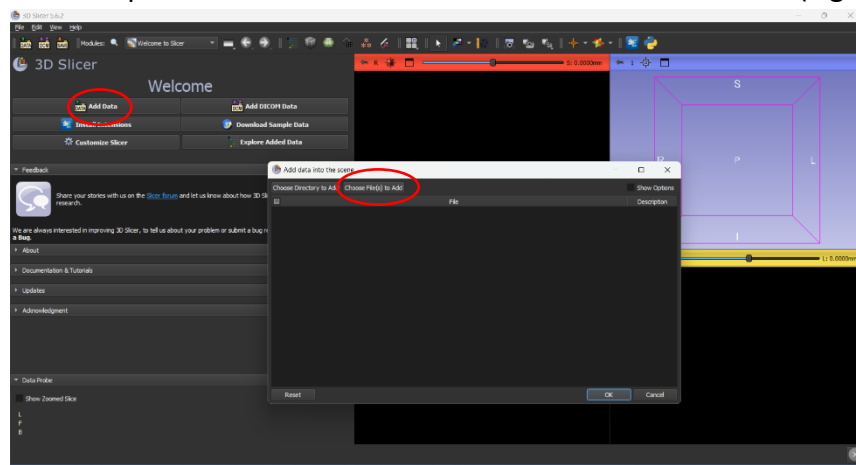


Figure 2: Adding data in Slicer

2. Select in ‘Choose File(s) to Add’ the files ending in ‘Shanks-Feet.nrrd’ and ‘Shanks-Feet_Reconstruction.seg.nrrd’, and for the folders starting with ‘z’ also the ‘Transform-Upside-Down.h5’ file.

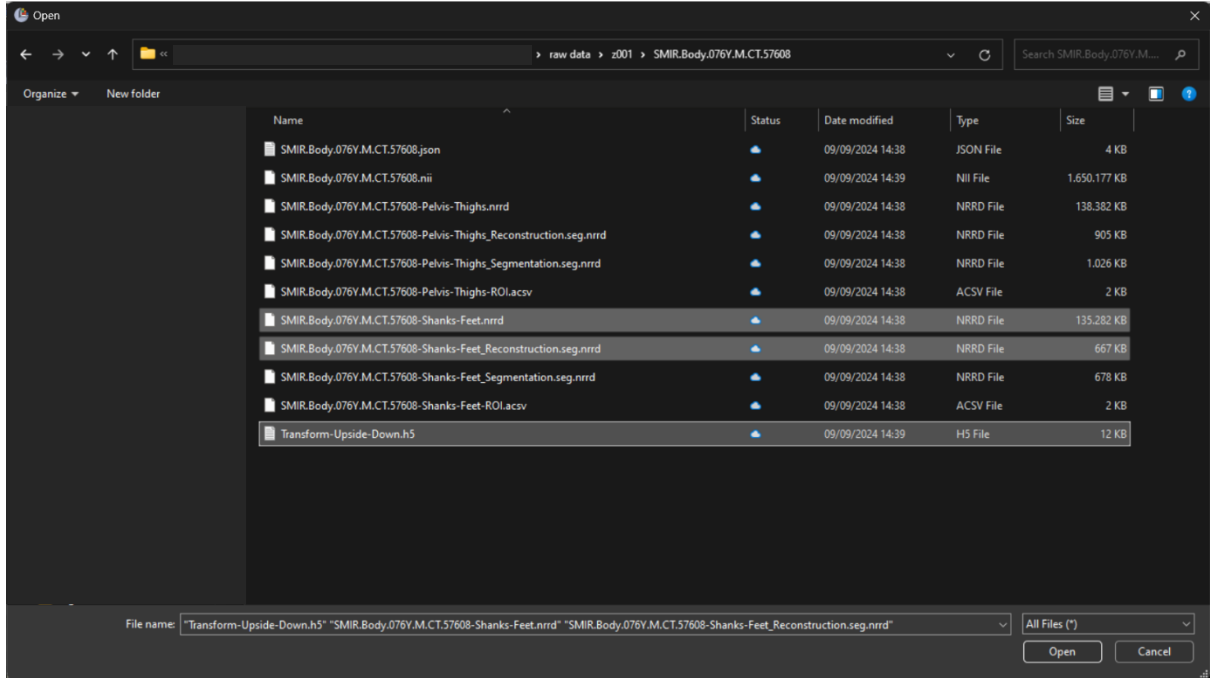


Figure 3: Selecting the CT scan and segmentation files

3. Click ‘OK’

1.3 Transforming the CT scan

This section is only applicable for the ‘z’-folders (such as ‘z001’, ‘z004’, etc.) as those have been transformed upside-down. For preprocessing the data in the non-‘z’-folders (such as ‘002’, ‘006’, etc.) skip this section and continue with section 1.4.

1. Go to the ‘Transforms’ menu (Fig. 4)

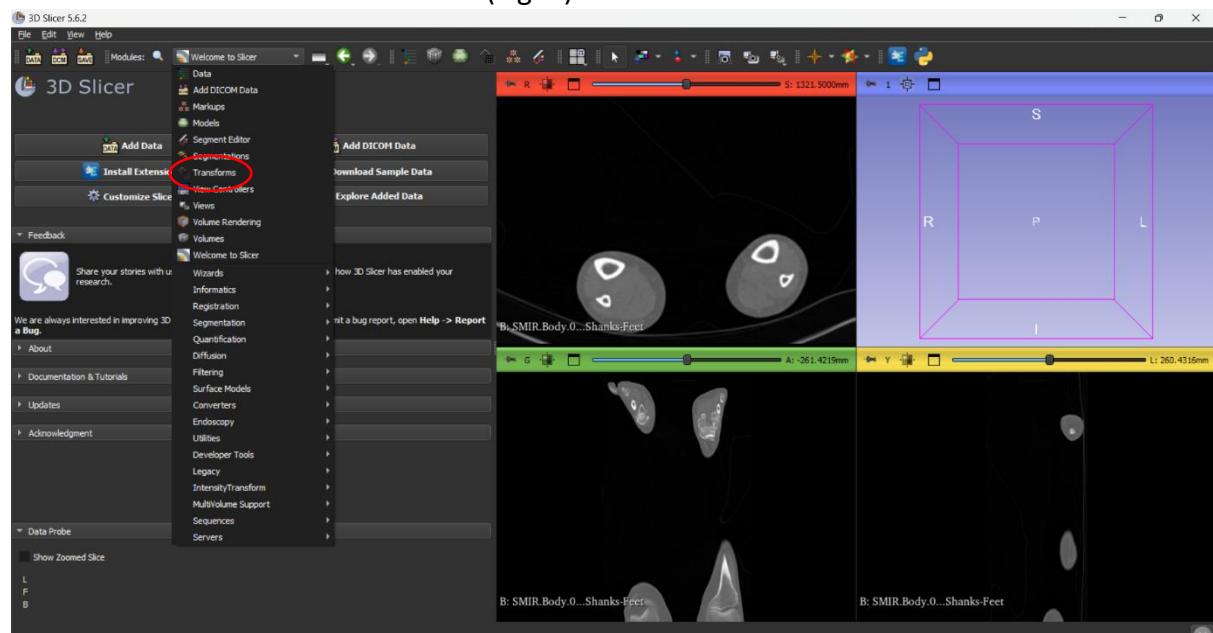


Figure 4: Navigating to the ‘Transforms’ menu

2. In the ‘Transforms’ menu, the active transform is already set to ‘Transform-Upside-Down’ if it has been loaded. This transformation matrix rotates the CT scan along the y-axis to align with the segmentations (Fig. 5).
3. In the ‘Apply transform’ section, select the scan (file ending in ‘Shanks-Feet’), click the green arrow to the right and then the bottom button to ‘Harden’ the transformation (Fig. 5).

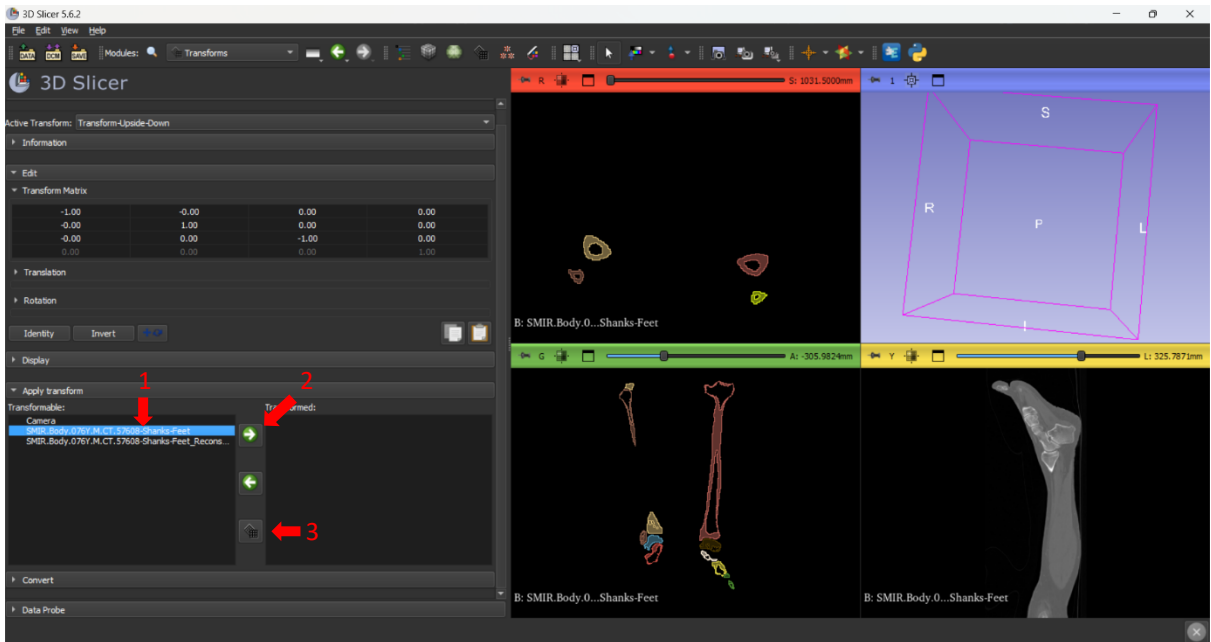


Figure 5: Transforming the upside-down image to normal orientation

4. You will find that the scan is gone from the image viewer, but this is due to the field of view of the upside-down scan not corresponding to the normal scan. To fix this, simply right click on the three scan views and select ‘Reset Field of View’ (Fig. 6)

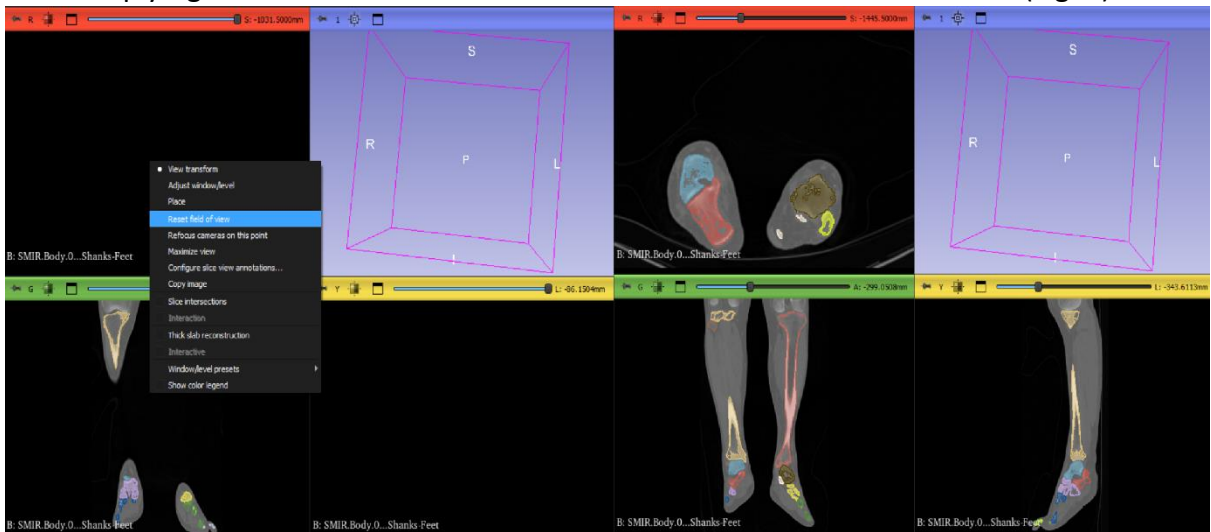


Figure 6: Before and after resetting the field of view for the transformed CT scan

1.4 Cropping the CT scan and segmentation

Since this protocol focuses on training nnU-Net to segment foot and ankle CT scans, we are only interested in everything below ~5 cm above the Talus. For that reason, the CT scan and segmentation should be cropped to only include the necessary data.

1. In the navigation menu, go to ‘Converters’ and select ‘Crop Volume’ (Fig. 7).

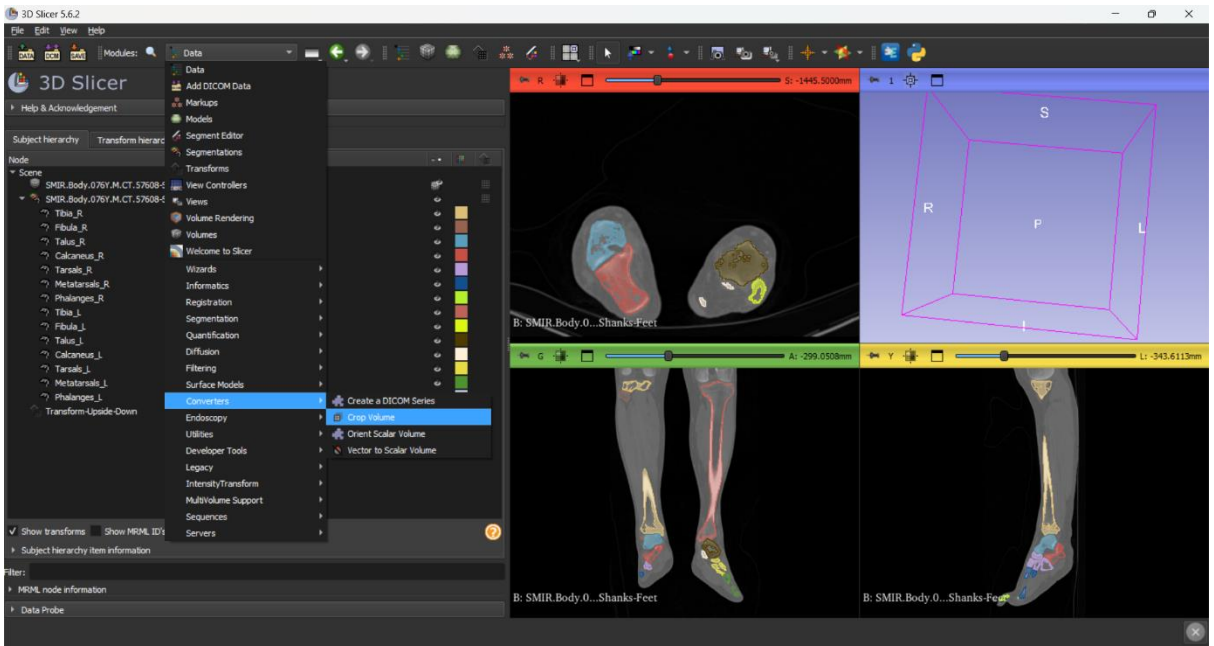


Figure 7: Navigating to ‘Crop Volume’

2. The ‘Input volume’ should display the CT scan. At ‘Input ROI’ select ‘Create new ROI as...’ and name it something recognizable. At ‘Output volume’ select ‘Create new volume as...’ and name it according to the naming conventions of nnU-Net (explained in Chapter 2). The format is ‘DatasetName_ScanNumber_0000’, so for example ‘Foot_001_0000’. For the rest of this protocol, the name of the new volume is Foot_001_0000.
3. Position the ROI box over the scan and include everything of both feet under ~5 cm above the Talus (Fig. 8).

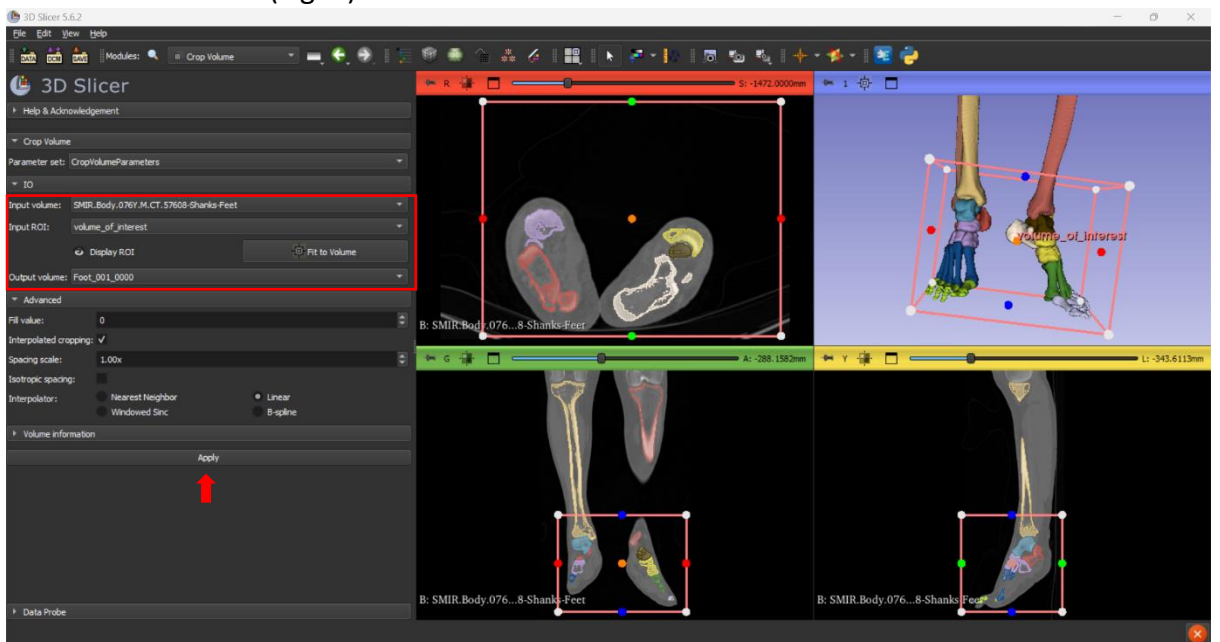


Figure 8: Cropping the CT scan volume to only include everything below 5cm above Talus

4. Click ‘Apply’

- Now go back to the ‘Data’ menu and unselect the eye on the old volume to not show it anymore and select the eye on the ‘Foot_001_0000’ to show it.
- Go to ‘Segment Editor’ (Fig. 9).

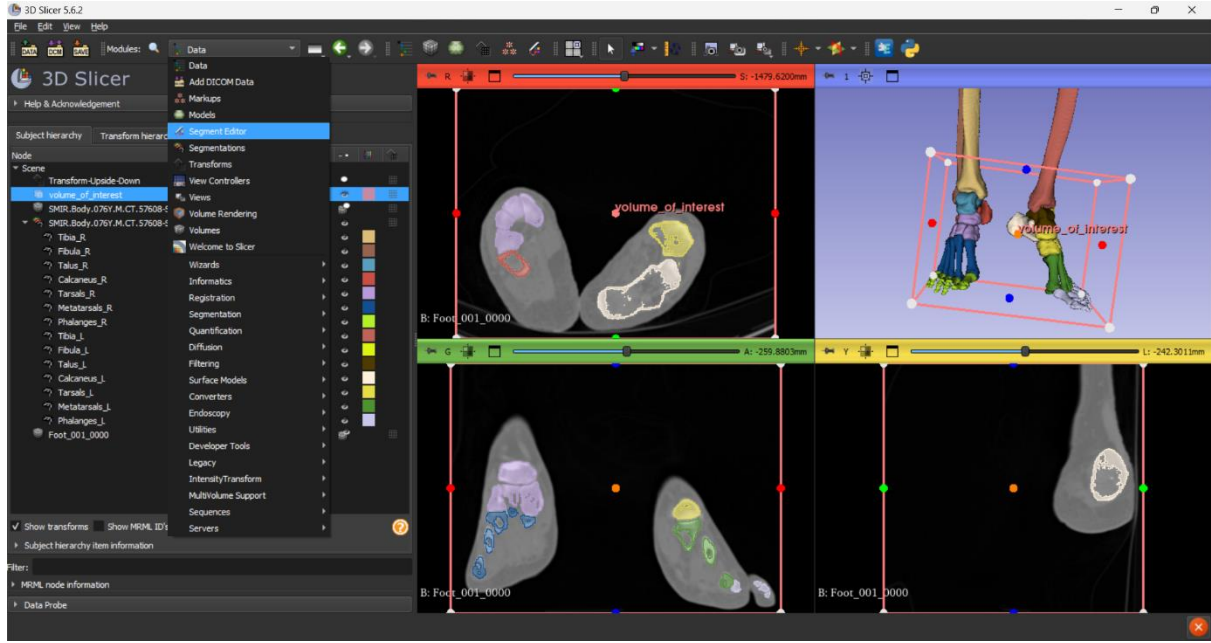


Figure 9: Navigating to ‘Segment Editor’

- The segmentations outside the ROI should be removed. To do this, select the segmentations one at a time and use the ‘Scissors’ tool to ‘Erase outside’ the ROI (Fig. 10). Do this for ‘Tibia_R’, ‘Fibula_R’, ‘Tibia_L’, and ‘Fibula_L’.

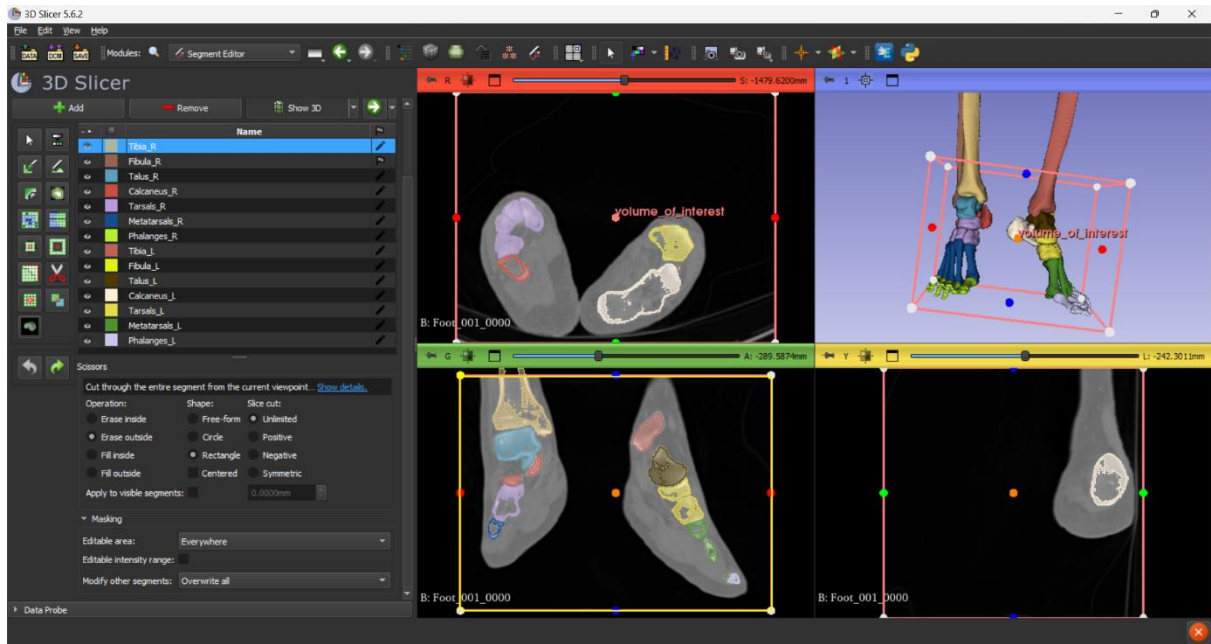


Figure 10: With ‘Tibia_R’ selected, use the ‘Scissors’ tool, operation ‘Erase outside’ with ‘Rectangle’ shape and follow the shape of the ROI in the Coronal view (bottom right). This removes everything from the ‘Tibia_R’ segment outside the ROI.

8. The final step is to make sure that the geometry of ‘Foot_001_0000’ and the cropped segmentations is the same. To do this, go to ‘Segmentation geometry’, select the ‘Foot_001_0000’ for ‘Source geometry’ and click ‘OK’ (Fig. 11).

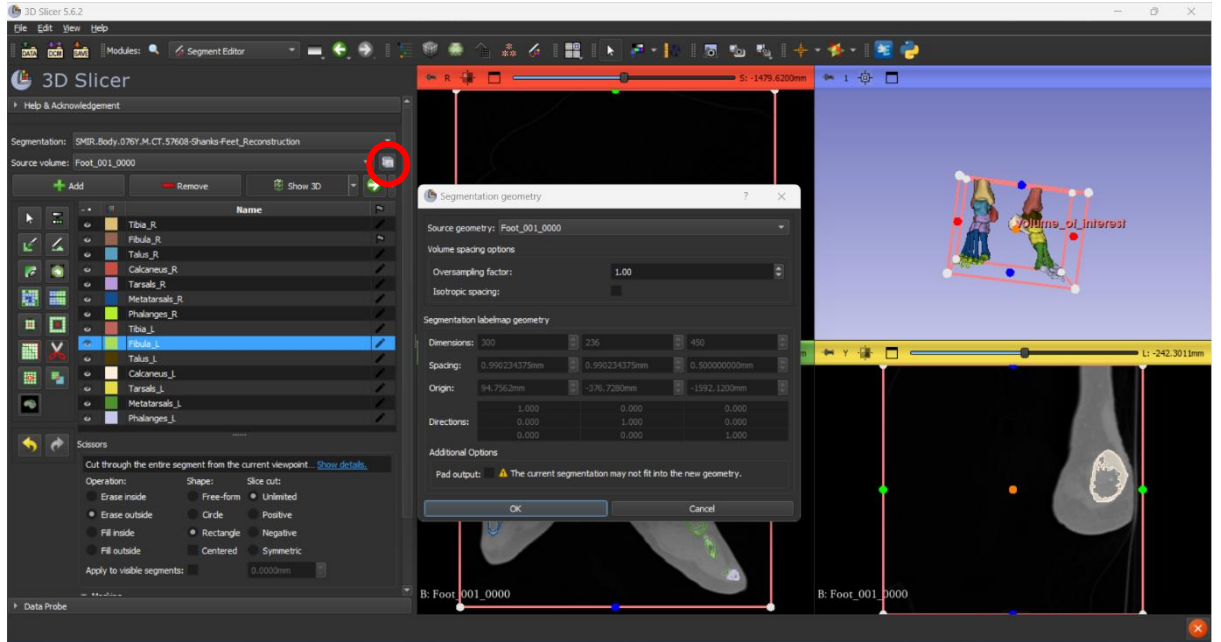


Figure 11: Aligning the geometry of Foot_001_0000 and the cropped segmentation

1.5 Removing unwanted segments / altering segments

If you want your nnU-Net segmentation model to segment only a couple of foot bones or segment each bone separately, you can change the segments using the ‘Segment Editor’. For this protocol, the current segmentation is enough so we won’t change them. For tutorials on how to edit segments in Slicer, see the online documentation:

https://slicer.readthedocs.io/en/5.6/user_guide/modules/segmentededitor.html.

1.6 Create labelmap and export data

Once the scan and segmentation are cropped (and edited), it’s time to export the data.

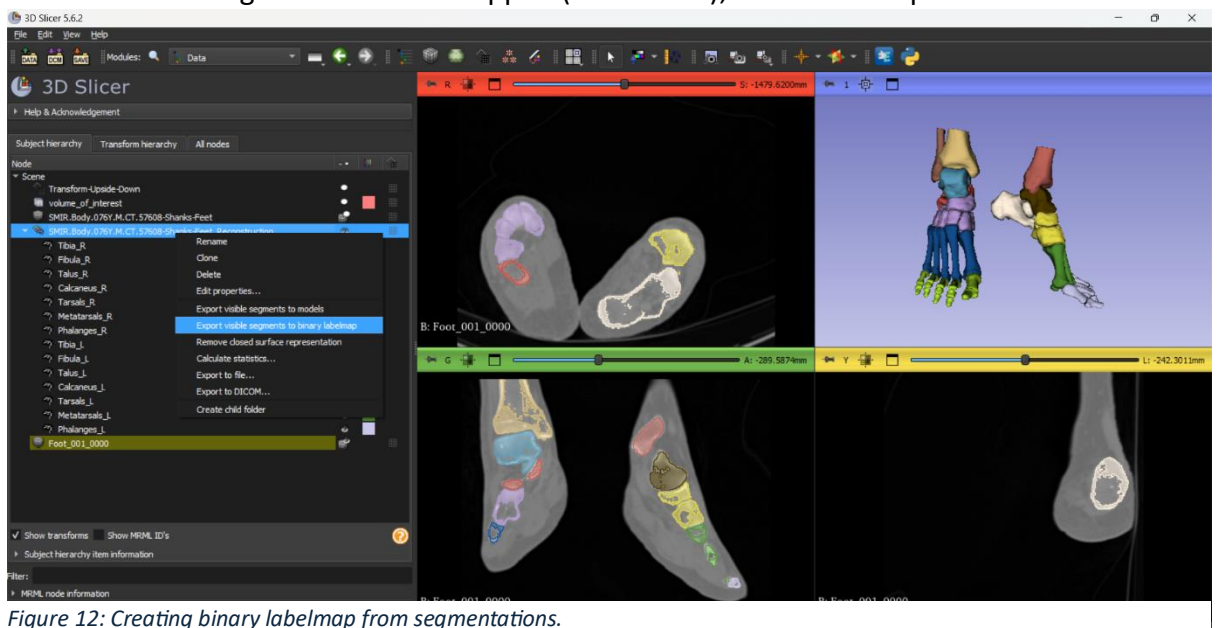


Figure 12: Creating binary labelmap from segmentations.

1. Go to the 'Data' menu and select the segmentation object. Right click and select 'Export visible segments to binary labelmap' (Fig. 12). This creates a labelmap object, a 3D-matrix with 0's for the background and integers corresponding to the labels. In this case, 1 up until 14 corresponding to 'Tibia_R' up until 'Phalanges_L', respectively.
2. Right click on the labelmap and rename to the correct naming convention for labels in nnU-Net. For this case, it's 'Foot_001'. Right click again and select 'Export to file'. Select the correct directory, change the 'Export format' to 'NifTI (.nii.gz.)' and uncheck 'Compress'. The filename should automatically change to Foot_001.nii.gz. Click 'Export' (Fig. 13).
3. Do the same to export 'Foot_001_0000.nii.gz'.

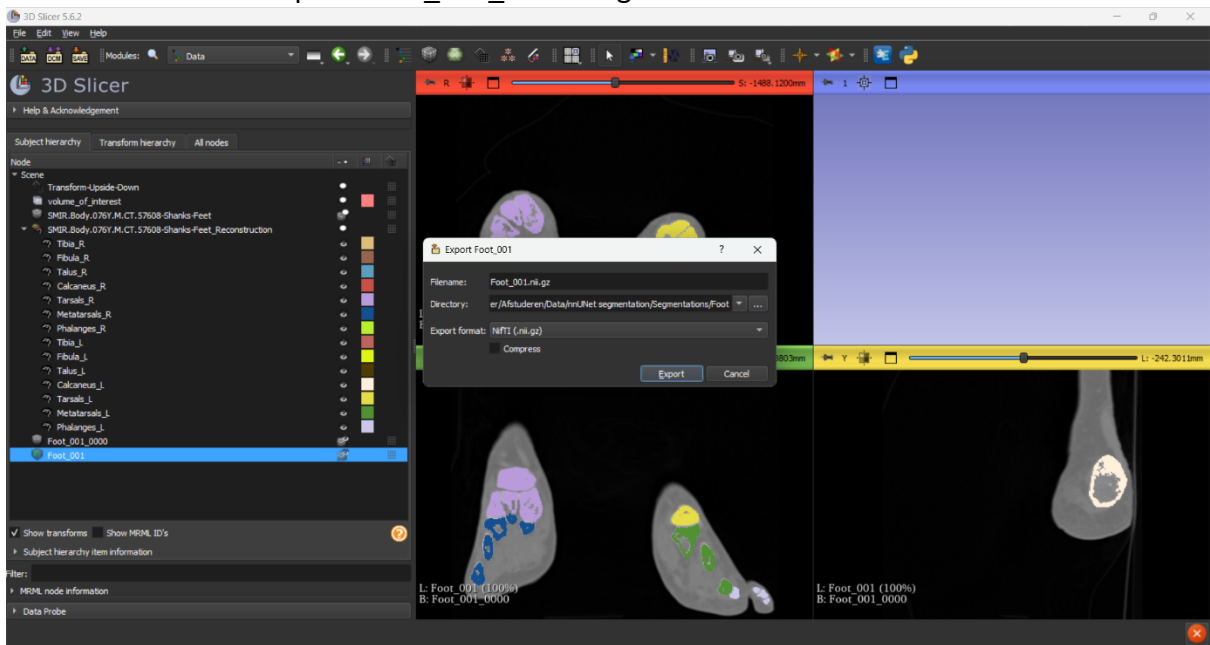


Figure 13: Export to NifTI file

1.7 Repeat for all remaining scans

The folder where the NifTI files are stored should include one CT scan (Foot_001_0000.nii.gz) and one labelmap (Foot_001.nii.gz) for all 29 segmented scans.

2. Setting up nnU-Net in an online environment

In this chapter, the nnU-Net environment is set up, and the preprocessed data is stored according to the conventions of nnU-Net. This protocol uses an online environment to access high performance GPUs necessary for training. For TU/e students and employees, see <https://hpc.tue.nl>. For people outside of TU/e, check how you can access high performance GPUs with a virtual environment.

The steps in this chapter are also described on the Github page of nnU-Net:
<https://github.com/MIC-DKFZ/nnUNet/tree/master/documentation>

2.1 Install nnU-Net

To install nnU-Net in a virtual environment, you need to use a program with a terminal to execute pip code. This protocol uses JupyterLab.

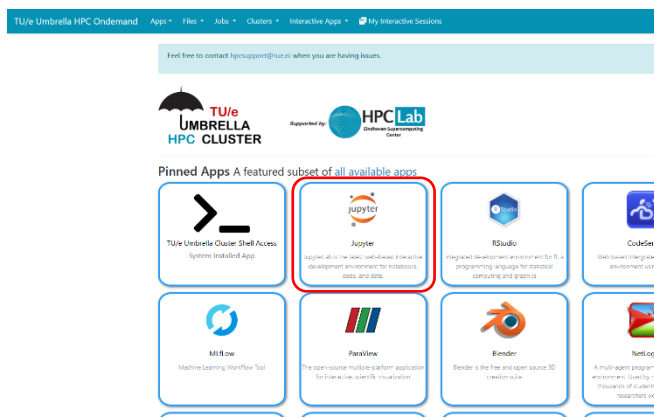


Figure 14: TU/e Umbrella HPC Cluster homepage with JupyterLab

A screenshot of the JupyterLab server setup interface. It includes fields for Jupyter version (4.0.5 with CUDA 12.1, SciPy-bundle, PyTorch 2.x, TensorFlow and H5py), Partition/Queue where Jupyter will be running (bmc_gpustudent.q), Maximum number of hours Jupyter will be running (4), Number of CPU cores available to Jupyter (6), Total CPU Memory available to Jupyter (16GB), and Number of GPU available to Jupyter (1). There is also a checkbox for "I would like to receive an email when the session starts" and a "Launch" button at the bottom. A note at the bottom states: "* The Jupyter session data for this session can be accessed under the data root directory."

Figure 15: JupyterLab server presets

1. Select JupyterLab (Fig. 14) and choose the type of JupyterLab server needed for the task (Fig. 15). Make sure you select the version with PyTorch 2.x and Tensorflow. The Partition should have a gpu. Select the highest possible running time, 6 CPU cores should be enough, and 16GB of CPU memory is advised.
2. JupyterLab automatically opens a terminal for bash commands. To install nnU-Net as an integrative framework (a copy of the nnU-Net code in the folder so the code can be modified), write the following code in the terminal one row at a time:

```
git clone https://github.com/MIC-DKFZ/nnUNet.git  
cd nnUNet  
pip install -e .
```

- The first line clones the nnU-Net Github repository to the home directory, creating a folder 'nnUNet' containing the contents of the repository
- The second line changes the current directory to the nnUNet folder
- The final line installs the nnU-Net environment functions. Make sure not to forget the . after pip install -e

2.2 Setting up data folders

Now that nnU-Net is successfully installed, the next step is to create the directories where training and testing data are stored. The architecture of nnU-Net is composed such that it

relies on specific variables to know where the data is stored. To this end, the following three directories must be set: nnUNet_raw, nnUNet_preprocessed, and nnUNet_results.

nnUNet_raw contains the train and test scans and labels as well as metadata for each dataset. nnUNet_preprocessed is where preprocessed data and train presets are stored. nnUNet_results is where model weights and training results are stored.

nnUNet_preprocessed and nnUNet_results are empty to start with.

Extensive information on the nnU-Net dataset format can be found on:

https://github.com/MIC-DKFZ/nnUNet/blob/master/documentation/dataset_format.md

1. In the nnUNet folder, create the three above subfolders such that the folder looks like this (Fig. 16)

Type	Name	Size	Modified at
directory	documentation	-	13-12-2024 16:57:23
directory	nnUNet_preprocessed	-	13-12-2024 17:15:22
directory	nnUNet_raw	-	13-12-2024 17:15:16
directory	nnUNet_results	-	13-12-2024 17:15:26
directory	nnunetv2	-	13-12-2024 16:57:23
directory	nnunetv2.egg-info	-	13-12-2024 17:00:32
file	LICENSE	11.43 kB	13-12-2024 16:57:23
file	pyproject.toml	4.27 kB	13-12-2024 16:57:23
file	readme.md	10.57 kB	13-12-2024 16:57:23
file	setup.py	69.00 B	13-12-2024 16:57:23

Figure 16: nnUNet folder containing the contents from the Github repository and the three data storage folders

2. Enter nnUNet_raw and create folders for your datasets. Datasets are identified according to the following naming convention: Dataset{dataset ID}_{dataset name}. The dataset ID is a three digit integer and the dataset name can be freely chosen: for example, Dataset001_Foot has ‘Foot’ as dataset name and the dataset ID is 1. If you have multiple segmentation datasets, create a folder for each one.

Each dataset folder contains the following four structures:

- A dataset.json file which contains the metadata information for the dataset,
- Folder imagesTr which contains the training images,
- Folder imagesTs which contains testing images (if needed),
- Folder labelsTr which contains the labelmaps for the training images.

3. In the Dataset001_Foot folder, create the dataset.json file and put the following information in:

```
{
  "name": "Foot_multilabel",
  "description": "Foot segmentation",
  "channel_names": {
    "0": "CT"
  },
  "labels": {
    "background" : 0,
    "skin" : 1,
    "fatty_tissue" : 2,
    "muscle" : 3,
    "tendon" : 4,
    "ligament" : 5,
    "cartilage" : 6,
    "bone" : 7
  }
}
```

```

    "Tibia_R" : 1,
    "Fibula_R" : 2,
    "Talus_R" : 3,
    "Calcaneus_R" : 4,
    "Tarsals_R" : 5,
    "Metatarsals_R" : 6,
    "Phalanges_R" : 7,
    "Tibia_L" : 8,
    "Fibula_L" : 9,
    "Talus_L" : 10,
    "Calcaneus_L" : 11,
    "Tarsals_L": 12,
    "Metatarsals_L" : 13,
    "Phalanges_L" : 14
},
"numTraining": 23,
"file_ending": ".nii.gz"
}

```

numTraining can be altered depending on the number of training images. A common train/test split is 80/20.

4. Add the train images and labels to the imagesTr and labelsTr folders, respectively. As mentioned in Section 1.4, each image should follow the same naming convention and the labelmaps should correspond in name and number. This means that label Foot_001.nii.gz corresponds to image Foot_001_0000.nii.gz.
5. Add the test images (if you have them) to the imagesTs folder. These should also follow the same naming convention. When testing the model with the test images, the resulting labelmaps will then have a corresponding name to the test images.
6. The folder Dataset001_Foot should then look like this (Fig. 17).

	Type	Name	Size	Modified at
□	📁	imagesTr	-	13-12-2024 17:49:22
□	📁	imagesTs	-	13-12-2024 17:49:26
□	📁	labelsTr	-	13-12-2024 17:49:30
□	📄	dataset.json	500.00 B	13-12-2024 17:41:29

Figure 17: Structure of dataset directories

2.3 Setting up paths

For nnU-Net to know where the raw data, preprocessed data, and trained models are located, some environment variables need to be set every time you start a new virtual environment (every new JupyterLab session and terminal).

1. First, make sure that the nnUNet directory is selected with `cd nnUNet`
2. Next, set up the following paths:

```

export PATH=$PATH:/home/20193158/.local/bin
export nnUNet_raw="/home/20193158/nnUNet/nnUNet_raw"
export nnUNet_preprocessed="/home/20193158/nnUNet/nnUNet_preprocessed"
export nnUNet_results="/home/20193158/nnUNet/nnUNet_results"

```

3. The exact path is specific to you, so make sure you copy it correctly. In the first row, the information between PATH: and ./local/bin should be changed

- DISCLAIMER: This step needs to happen for every new session or new terminal for nnU-Net to correctly find the directories.

2.4 Planning and preprocessing

The final step before model training is planning and preprocessing. During this step, nnU-Net extracts a dataset fingerprint from the new dataset. The fingerprint includes properties such as image sizes, voxel spacing, greyscale intensities, etc. Using these properties, an experiment plan is created for different U-Net configurations: 2D, 3D_fullres, 3D_lowres, and 3D_cascade_fullres.

- In the terminal (which was set up in 2.3), paste the following code and hit enter:

```
nnUNetv2_plan_and_preprocess -d 1 --verify_dataset_integrity
```

- nnUNetv2 calls on the library
- plan and preprocess is the function call
- d 1 calls Dataset001_Foot
- verify_dataset_integrity is a command that checks whether the dataset is correct

- If there are problems with the images and / or segmentations, this will result in an error. Find which images causes the errors and check in Slicer if the geometry was correctly matched between the image and segmentation (step 8 of section 1.4). You can easily check this by loading the labelmap and image in Slicer, navigating to 'Crop Volume' and comparing the volume information.
- If there are no errors, you should see this once the code is executed (Fig. 18).

```
Plans were saved to /home/20193158/nnUNet/nnUNet_preprocessed/Dataset001_Foot/nnUNetPlans.json
Preprocessing...
Preprocessing dataset Dataset001_Foot
Configuration: 2d...
100%|██████████| 23/23 [02:46<00:00,  7.25s/it]
Configuration: 3d_fullres...
100%|██████████| 23/23 [03:58<00:00, 10.38s/it]
Configuration: 3d_lowres...
100%|██████████| 23/23 [01:43<00:00,  4.49s/it]
```

Figure 18: Successful planning and preprocessing

- The preprocessed data is saved in the nnUNet_preprocessed folder for the dataset, distributed in folders for each configuration.
 - The dataset.json file is copied to the folder
 - A dataset_fingerprint.json file is created containing metadata for the dataset
 - An nnUNetPlans.json file is created containing information necessary for training the model with the different configurations.

3. Training nnU-Net using Slurm

In this chapter, nnU-Net is trained on the data and model performance is evaluated. First, the process of training is explained, then the training script is adjusted to have a better starting off point for training, then training is performed using Slurm for batch tasks, and finally the model performance is evaluated.

3.1 nnU-Net training

As mentioned Section 2.4, nnU-Net uses different configurations to train the model. Each of these configurations focuses on different parts and structures and thus result in a different model. nnU-Net has an integrated feature which can compare the models from different configurations and find the optimal model by combining them or choosing the best configuration. For this reason, it's best to just train nnU-Net for your dataset using all four configurations.

For each configuration, nnU-Net uses 5-fold cross-validation over the training cases. This means that the model is trained 5 times using a different set of training and validation cases. In this case, we have 23 training cases in total which is then split in 18 training and 5 validation cases. nnU-Net randomly chooses the validation split. The 5-fold cross-validation is needed so nnU-Net can estimate the model performance, and it allows for combining the 5 models for better performance, even when the dataset is not very large.

Training nnU-Net requires one command with the following structure:

```
nnUNetv2_train DATASET_NAME_OR_ID UNET_CONFIGURATION FOLD --npz
```

or

```
nnUNetv2_train 1 2d 0 --npz
```

In Section 3.3 it is explained how to efficiently train the model for multiple configurations and folds at the same time.

3.2 Investigating and adjusting training scripts

nnU-Net has a vast library of python scripts responsible for each step from pre-processing, to training, to scan inference, to finally post-processing. Generally, these scripts are good-to-go and can be used immediately and obtain good results. This is due to nnU-Net having integrated methods for adjusting processes depending on the dataset. For this reason, the pre-processing step is very important as it gives nnU-Net the necessary information for training. However, it might be useful to be aware of some adjustments you can do to improve model performance. These adjustments can be made in nnUNetTrainer.py.

1. From the main nnUNet folder, navigate to nnunetv2 (Fig. 19).

	Type	Name	Size	Modified at
□	📁	documentation	-	13-12-2024 16:57:23
□	📁	nnUNet_preprocessed	-	16-12-2024 16:14:10
□	📁	nnUNet_raw	-	13-12-2024 17:22:53
□	📁	nnUNet_results	-	13-12-2024 17:15:26
□	📁	nnunetv2	-	16-12-2024 15:16:05
□	📁	nnunetv2.egg-info	-	13-12-2024 17:00:32
□	📄	LICENSE	11.43 kB	13-12-2024 16:57:23
□	📄	pyproject.toml	4.27 kB	13-12-2024 16:57:23
□	📄	readme.md	10.57 kB	13-12-2024 16:57:23
□	📄	setup.py	69.00 B	13-12-2024 16:57:23

Figure 19: Navigating to the nnunetv2 folder with the code library

2. Go to ‘training/nヌNetTrainer/nヌNetTrainer.py’ and click ‘Edit’ (Fig. 20).

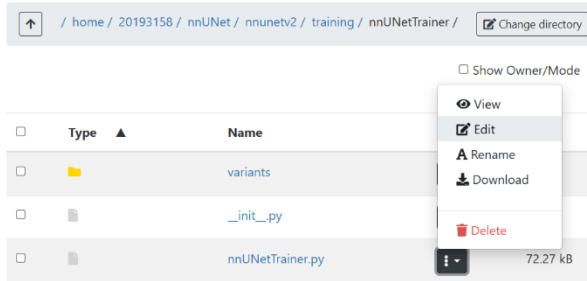


Figure 20: Opening nnUNetTrainer.py to edit

3. Scroll down to row 146 “### Some hyperparameters for you to fiddle with”. You will find some hyperparameters. It is advised to fiddle with these to see which work best for your dataset. For this dataset, these are the hyperparameters used:

```
### Some hyperparameters for you to fiddle with
self.initial_lr = 1e-3
self.weight_decay = 3e-5
self.oversample_foreground_percent = 0.7
self.num_iterations_per_epoch = 250
self.num_val_iterations_per_epoch = 50
self.num_epochs = 400
self.current_epoch = 0
self.enable_deep_supervision = True
```

- Initial_Lr is lowered from 1e-2 to 1e-3 to start more accurate
- Oversample_foreground_percent is increased from 0.33 to 0.7 to focus more on foreground voxels
- Num_epochs is reduced from 1000 to 400 to decrease training time and reduce the risk of overfitting

4. Scroll down to row 425 “def configure_rotation_dummyDA_mirroring_and_initial_patch_size(self). This function causes rotation and mirroring of the scans for a better fit. The mirroring is very useful in bodyparts where the anatomy is not mirrored, such as the abdomen. But as this dataset is of two feet (which are

mirrored) and we want the model to segment left and right separately, mirroring should be disabled.

5. To do this, find the variable ‘mirror_axes’ in both ‘if dim == 2’ and ‘elif dim == 3’ and replace the tuple (0, 1) or (0, 1, 2) with None.
6. Now you’ve disabled mirroring in the training script, the model should perform accurately, but mirroring also then needs to be disabled in the prediction script.
7. Navigate to “nnUNet/nunetv2/inference/predict_from_raw_data.py” and edit the file.
8. Scroll down to row 538 and set mirror_axes to None. This also disables mirroring during prediction with new data.

3.3 Slurm batch training

Now it’s time for training. The training command from Section 3.1 can be executed directly in the command terminal, but that way, it is not possible to run multiple trainings at the same time and be sure that everything goes well. To perform batch training, we use Slurm. From the TU/e supercomputing wiki “Slurm allows users to submit jobs to be performed on one or many nodes in a cluster, manage job queues, and query the status of jobs and queues.” See, <https://supercomputing.tue.nl/documentation/steps/jobs/>. How to use Slurm.

1. In JupyterLab, create a new text file in the nnUNet folder, put the following information in and save as ‘nnUNet_train_2d.sh’. This automatically makes it a Slurm job script.

```
#!/bin/bash

#SBATCH --job-name=train_2d          # Name that shows up in the job screen
#SBATCH --output=train_2d_%j.txt      # Name of the output file
#SBATCH --partition=tue.gpu.q        # Choose a partition that has GPUs
#SBATCH --time=1-23:00:00             # Choose a time long enough for the whole fold
training
#SBATCH --nodes=1                    # Ensure only 1 task runs at a time
#SBATCH --ntasks-per-node=1
#SBATCH --cpus-per-task=8
#SBATCH --mem=1G
#SBATCH --gres=gpu:1

# Load necessary modules
module load PyTorch/2.1.2-foss-2023a-CUDA-12.1.1
module load matplotlib/3.7.2-gfbf-2023a

# Set environment variables
export PATH=$PATH:/home/20193158/.local/bin
export nnUNet_raw="/home/20193158/nnUNet/nnUNet_raw"
export nnUNet_preprocessed="/home/20193158/nnUNet/nnUNet_preprocessed"
export nnUNet_results="/home/20193158/nnUNet/nnUNet_results"

nnUNetv2_train 1 2d 0 --npz      # Change the fold number (last integer) for every training
```

- Make sure that the partition you choose has GPUs and that you have access to it
- Use this script for every fold, just change the fold number. The folds range from 0 to 4 (5 folds)
- The --npz flag makes sure that predicted probabilities of the validation data is saved as .npz files. These are needed for emsembling later on.

- Create the same scripts for 3d_fullres, 3d_lowres, 3d_fullres_cascade (if there are plans in the preprocessing) and name accordingly.
- In the terminal, write the following command to submit the job:

```
sbatch nnUNet_train_2d.sh
```

- Do the same for the other four folds, such that all 5 folds for 2d are running.
- Do the same for the other configurations. Mind, there is a limit on the number of tasks that you can submit.

3.4 Evaluate model performance

Results of the training are stored in the nnUNet_results directory. For each dataset, there are folders for the different configurations (Fig. 21). These then contain folders for the

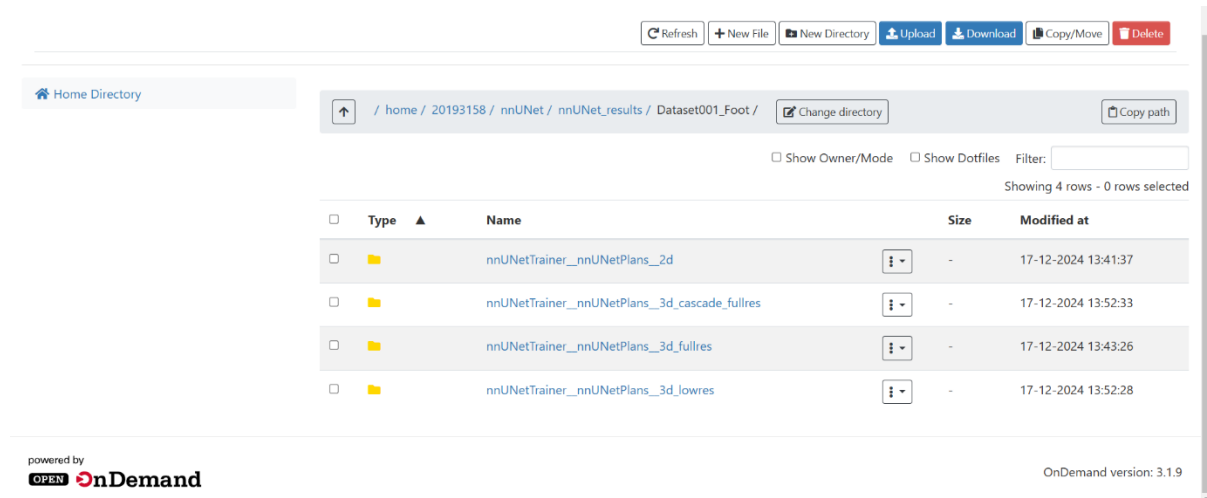


Figure 22: Results directory with folders for the 4 configurations

different folds, each with checkpoint files (useful when a training is interrupted); a debug.json file; a progress.png graph plotting the training loss, validation loss and pseudo dice scores for each epoch; and a training log updating for each epoch, showing the current learning rate, losses, epoch time, and pseudo dice scores (Fig. 22).

```
2024-12-17 13:48:07.034895: Epoch 3
2024-12-17 13:51:07.035025: Current learning rate: 0.00099
2024-12-17 13:51:16.019360: train_loss 0.0902
2024-12-17 13:51:16.020623: val_loss 0.0631
2024-12-17 13:51:16.821211: Pseudo dice [0.0033, 0.0, 0.0213, 0.0069, 0.0366, 0.2015, 0.0, 0.0688, 0.0, 0.0, 0.0, 0.0, 0.0142, 0.0]
2024-12-17 13:51:16.821677: Epoch time: 188.99 s
2024-12-17 13:51:16.822217: Yay! New best EMA pseudo Dice: 0.0106
2024-12-17 13:51:25.019360: train_loss 0.0778
2024-12-17 13:51:25.020623: val_loss 0.0529
2024-12-17 13:51:25.161040: Pseudo dice [0.0497, 0.0, 0.1699, 0.2131, 0.0394, 0.2, 0.0, 0.0831, 0.0, 0.0, 0.0, 0.0, 0.0638, 0.0]
2024-12-17 13:51:25.161523: Epoch time: 189.02 s
2024-12-17 13:51:35.051093: Yay! New best EMA pseudo Dice: 0.0153
2024-12-17 13:51:35.051545: Epoch 5
2024-12-17 13:51:35.053131: Current learning rate: 0.00099
```

Figure 21: Training log for 2d fold 0

nnU-Net uses the Dice-Sørensen index, or Dice score, to determine the difference between the ground-truth labelmaps and the predicted labels. The score scales between 0 and 1: the higher the Dice score, the more accurate the model.

3.5 Determine optimal model

Once every fold for every configuration is trained, it's time to find the optimal model. nnU-Net takes the .npz files from the validation and uses them to find the combination of trained models with the highest Dice scores.

1. In the terminal, write the following code:

```
nnUNetv2_find_best_configuration 1
```

This command will combine the trained models and also determine the best postprocessing of the applied model. Postprocessing means removal of all but the largest component in the predicted labelmap. If postprocessing is applied, it will result in a prediction which is less focused on details and more on the overall shape of the bones.

2. If you want to only use specific configurations, you can do so by adding to the command `-c "3d_fullres" "3d_lowres" "3d_cascade_fullres"`, for example.
3. Once completed, the command will print to your console exactly what commands you need to run to make predictions. It will also create two files in the results folder for you to inspect:
 - `inference_instructions.txt` again contains the exact commands you need to use for predictions
 - `inference_information.json` can be inspected to see the performance of all configurations and ensembles, as well as the effect of the postprocessing plus some debug information.
4. The output console will look something like this, giving you information about what steps were performed (Fig. 23)
5. In this case, nnU-Net found that the best possible model is an ensemble of “3d_fullres” 3d_cascade_fullres”, so these configurations are used for segmentation.

```
[20193158@bmc-gpu001 nnUNet]$ nnUNetv2_find_best_configuration 1 -c "3d_fullres" "3d_lowres" "3d_cascade_fullres"

***All results:***
nnUNetTrainer_nnUNetPlans_3d_fullres: 0.872940697940141
nnUNetTrainer_nnUNetPlans_3d_lowres: 0.8614548610191865
nnUNetTrainer_nnUNetPlans_3d_cascade_fullres: 0.8667548636842304
ensemble_nnUNetTrainer_nnUNetPlans_3d_fullres_nnUNetTrainer_nnUNetPlans_3d_lowres_nnUNetTrainer_nnUNetPlans_3d_cascade_fullres_0_1_2_3_4: 0.8722636241610077
ensemble_nnUNetTrainer_nnUNetPlans_3d_fullres_nnUNetTrainer_nnUNetPlans_3d_lowres_nnUNetTrainer_nnUNetPlans_3d_cascade_fullres_0_1_2_3_4: 0.873437121832091
ensemble_nnUNetTrainer_nnUNetPlans_3d_lowres_nnUNetTrainer_nnUNetPlans_3d_cascade_fullres_0_1_2_3_4: 0.8678292638983196
ensemble_nnUNetTrainer_nnUNetPlans_3d_fullres_nnUNetTrainer_nnUNetPlans_3d_cascade_fullres_0_1_2_3_4: 0.8734371218332091

*Best*: ensemble_nnUNetTrainer_nnUNetPlans_nnUNetTrainer_nnUNetPlans_3d_cascade_fullres_0_1_2_3_4: 0.8734371218332091

***Determining postprocessing for best model/ensemble:***
Removing all but the largest foreground regions did not improve results!
Removing all but the largest component for 1 did not improve results! Dice before: 0.8832 after: 0.87843
Results were improved by removing all but the largest component for 2. Dice before: 0.86847 after: 0.86849
Results were improved by removing all but the largest component for 3. Dice before: 0.90278 after: 0.90281
Results were improved by removing all but the largest component for 4. Dice before: 0.88241 after: 0.88242
Results were improved by removing all but the largest component for 5. Dice before: 0.87092 after: 0.87092
Results were improved by removing all but the largest component for 6. Dice before: 0.87338 after: 0.87305
Removing all but the largest component for 7 did not improve results! Dice before: 0.84013 after: 0.56887
Results were improved by removing all but the largest component for 8. Dice before: 0.90193 after: 0.91206
Results were improved by removing all but the largest component for 9. Dice before: 0.89254 after: 0.89661
Results were improved by removing all but the largest component for 10. Dice before: 0.93237 after: 0.94566
Results were improved by removing all but the largest component for 11. Dice before: 0.88441 after: 0.88442
Results were improved by removing all but the largest component for 12. Dice before: 0.848 after: 0.85912
Results were improved by removing all but the largest component for 13. Dice before: 0.82407 after: 0.84311
Removing all but the largest component for 14 did not improve results! Dice before: 0.8039 after: 0.51338

***Run inference like this:***
An ensemble won! What a surprise! Run the following commands to run predictions with the ensemble members:
nnUNetv2_predict -d Dataset001_Foot -i INPUT_FOLDER -o OUTPUT_FOLDER_MODEL_1 -f 0 1 2 3 4 -tr nnUNetTrainer -c 3d_fullres -p nnUNetPlans --save_probabilities
nnUNetv2_predict -d Dataset001_Foot -i INPUT_FOLDER -o OUTPUT_FOLDER_MODEL_2 -f 0 1 2 3 4 -tr nnUNetTrainer -c 3d_cascade_fullres -p nnUNetPlans --save_probabilities

The run ensembling with:
nnUNetv2_ensemble -i OUTPUT_FOLDER_MODEL_1 OUTPUT_FOLDER_MODEL_2 -o OUTPUT_FOLDER -np 8
***Once inference is completed, run postprocessing like this:***
nnUNetv2_apply_postprocessing -i OUTPUT_FOLDER -o OUTPUT_FOLDER_PP -pp_pk1_file /home/20193158/nnUNet/nnUNet_results/Dataset001_Foot/ensembles/ensemble_nnUNetTrainer_nnUNetPlans_3d_fullres_nnUNetTrainer_nnUNetPlans_3d_cascade_fullres_0_1_2_3_4/planc.json
```

Figure 23: nnU-Net configuration ensembling output

4. Scan segmentation and postprocessing

In this chapter, the trained model is used to segment the test scans and postprocess them for further use. The new labelmaps are loaded into Slicer where they can be converted into segmentation files or digital models.

4.1 Perform inference on the test scans

Once the model is trained and the best model is chosen, it's time to apply the model on the test scans to see the results.

1. Go to the results folder and open the file “inference_instructions.txt”
2. At the top, it reads “***Run inference like this:***”. Edit the command (or commands if an ensemble of multiple configurations was the best combination) and replace “INPUT_FOLDER” with the path to the folder containing the test scans in the “nnUNet_raw” directory.
3. In the results folder, create a new folder (or multiple for an ensemble) to store the new labelmaps. In this case, five folders were created (Fig. 24).



Figure 24: Output folders for the test scan inference results.

4. In the inference instructions, replace “OUTPUT_FOLDER” with the output folder path.
5. This model uses an ensemble of “3d_fullres” and “3d_cascade_fullres”. As the model includes the configuration “3d_cascade_fullres”, the flag `-prev_stage_predictions` should be added with the output from the `3d_lowres` model. Therefore the output folder in the first command is “inf_3dfull”, the second command has output “inf_3dlow”, and the third command has output “inf_3dcas”.
6. For ensembling, also add the correct paths and replace “OUTPUT_FOLDER” with “inf_tot”.
7. For postprocessing, there is a command at the bottom of the file. In this command, replace “OUTPUT_FOLDER” with the complete output folder path and “OUTPUT_FOLDER_PP” with a new folder for postprocessed labelmaps (“inf_pp”).
8. The instructions in the “inference_instructions.txt” file could be a little vague, especially when using ensembling with a cascaded network, so hopefully the code below is clear to understand and use. “\” is used as a line separator to make the code cleaner. Change some parts if needed.

```

Prediction 1 (fullres):
nnUNetv2_predict -d Dataset001_Foot \
-i /home/20193158/nnUNet/nnUNet_raw/Dataset001_Foot/imagesTs \
-o /home/20193158/nnUNet/nnUNet_results/Dataset001_Foot/inference/inf_3dfull \
-f 0 1 2 3 4 \
-tr nnUNetTrainer \
-c 3d_fullres \
-p nnUNetPlans \
--save_probabilities

Prediction 2 (lowres):
nnUNetv2_predict -d Dataset001_Foot \
-i /home/20193158/nnUNet/nnUNet_raw/Dataset001_Foot/imagesTs \
-o /home/20193158/nnUNet/nnUNet_results/Dataset001_Foot/inference/inf_3dlow \
-f 0 1 2 3 4 \
-tr nnUNetTrainer \
-c 3d_lowres \
-p nnUNetPlans \
--save_probabilities

Prediction 3 (cascade fullres):
nnUNetv2_predict -d Dataset001_Foot \
-i /home/20193158/nnUNet/nnUNet_raw/Dataset001_Foot/imagesTs \
-o /home/20193158/nnUNet/nnUNet_results/Dataset001_Foot/inference/inf_3dcas \
-f 0 1 2 3 4 \
-tr nnUNetTrainer \
-c 3d_cascade_fullres \
-p nnUNetPlans \
--save_probabilities \
--prev_stage_predictions \
/home/20193158/nnUNet/nnUNet_results/Dataset001_Foot/inference/inf_3dlow

Ensembling fullres and cascade:
nnUNetv2_ensemble \
-i /home/20193158/nnUNet/nnUNet_results/Dataset001_Foot/inference/inf_3dfull \
/home/20193158/nnUNet/nnUNet_results/Dataset001_Foot/inference/inf_3dcas \
-o /home/20193158/nnUNet/nnUNet_results/Dataset001_Foot/inference/inf_tot \
-np 8

Postprocessing
nnUNetv2_apply_postprocessing \
-i /home/20193158/nnUNet/nnUNet_results/Dataset001_Foot/inference/inf_tot \
-o /home/20193158/nnUNet/nnUNet_results/Dataset001_Foot/inference/inf_pp \
-pp_pkl_file \
/home/20193158/nnUNet/nnUNet_results/Dataset001_Foot/ensembles/ensemble__nnUNetTrainer_n \
nUNetPlans__3d_fullres__nnUNetTrainer__nnUNetPlans__3d_cascade_fullres__0_1_2_3_4/postpr \
ocessing.pkl \
-np 8 \
-plans_json \
/home/20193158/nnUNet/nnUNet_results/Dataset001_Foot/ensembles/ensemble__nnUNetTrainer_n \
nUNetPlans__3d_fullres__nnUNetTrainer__nnUNetPlans__3d_cascade_fullres__0_1_2_3_4/plans.json

```

9. Copy and paste the commands one-by-one in the terminal and wait for the model to perform the inference on the test scans. Once the first command is completely executed, the second can be executed, etc.
10. You should end up with each of your output files containing the “dataset.json”, “plans.json” and “predict_from_raw_data_args.json” files as well as a “.nii.gz”, “.npz” and “.pkl” file for each of the test scans.
11. The ensemble output folder “inf_tot” should contain the “dataset.json” file as well as a “.nii.gz” labelmap file for each of the test scans.
12. The postprocessed folder “inf_pp” should contain the “.nii.gz” labelmap file for each of the test scans.
13. Download the postprocessed labelmaps onto your computer to use in Slicer.

14. Inference of the test scans is complete! If you wish to segment other scans, just add them to the imagesTs folder or create a new folder and make sure the input path refers to that folder.

4.2 Loading the segmented labelmaps into Slicer

Now that the test scans are segmented, it's time to load them into 3D Slicer and see how well the model performed.

1. Open Slicer and click 'Add Data' to load the test scans, first only the scans without labels (Foot_024_0000.nii.gz, etc.) and click 'OK' (Fig. 25).

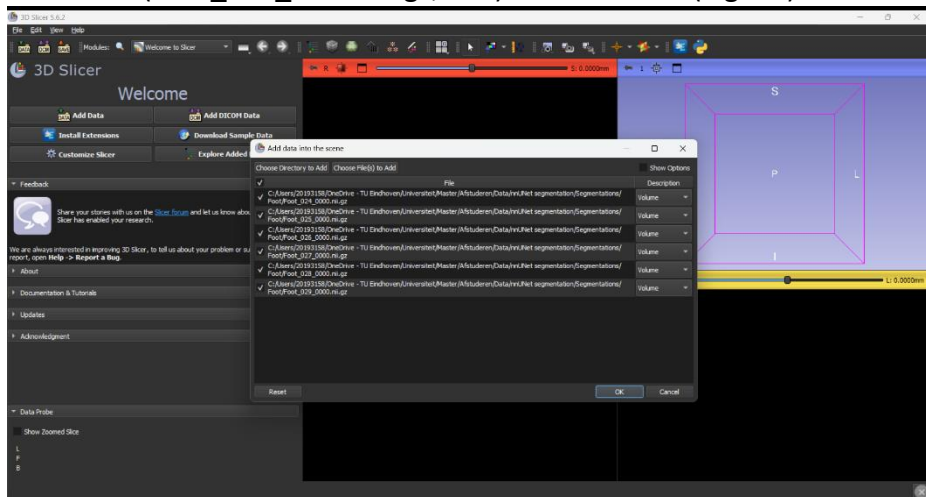


Figure 25: Loading the test scans into Slicer

2. Now add the newly segmented labelmaps by clicking 'Add Data', navigating to the folder where you downloaded the labelmaps to and select them.
3. In the 'Add data into the scene' screen, don't click on 'OK' but first check 'Show Options' at the top right of the screen. This enables you to select the file type that Slicer will recognize.
4. Check the box 'LabelMap' for each labelmap file and click 'OK' (Fig. 26).

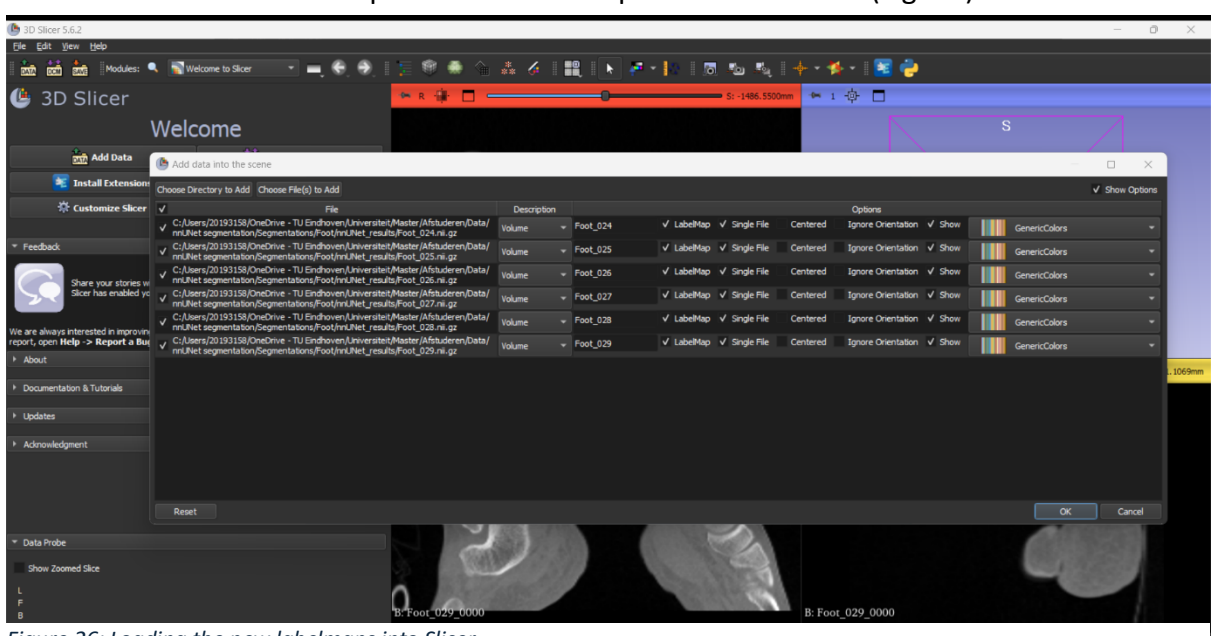


Figure 26: Loading the new labelmaps into Slicer

- Now go to the ‘Data’ module and convert each labelmap into a segmentation node (Fig. 27).

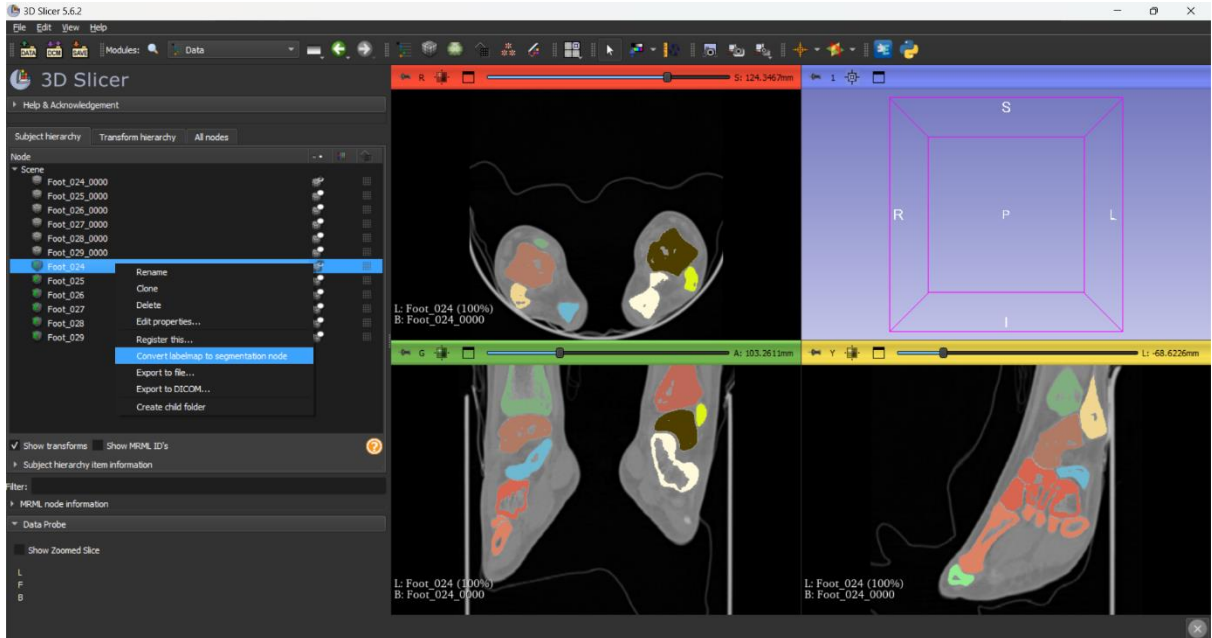


Figure 27: Convert new labelmap into segmentation node

4.3 Accuracy analysis

Now you can inspect the resulting segmentation and use it for further analysis. Slicer has a multitude of extension software which include tools to inspect the similarities between the test scan segmentation by nnUNet and the segmentation from the dataset (ground truth) and compute the DICE score.

- Click ‘Edit’ in the top left of the screen and select ‘Application Settings’ (Fig. 28).

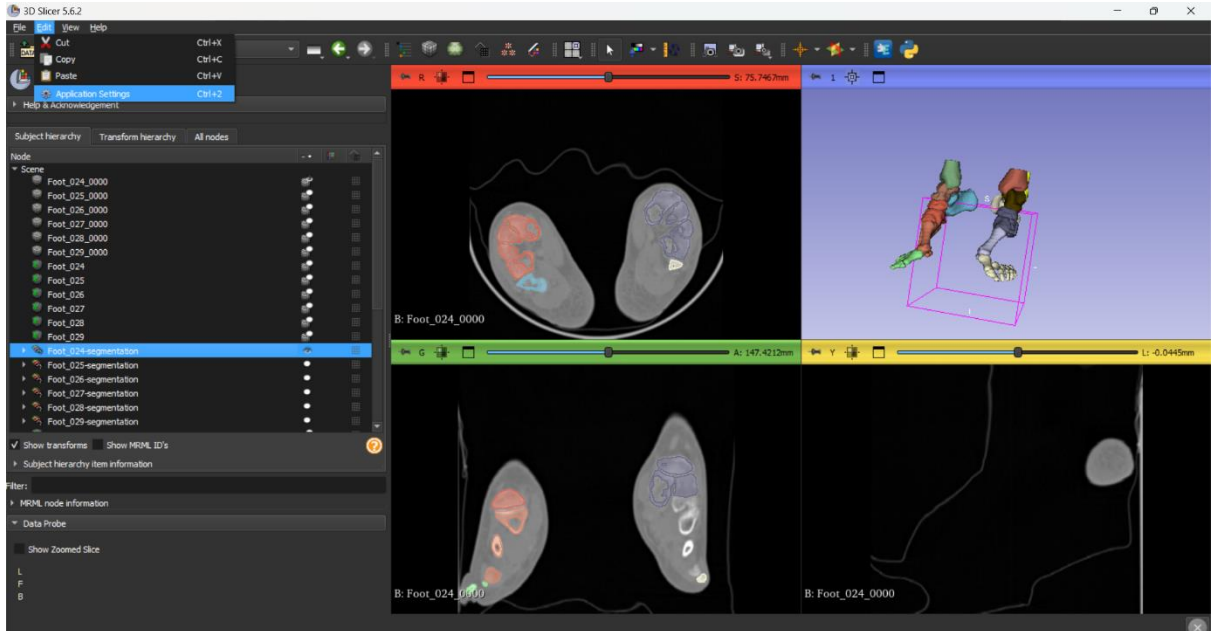


Figure 28: Finding the ‘Application Settings’ menu

- Navigate to ‘Extensions’ and click ‘Open Extensions Manager...’.

- In the ‘Install Extensions’ tab, search for ‘SlicerRT’ and click ‘INSTALL’. A restart of Slicer is required for installation so after the installation is complete, click ‘Restart’ at the bottom right of the screen.
- Again, import the model segmented labelmaps (with added _test) and Test CT scans. Also add the ground truth segmentations the same way as you imported the test segmentations (with added _gt). Use the labelmaps created in Section 1.6 (Fig. 29).

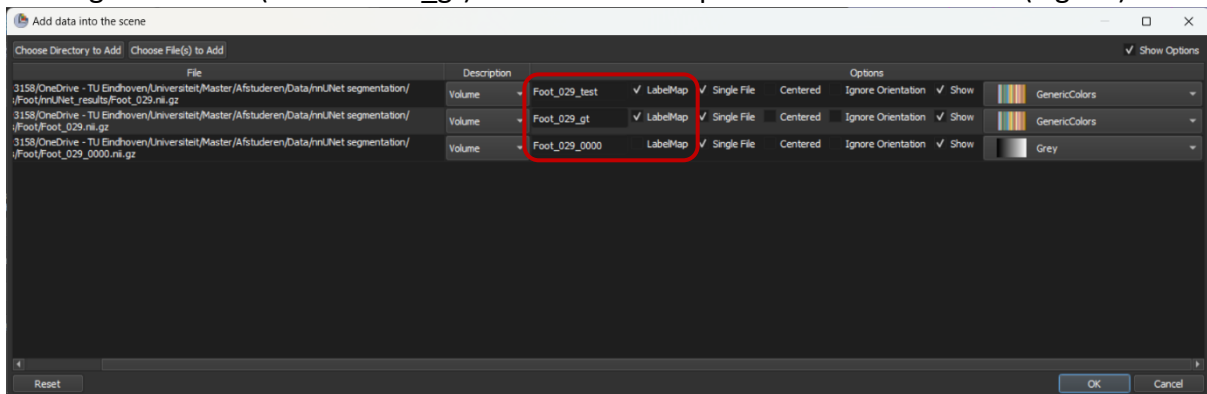


Figure 29: Importing the test and ground truth labelmap for comparison analysis

- Convert the labelmaps into segmentations to compare the segmentations.
- Open the module ‘Segment Comparison’. Here you can let Slicer compute the DICE scores for each segment comparison.
- Set the GT segmentation as ‘Reference segment’ and the Test segmentation as ‘Compare segment’ and compute the Dice metrics for each individual segment (Fig. 30).

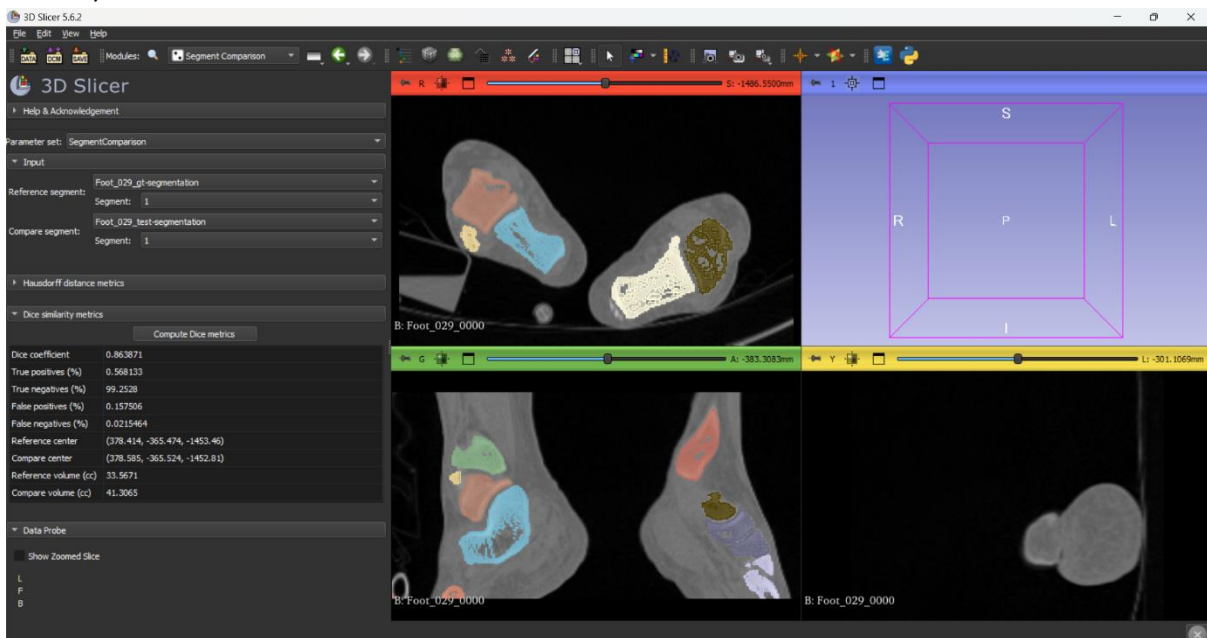


Figure 30: Segment Comparison module with DICE score analysis

4.4 Further use of the segmentations

If you want to perform 3D modeling such as FEM, you can convert the segmentation node into models and export them to your desired output file.